



Hochschule für Angewandte Wissenschaften Hamburg
Hamburg University of Applied Sciences

Master Thesis

Department Fahrzeugtechnik und Flugzeugbau

**Multi-Disciplinary Conceptual Aircraft Design using
CEASIOM**

Maria Pester

10. December 2010



Hochschule für Angewandte Wissenschaften Hamburg
Fakultät Technik und Informatik
Department Fahrzeugtechnik und Flugzeugbau
Berliner Tor 9
20099 Hamburg

Verfasserin: Maria Pester
Abgabedatum: 11.12.2010

1. Prüfer: Prof. Dr.-Ing. Dieter Scholz, MSME

2. Prüfer: Prof. Dr.-Ing. Hartmut Zingel

Abstract

The subject of this study is the programme CEASIOM. CEASIOM is a physics based multi-disciplinary programme which includes aerodynamic and structural calculations as well as analyses of stability and control. It was developed for the conceptual design phase, in order to reduce technical and financial risks. CEASIOM includes six tools: AcBuilder, a parametric aircraft builder; SUMO, a 3D mesh generator; AMB, a tool to consider the aerodynamic effects; NeoCASS, for structure and aeroelastic modelling; SDSA, a tool for analysing stability and control and FCSDT, a tool to generate the flight control architecture. All six tools are tested with the example of an Airbus A320. The results given by CAESIOM are compared to results from generally valid equations or data from Airbus. Thereby inadequacies of AcBuilder, NeoCASS and FCSDT become apparent. A number of these failures are already solved, but here remains a certain rest that is still in process and will be corrected with the next version of CEASIOM. With the help of the working features, a new aircraft concept is tested. A shoulder wing aircraft based on the A320 is implemented into CEASIOM. The shoulder wing aircraft is powered by turboprops and not by jet engines. It is proven that the conceptual shoulder wing aircraft meets the same requirements as the A320. CEASIOM acts out being a helpful programme during the conceptual design phase. Current problems will be solved. As soon as this is done, CEASIOM will become an accessible and timesaving device in the conceptual design.



DEPARTMENT FAHRZEUGTECHNIK UND FLUGZEUGBAU

Multi-Disciplinary Conceptual Aircraft Design using CEASIOM

Aufgabenstellung zur *Masterarbeit* gemäß Prüfungsordnung

Background

An aircraft conceptual design process can be segmented into two cycles (**Raymer 2006**): the initial layout and the revised layout. For the latter one, stability and control analysis among aerodynamics, weights, propulsion, structures, subsystems and costs becomes decisive. In order to be “First-time-right” with the flight control systems design architecture already in an early stage of conceptual design level, an accurate and appropriate stability and control analysis becomes necessary (**Von Kaenel 2008**).

The software package CEASIOM (Computerized Environment for Aircraft Synthesis and Integrated Optimization Methods), developed within the frame of the SimSAC¹, aims at supporting the conceptual aircraft design process with emphasis on the improved prediction of stability and control properties. CEASIOM therefore features rapid low fidelity analysis as well as higher fidelity numerical simulations and integrates the main design disciplines *aerodynamics*, *structures* and *flight dynamics* into one application. It is therefore a tri-disciplinary analysis on the aero-servoelastic aircraft (**Von Kaenel 2008**).

To run CEASIOM, the initial layout of the aircraft to be investigated has to be provided. CEASIOM then refines and outputs the baseline configuration by calculating performance, loads and stability and control parameters. The information obtained is sufficient to be input into a six Degree of Freedom flight simulator.

The baseline aircraft selected for this Master thesis is a 150 passenger, twin engine subsonic transport aircraft. Low and high fidelity tri-disciplinary analysis shall be conducted with the

¹ SimSAC (Simulating Aircraft Stability And Control Characteristics for Use in Conceptual Design) Specific Targeted Research Project (STREP) approved for funding by the European Commission 6th Framework Programme on Research, Technological Development and Demonstration. Work began 1 November 2006 and last 3 years (see www.simsacdesign.eu). The SimSAC project aims at significantly enhancing CEASIOM functionality (**CFS Engineering 2010**)

help of all available CEASIOM modules. Wherever possible, results shall be compared with values found in literature or in-house databases. The course of action in each module and the interrelation to others shall be explained and documented. The final result is thus a composition of results obtained from each CAESIOM module of the baseline aircraft. If time permits, further analyses can be conducted with an adapted aircraft layout (e.g. shoulder wing aircraft).

Task

- Literature research and familiarization with CEASIOM
- Generation of the input files (XML based) of the baseline aircraft (if appl. also of the adapted aircraft layout) for input in CEASIOM with help of the Aircraft Builder Module (AcBuilder)
- Tri-disciplinary analysis of the baseline aircraft with help of
 - Aerodynamic Model Builder (AMB)
 - Next generation Conceptual Aero-Structural Sizing Suite (NeoCASS)
 - Simulation and Dynamic Stability Analyser (SDSA)
 - Flight Control System Design Toolkit (FCSDT)
- Verification of results obtained
- Documentation of course of actions in each module and the interrelation to others
- Discussion on results and CEASIOM practicability

The report has to be written in English based on German or international standards on report writing.

Basic Literature

CFS Engineering 2010

CFS ENGINEERING: CEASIOM: Computerised Environment for Aircraft Synthesis and Integrated Optimisation Methods. Lausanne, Switzerland : CFS Engineering, 2010. – URL: www.CEASIOM.com (2010-05-21)

Raymer 2006

RAYMER, Daniel P.: *Aircraft Design: A Conceptual Approach*. Fourth Edition. New York : AIAA Education Series, 2006 – ISBN 1-56347-829-3

Von Kaenel 2008

VON KAENEL, R.; RIZZI, A.; OPPELSTRUP, J.; et al.: CEASIOM: Simulating Stability & Control with CFD/CSM in Aircraft Conceptual Design. In: *CD Proceedings : ICAS 2008 - 26th Congress of the International Council of the Aeronautical Sciences including the 8th AIAA Aviation Technology, Integration, and Operations (ATIO) Conference* (Anchorage, Alaska, USA, 14-19 September 2008). Edinburgh, UK : Optimage Ltd, 2008. - Paper: ICAS 2008-1.6.3 (061.pdf), ISBN: 0-9533991-9-2

Declaration

This project is entirely my own work. Where use has been made of the work of others, it has been fully acknowledged and referenced.

Date signature student

Table of Content

| | Page |
|--|-----------|
| List of Figures | v |
| List of Tables. | ix |
| List of Symbols | x |
| Greek Symbols | xi |
| Indices | xi |
| List of Abbreviations | xii |
| Explanation | xiii |
| | |
| 1 Introduction | 1 |
| 1.1 Motivation | 1 |
| 1.2 Aim of the Work..... | 1 |
| 1.3 Definitions | 1 |
| 1.4 Literature | 2 |
| 1.5 Thesis Breakdown | 2 |
| | |
| 2 Description of CEASIOM..... | 4 |
| 2.1 CEASIOM | 4 |
| 2.1.1 Handling of CEASIOM..... | 7 |
| 2.2 Tools of CEASIOM..... | 7 |
| 2.2.1 AcBuilder | 7 |
| 2.2.2 SUMO | 9 |
| 2.2.3 AMB | 9 |
| 2.2.4 Propulsion..... | 12 |
| 2.2.5 SDSA..... | 12 |
| 2.2.6 NeoCASS | 16 |
| 2.2.7 FCSDT..... | 21 |
| | |
| 3 Reference Aircraft A320 in CEASIOM..... | 23 |
| 3.1 A320 | 23 |

| | | |
|----------|---|-----------|
| 3.2 | A320 in AcBuilder | 24 |
| 3.2.1 | Implementation..... | 24 |
| 3.2.2 | Evaluation of the Results of AcBuilder..... | 27 |
| 3.2.3 | Discussion on the Practicability of AcBuilder | 30 |
| 3.3 | A320 in SUMO | 31 |
| 3.3.1 | Implementation..... | 31 |
| 3.3.2 | Discussion on the Practicability of SUMO | 34 |
| 3.4 | A320 in AMB | 35 |
| 3.4.1 | Implementation..... | 35 |
| 3.4.2 | Evaluation of the Results of AMB | 37 |
| 3.4.3 | Discussion on the Practicability of AMB | 43 |
| 3.5 | A320 in Propulsion..... | 44 |
| 3.5.1 | Implementation..... | 44 |
| 3.5.2 | Results | 44 |
| 3.6 | A320 in SDSA..... | 45 |
| 3.6.1 | Implementation..... | 45 |
| 3.6.2 | Evaluation of the Results of SDSA | 48 |
| 3.6.3 | Discussion on the practicability of SDSA..... | 56 |
| 3.7 | A320 in NeoCASS | 57 |
| 3.7.1 | Implementation in GUESS | 57 |
| 3.7.2 | Evaluations of the Results of GUESS | 58 |
| 3.7.3 | Implementation in SMARTCAD | 62 |
| 3.7.4 | Evaluation of the Results of SMARTCAD | 64 |
| 3.7.5 | Discussion on the Practicability of NeoCASS | 70 |
| 3.8 | A320 in FCSDT..... | 71 |
| 3.8.1 | Implementation..... | 71 |
| 3.8.2 | Discussion on Practicability of FCSDT | 75 |
| 4 | Analysis of a Shoulder Wing Aircraft | 76 |
| 4.1 | Description of the Configuration..... | 76 |
| 4.2 | Implementation in CEASIOM..... | 80 |
| 4.2.1 | AcBuilder | 80 |

| | | |
|----------|-------------------------------------|-----------|
| 4.2.2 | SUMO | 81 |
| 4.2.3 | AMB | 82 |
| 4.2.4 | SDSA..... | 84 |
| 4.2.5 | NeoCASS | 86 |
| 5 | Conclusion and Outlook | 89 |
| 6 | References | 90 |
| 7 | Appendix | 93 |

List of Figures

| | |
|---|----|
| Fig. 1: Conceptual design phase (Raymers 1992)..... | 4 |
| Fig. 2: Virtual Aircraft Simulation model..... | 5 |
| Fig. 3: Tree structure of the aircraft geometrical data..... | 5 |
| Fig. 4: Data flow of CEASIOM..... | 6 |
| Fig. 5: Adaptable fidelity modules..... | 10 |
| Fig. 6: Adaptive fidelity geometry modeling (Molitor 2009)..... | 11 |
| Fig. 7: SDSA coordinate system (SimSAC 2009)..... | 13 |
| Fig. 8: Velocity axis system (SimSAC 2009)..... | 14 |
| Fig. 9: Stability analysis scheme (SimSAC 2009)..... | 15 |
| Fig. 10: Scheme of flight simulation (SimSAC 2009)..... | 15 |
| Fig. 11: NeoCASS (Cavagna 2009a)..... | 16 |
| Fig. 12: GUESS (Cavagna 2009a)..... | 17 |
| Fig. 13: Sizing tool (Cavagna 2009a)..... | 18 |
| Fig. 14: DLM (DaRonch 2007)..... | 20 |
| Fig. 15: Example - design law..... | 22 |
| Fig. 16: Three view drawing A320 (Aerospace 2010)..... | 23 |
| Fig. 17: Toolbar - Geometry..... | 24 |
| Fig. 18: Geometrical visualization..... | 24 |
| Fig. 19: Fuel visualization..... | 24 |
| Fig. 20: Winglet A320..... | 25 |
| Fig. 21: Winglet A320 new version..... | 25 |
| Fig. 22: Cant angle definition..... | 25 |
| Fig. 23: Visualisation of the Weight & Balance..... | 26 |
| Fig. 24: Visualisation of the Centres of gravity..... | 26 |
| Fig. 25: Structural mesh..... | 26 |
| Fig. 26: Aero mesh..... | 26 |
| Fig. 27: Geometry output AcBuilder..... | 27 |
| Fig. 28: Center of gravity – structure..... | 30 |
| Fig. 29: GUI of SUMO..... | 31 |
| Fig. 30: Skeleton of the fuselage..... | 32 |
| Fig. 31: Rendering of the A320..... | 32 |
| Fig. 32: Control surface definition in SUMO..... | 33 |
| Fig. 33: Surface mesh of the A320..... | 33 |
| Fig. 34: Volume mesh of the A320- refinement 3..... | 34 |
| Fig. 37: States AMB..... | 35 |
| Fig. 38: Tables AMB..... | 35 |
| Fig. 35: Three view drawing..... | 35 |
| Fig. 36: Edit Plot..... | 35 |

| | |
|---|----|
| Fig. 39: Tornado 3D wing and partition layout..... | 36 |
| Fig. 40: Tornado 3D panels, collocation points and normals..... | 36 |
| Fig. 41: Solver AMB..... | 36 |
| Fig. 42: Output of results..... | 36 |
| Fig. 43: Results calculated on equations | 38 |
| Fig. 44: Results C_L over AoA Tornado and DATCOM..... | 38 |
| Fig. 45: NACA 4412 C_L over AoA..... | 39 |
| Fig. 46: C_{Di} calculated on the equations..... | 39 |
| Fig. 47: C_D calculated on the equations | 40 |
| Fig. 48: C_D Tornado and DATCOM | 40 |
| Fig. 49: Grid convergence C_L | 40 |
| Fig. 50: Grid convergence C_D | 40 |
| Fig. 51: C_L over AoA Matlab output Edge Euler..... | 41 |
| Fig. 52: C_L over AoA logfile output..... | 41 |
| Fig. 53: C_D over AoA Matlab output Edge | 41 |
| Fig. 54: C_D over AoA logfile output | 41 |
| Fig. 55: Drag polar SC(2)-0612 (Krauss 2010)..... | 42 |
| Fig. 56: CD for a NASA SC(2)-0612..... | 42 |
| Fig. 57: Mach 0.75 AoA 0° c_p distribution | 42 |
| Fig. 58: Mach 0.75 AoA 5° c_p distribution | 42 |
| Fig. 59: Mach 0.75 alpha 0° Mach distribution..... | 43 |
| Fig. 60: Propulsion GUI..... | 44 |
| Fig. 61: Propulsion output..... | 44 |
| Fig. 62: Input range | 45 |
| Fig. 64: External performance module..... | 46 |
| Fig. 63: Input box | 46 |
| Fig. 65: Basic FCS parameters..... | 46 |
| Fig. 66: Stability GUI..... | 47 |
| Fig. 67: Results GUI..... | 47 |
| Fig. 68: Glide ratio SDSA | 49 |
| Fig. 69: Constant roll angle regular turn | 50 |
| Fig. 70: Constant roll angle calculated by equations | 50 |
| Fig. 71: Simulating tool..... | 51 |
| Fig. 72: Path angle for simulation | 51 |
| Fig. 73: Simulation 2 run 1..... | 52 |
| Fig. 74: Simulation 2 run 2..... | 52 |
| Fig. 75: Control window at the beginning of | 53 |
| Fig. 76: Control window at the simulation..... | 53 |
| Fig. 77: Phugoid..... | 54 |
| Fig. 78: Short period..... | 56 |
| Fig. 79: GUI NeoCASS..... | 57 |
| Fig. 80: GUI Results..... | 58 |
| Fig. 81: Shear force over $b/2$ V3b | 61 |

| | |
|---|----|
| Fig. 82: Bending moment over $b/2 V3b$ | 61 |
| Fig. 83: Shear force on equations..... | 61 |
| Fig. 84: Bending moment on equations | 61 |
| Fig. 85: SMARTCAD Input..... | 62 |
| Fig. 86: Flight condition..... | 62 |
| Fig. 87: GUI structural settings | 64 |
| Fig. 88: GUI Run..... | 64 |
| Fig. 89: Model | 65 |
| Fig. 90: Vibration mode 1 | 65 |
| Fig. 91: V-g plot flutter analysis | 66 |
| Fig. 92: Characteristic ratio of flutter and (Bisplinghoff 1983) | 66 |
| Fig. 93: Mode shape 7 - deformed model | 67 |
| Fig. 94: Mode shape 8 - deformed model | 67 |
| Fig. 95: Mode shape 9 - deformed model | 68 |
| Fig. 96: Mode shape 12 - deformed model | 68 |
| Fig. 97: Mode shape 13 - deformed model | 69 |
| Fig. 98: Model shape 14 - deformed model | 69 |
| Fig. 99: GUI FSCA | 71 |
| Fig. 100: FSCA A320 (Briere 2001)..... | 71 |
| Fig. 101: Fly by wire (Briere 2001) | 72 |
| Fig. 102: Build up FCSA..... | 72 |
| Fig. 103: Failure rate definition for the aileron | 73 |
| Fig. 104: Reliability analysis..... | 73 |
| Fig. 105: A320 flight envelope protection (Briere 2001)..... | 74 |
| Fig. 106: Options for laws and protections | 75 |
| Fig. 107: Definition of the laws | 75 |
| Fig. 108: Definition of the protections | 75 |
| Fig. 109: Fuel fraction turboprop | 79 |
| Fig. 110: SW – geometry | 80 |
| Fig. 111: SW - aero panel..... | 80 |
| Fig. 112: SW - centre of gravity..... | 80 |
| Fig. 113: SW - reference data..... | 80 |
| Fig. 114: SW - rendering in SUMO | 81 |
| Fig. 115: SW - volume mesh..... | 81 |
| Fig. 118: SW - rolling moment coefficient | 82 |
| Fig. 116: SW - drag coefficient..... | 82 |
| Fig. 117: SW - lift coefficient | 82 |
| Fig. 119: SW - pitching moment coefficient..... | 83 |
| Fig. 120: A320 model - pitching moment coefficient..... | 83 |
| Fig. 121: SW - Mach distribution..... | 83 |
| Fig. 122: SW - pressure coefficient distribution | 83 |
| Fig. 123: SW - short period..... | 84 |
| Fig. 124: SW – Phugoid | 84 |

| | |
|--|-----|
| Fig. 125: SW - range | 85 |
| Fig. 126: SW - shear force | 86 |
| Fig. 127: SW - bending moment | 86 |
| Fig. 128: Model A320 - shear force | 86 |
| Fig. 129: Model A320 - bending moment..... | 86 |
| Fig. 130: V-g plot Mach 0,69 altitude 9 900 meters | 87 |
| Fig. 131: Mode shape 11 - deformed model SW | 88 |
| | |
| Fig.A1 1: Input fuselage..... | 93 |
| Fig.A1 2: Input horizontal tail..... | 93 |
| Fig.A1 3: Input wing | 94 |
| Fig.A1 4: Input vertical tail..... | 94 |
| Fig.A1 5: Input engine | 94 |
| Fig.A1 6: Input Weight & Balance | 95 |
| Fig.A1 7: Input beam model (technology) | 95 |
| Fig.A1 8: Input aero panel (technology) | 95 |
| Fig.A1 9: Input spar location (technology) | 96 |
| Fig.A1 10: Input Material (technology) | 96 |
| | |
| Fig.B 1: List for aerodynamic output (SDSA) | 98 |
| Fig.B 2: LQR matrix | 98 |
| Fig.B 3: External SDSA tool endurance | 99 |
| Fig.B 4: External tool range | 99 |
| Fig.B 5: SDSA range - C_L constant..... | 100 |
| Fig.B 6: SDSA range - V constant (simple)..... | 100 |
| Fig.B 7: SDSA range - V constant | 101 |
| Fig.B 8: SDSA radius regular turn | 101 |
| | |
| Fig.D 1: PreSTo result - SW 2 turboprop engines | 103 |
| Fig.D 2: PreSTo result - SW 2 turboprop engines | 103 |
| | |
| Fig.E 1: V-g plot 0.2 Mach h=0 m | 104 |
| Fig.E 2: V-g plot 0.4 Mach h=0 m | 104 |
| Fig.E 3: V-g plot 0.6 Mach h=0 m | 105 |
| Fig.E 4: V-g plot 0.8 Mach h=0 m | 105 |
| Fig.E 5: V-g plot 0.6 Mach h=9 900 m | 106 |
| Fig.E 6: V-g plot 0.8 Mach h=9 900 m | 106 |

List of Tables

| | |
|--|----|
| Tab. 1: Initial conditions | 23 |
| Tab. 2: Winglet parameters | 25 |
| Tab. 3: Weights of the A320 | 28 |
| Tab. 4: AcBuilder V3_b | 28 |
| Tab. 5: Centre of gravity | 30 |
| Tab. 6: Details of the surface mesh | 33 |
| Tab. 7: Data of the volume mesh | 34 |
| Tab. 8: Endurance and range | 49 |
| Tab. 9: GUESS weight estimation | 59 |
| Tab. 10: GUESS weight estimation input V3_b | 59 |
| Tab. 11: Flight conditions | 63 |
| Tab. 12: Parameters V-g plot | 63 |
| Tab. 13: Mode description | 67 |
| Tab. 14: Values of A-C Preliminary sizing | 77 |
| Tab. 15: Comparison of turboprop aircrafts | 77 |
| Tab. 16: Flight mission..... | 78 |
| Tab. 17: Determination of the cruise Mach number | 78 |
| Tab. 18: Comparison with reference aircraft | 79 |
| Tab. 19: SW - weights..... | 81 |
| Tab. 20: Flutter speed for SW | 87 |

List of Symbols

| | |
|--------------------------|--|
| a | Speed of sound or parameter for description of equations |
| A | Aspect ratio |
| b | Wing span |
| c | Chord, coefficient |
| B | Breguet factor |
| d | Diameter |
| D | Drag |
| c_D, C_D | Drag coefficient |
| c_L, C_L | Lift coefficient |
| e | Oswald-Factor |
| E | Glide ratio, engine |
| f | Frequency |
| g | Earth acceleration |
| G_z | Load factor |
| h | Altitude |
| l | Length |
| L | Lift |
| m | Mass |
| M | Moment |
| Ma | Mach number |
| M_{ff} | Mission fuel fraction |
| $O\text{-}xyz$ | body axis system |
| $O_I\text{-}x_Iy_Iz_I$ | coordinate system of the earth |
| $O_a\text{-}x_a y_a z_a$ | velocity coordinate system |
| $O_g\text{-}x_g y_g z_g$ | movable coordinate system = gravity coordinate system |
| p | rotation in roll |
| P | Power |
| $P/(mg)$ | Power to weight ratio |
| q | Dynamic pressure or , rotation in pitch |
| r | rotation in yaw or radius |
| Re | Reynolds number |
| S | Surface |
| t | Thickness, time |
| T | Period |
| t/c | Relative thickness |
| Th | Thrust |
| $Th/(mg)$ | Thrust to weight ratio |
| V | Velocity |

Greek Symbols

| | |
|------------|---|
| α | Angle of attack |
| α_0 | Angle of attack at zero lift |
| β | sideslip angle |
| δ | Angle of a control surface (e –elevator, r- rudder, a – aileron), damping constant |
| η | control variable |
| λ | Taper ratio |
| μ | Dynamic viscosity |
| ν | Cinematic viscosity |
| ρ | Air density |
| σ | Relative density |
| π | PI |
| ξ | Damping |
| ω | Circular frequency |
| ω_0 | Eigenfrequency |
| Λ | Aspect raio |

Indices

| | |
|----------------|-----------------------------------|
| () <i>i</i> | Inner |
| () <i>cg</i> | Center of gravity |
| () <i>D,0</i> | Zero lift drag |
| () <i>D,i</i> | induced Drag |
| () <i>E</i> | Engine |
| () <i>F</i> | Fuselage |
| () <i>fe</i> | viscous drag |
| () <i>MAC</i> | Related to mean aerodynamic chord |
| () <i>o</i> | Outer |
| () <i>p</i> | Pressure |
| () <i>r</i> | Root |
| () <i>t</i> | Tip |
| () <i>W</i> | Wing |
| () <i>Wet</i> | Wetted |

List of Abbreviations

| | |
|-----------|---|
| AC | Aerodynamic center or Advisory Circular |
| AcBuilder | Aircraft Builder |
| AIC | Aerodynamic Influence Coefficient |
| AMB | Aerodynamic Model Builder |
| AoA | Angle of Attack |
| APU | Auxiliary Power Unit |
| CAD | Computer Aided Design |
| CEASIOM | Computerised Environment for Aircraft Synthesis and Integrated Optimisation Methods |
| CFD | Computational Fluid Dynamics |
| CLD | Control Laws Definition |
| DLM | Douplet-Lattice Methode |
| COG | Center of gravity |
| DATCOM | Stability and Control Data Compendium |
| EAS | Equivalent Air Speed |
| FAA | Federal Aviation Agency |
| FAR | Federal Aviation Regulations |
| FCS | Flight control System |
| FCSA | Flight Control System Architecture |
| FCSDT | Flight Control System Designer Toolkid |
| FORTTRAN | Formula Translator |
| FSim | Desktop Flight Simulator |
| GMEW | Green Manufacturing Empty Weight |
| GUESS | Generic Unknown Estimator in Structural Sizing |
| GUI | Graphical User Interface |
| HT | Horizontal Tail |
| ICAO | International Civil Aviation Organization |
| ICEM | Integrated Computer Engineering and Manufacturing |
| IGES | Initial Graphics Exchange Specification |
| ISA | International Standard Atmosphere |
| JAR | Joint Aviation Requirements |
| LE | Leading Edge |
| LTIS | Linear Time Invariant Synthesis |
| LQR | Linear-Quadratic Regulator |
| MAC | Mean aerodynamic chord |
| MIL | Military Specifications |
| MLS | Moving Least Squares |
| MPL | Maximum Payload |
| MTOW | Maximum Take Off Weight |

| | |
|----------|--|
| NACA | National Advisory Committee for Aeronautics |
| NeoCASS | Next generation Conceptual Aero-Structural Sizing |
| NM | Nautical Miles |
| OWE | Operating Empty Weight |
| PrADO | Preliminary Aircraft Design and Optimisation programme |
| RANS | Reynolds Average Navier Stokes |
| RBF | Radial Basic Functions |
| SCAA | Stability & Control Analyser and Assessor |
| SDSA | Stability |
| SFC | Specific Fuel Consumption |
| SMARTCAD | Simplified Models for Aeroelasticity in Conceptual Aircraft Design |
| SUMO | Surface Modeler |
| TAS | True Air Speed |
| TetGen | Tetrahedral Generator |
| USAF | United States Air Forces |
| VLM | Vortex-Lattice-Method |
| VT | Vertical Tail |
| WWW | World Wide Web |
| WB | Weight and Balance |

Explanation

CFSEngineering

CFS Engineering is a consultancy company founded in August 1999, located in the Business Park (PSE) of the Swiss Federal Institute of Technology (EPFL) in Lausanne, Switzerland. The mission of CFS Engineering is: To offer services in the Numerical Simulation of Fluid Mechanics and Structural Mechanics Engineering Problems.(CFS2005)

CFSEngineering is the support. When problems appear, they can be contacted and try to solve this problem.

1 Introduction

1.1 Motivation

The software package CEASIOM was developed to support the conceptual aircraft design process. Therefore the three design disciplines aerodynamics, structures and flight dynamics are covered. HAW Hamburg's research group AERO wants to participate on further development of CEASIOM. Therefore a basic understanding of the single tools is crucial. Because CEASIOM is a relatively new program, the handling and the possibilities of it are studied in this work. The integration of an A320 into CEASIOM serves to write a summarized documentation of the programme and to compare the output with given data. Subsequently a new configuration with the same reference data as the A320 is proved. Regarding the AERO project Airport 2030 a shoulder wing airplane is analysed with the help of CEASIOM.

1.2 Aim of the Work

The aim of this project is to understand the structure of CEASIOM. The application should be possible without any bigger problems. If any problems appear, the cause has to be detected and removed. In this case, CFS Engineering will be of help. First the known aircraft A320 is implemented into CEASIOM. Furthermore, a new configuration of a shoulder wing aircraft will be analysed and assessed with CEASIOM. In the end an impartial rating of CEASIOM can be given.

1.3 Definitions

The key words of this thesis are mentioned in the title:

- Multi-Disciplinary
- Conceptual Aircraft Design
- CEASIOM

Multi-Disciplinary makes clear that several fields of the aircraft design process are included. Several fields are examined.

Conceptual Aircraft Design indicates where the programme that is examined joins in. The conceptual aircraft design is at the beginning of the aircraft design process.

CEASIOM is the programme this thesis deals with. The advantages and disadvantages are identified in this work.

1.4 Literature

An important reference of papers and projects was the database included in the downloaded folder of CEASIOM. Moreover the homepage of CEASIMO serves as source.

To evaluate the results of CEASIOM lecture notes of the University of Applied Sciences, Hamburg were used. For example, it is referred to the lecture notes of Prof. Dieter Scholz “Flugzeugentwurf” (**Scholz 1999**) and the lecture notes of Prof. Seibel “Eine Vorlesung zur Gestaltung und Auslegung von Flugzeugzellen” (**Seibel 2008**).

1.5 Thesis Breakdown

Chapter 1: *Introduction* opens this work with the presentation of the motivation that leads to the study of CEASIOM. Here the potential advantages that should be analysed for the research group Aero are mentioned.

Chapter 2: *Description of CEASIOM* deals with the structure of CEASIOM. Moreover the idea of CEASIOM is characterised and the task of the single tools is depicted. Therefore the theoretical background is given and described.

Chapter 3: *Reference Aircraft A320 in CEASIOM* shows the handling of CEASIOM with the example of the A320. In this chapter a brief documentation of the programme is given. The A320 is modelled in each tool of CEASIOM and the results are compared to other methods and discussed. Furthermore the handling of the tool is described.

Chapter 4: *Analysis of a shoulder wing aircraft* examines a new configuration that is based on the A320. The position of the wings is changed and consequently the configuration of the tail as well. It is necessary to get adequate input data for CEASIOM. Hence, the shoulder wing aircraft is computed with the preliminary sizing tool PreSTo. The output data of this tool serves as input data for the AcBuilder. The findings of the CEASIOM analysis are discussed with regard to the A320.

Chapter 5: *Conclusion and outlook* close the master thesis with a summary of the results and an assessment of CEASIOM. Therefore the advantages and the handling are considered. Some further necessary steps are pointed out here, too.

Appendix A: includes contents according to the tool AcBuilder

Appendix B: includes contents according to the tool SDSA

Appendix C: includes the input data for the calculation of the bending moment and the shear force of the A320 wing

Appendix D: includes the results of PreSTO for the shoulder wing aircraft

Appendix E: includes the results of the flutter analysis for the shoulder wing aircraft

Appendix F: includes the structure of the attached CD

2 Description of CEASIOM

2.1 CEASIOM

CEASIOM stands for Computerised Environment for Aircraft Synthesis and Integrated Optimisation Methods. With the help of CEASIOM the technical and financial risks within aircraft design should be reduced.

CEASIOM is a physics based multi-disciplinary programme which steps in the conceptual design phase. If the design process is classified into three phases, the conceptual design phase stands at the beginning (**Raymers 1992**). Here many variants are defined at a system level and several concepts are proven. The basics related to the configuration arrangement, size, weight and performance are collected. In the following illustration (Fig. 1) the course of action at the conceptual design phase can be understood.

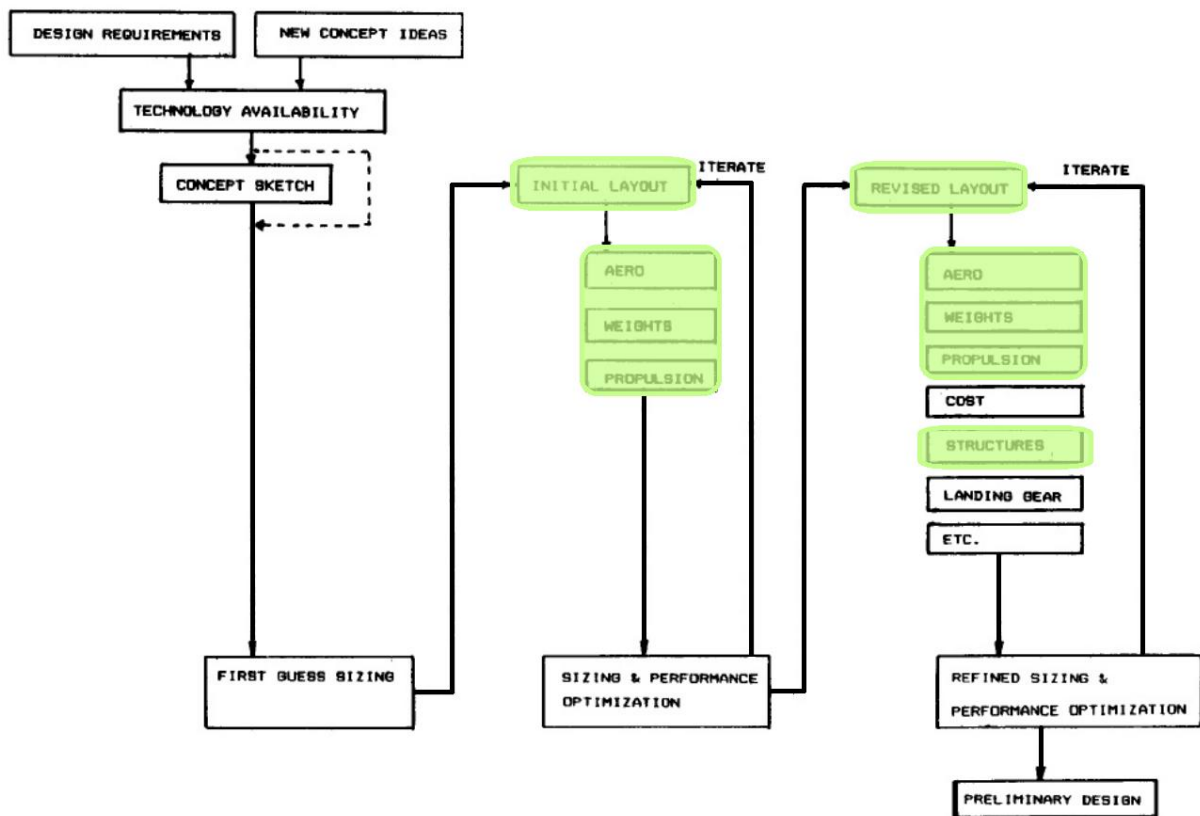


Fig. 1: Conceptual design phase (Raymers 1992)

The green marked items are the ones where CEASIOM joins in.

According to Raymer, the preliminary design follows the conceptual design. At this step the configuration will be frozen and first tests are initiated. The structure, the landing gear and the control system will be designed and analysed. Another important subject during the

preliminary design is “lofting”. Here the outer skin will be modelled mathematically to ensure the right interaction of the single components. Moreover in this phase it has to be clear, that the airplane can be built on time and that the estimated costs will be met (**Raymers 1992**).

The advantage of CEASIOM is the possibility to include aerodynamic and structural requirements very early into the process. A virtual aircraft model is built up. That allows comprising calculations regarding to aeroelasticity and stability and control as well. The CEASIOM main GUI comprises a parametric aircraft builder (AcBuilder) and a CAD modelling, a 3D mesh

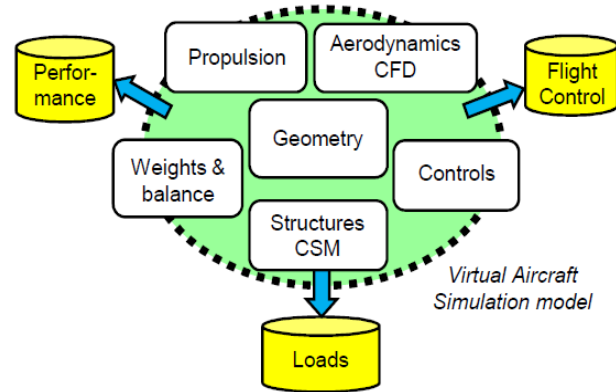


Fig. 2: Virtual Aircraft Simulation model (**CASIOM 2010**)

generator (SUMO), a tool to consider the aerodynamic effects (AMB), a tool for structure and aeroelastic modelling (NeoCASS) , a tool for stability and control analyses (SDSA) and a tool for Flight Control System architecture (FCSDT). In the end all elements allow a statement with regard to performance, flight controls and loads (cf. Fig. 2).

The whole CEASIOM process is based on an *.xml format. The input *.xml file contains all the parameters which are generally necessary for a geometrical description of the airplane. This description is based on a tree structure. The aircraft has several child elements, which have child elements by their own and so on. Fig. 3 shows an example of this. The elements of

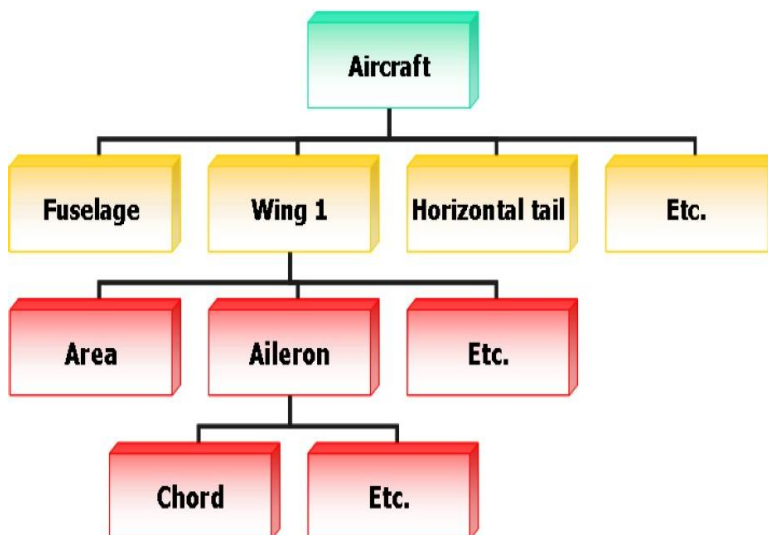


Fig. 3: Tree structure of the aircraft geometrical data (**Puelles 2010**)

the first level are Fuselage, Wing, Fairing, Horizontal tail, Vertical tail, Ventral fin, Engines, Fuel, Baggage, Cabin, Miscellaneous and Weight-Balance. The definition of the sub-items, which are necessary for a detailed description of the airplane, can be found in the document Ceasiom-xml File Definition (**Puelles 2010**). This paper belongs to the packet of the downloaded CEASIOM. For the path of Wing1 as to Fig. 3, the depending *.xml format is shown in the description field below.

```

<Wing1 idx="1" type="struct" size="1 1">
  <area idx="1" type="double" size="1 1">122.4</area>
  [...]
  <aileron idx="1" type="struct" size="1 1">
    <chord idx="1" type="double" size="1 1">0.275</chord>
    <Span idx="1" type="double" size="1 1">0.213</Span>
    [...]
  </aileron>
</Wing1>

```

To generate the *.xml file it is also possible to use the AcBuilder. In this case the file does not have to be typed. The GUI (Graphical User Interface) of the AcBuilder allows the user to define the parameters in a much simpler way. The AcBuilder also includes a Weight & Balance tool which is needed for working with NeoCass. The output file of the AcBuilder is also the base for SUMO and the Aerodynamic Model Builder (AMB). A mesh, generated in SUMO, can be imported by the AMB too. At the AMB the aerodynamic coefficients are calculated. The output of the AMB is a *.xml file that can be passed on to the tool called Propulsion. Here the data for the engine is added. After that the *.xml file can be transmitted to the SDSA or the FCSDT service program. With SDSA the stability and control can be analyzed. The FCSDT tool deals with the architecture of the control systems.

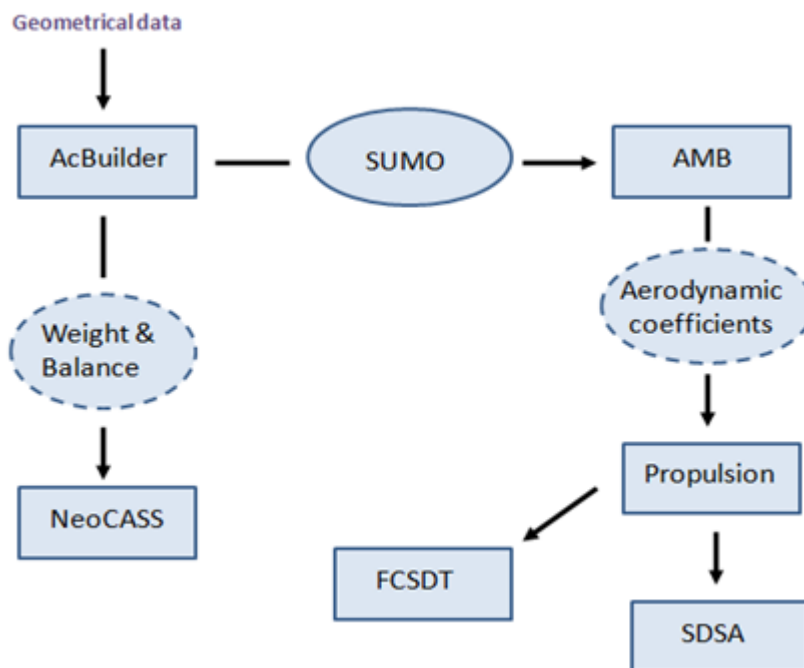


Fig. 4: Data flow of CEASIOM

Fig. 4 depicts the sequence of the data flow.

2.1.1 Handling of CEASIOM

For this thesis CEASIOM100v2-0 is downloaded from the relating homepage and installed on a computer working with Windows 7 (32bit). The available Matlab version is R2010a. The download includes a precise description how to start CEASIOM. Additional to the CEASIOM folder a new patch is downloaded during the project, also available on the CEASIOM homepage. Opening CEASIOM provides the opportunity to open an existing project, start a new project or to delete an existing project. When a user wants to get a first insight into the programme or wants to work on a current project, the user would have to open an existing project; this leads to the folder where the project files are stored. After selecting a project and the corresponding *.xml file the working surface of CEASIOM shows up. By choosing the button *Menu* the needed tool can be select. After starting one of the modules, a short introduction for the tool is given in the CEASIOM window. The available examples can be used as templates when starting a new project. The first tool to define the geometric data is the AcBuilder.

2.2 Tools of CEASIOM

2.2.1 AcBuilder

The AcBuilder serves to visualise an aircraft`s geometric data. Also the input of miscellaneous data can be set. At the AcBuilder the Geo and Weight & Balance tools are integrated. With the help of this module it is possible to import and export the parameters in *.xml format. This way an input file can be generated for the AMB module, the NeoCass module and FCSDT.

One sub-item of the AcBuilder is the Geometry. Here the single characteristics in view of the geometrical components and the fuel are set. A geometry output is available which contains the reference values that are used for the following calculations. One parameter of the wing is the airfoil. Several choices are listed here, but it is also possible to add some new airfoils. For this the data of the airfoils has to be implemented in diverse folders. One folder is under the path CEASIOM → Aerodynamics → Datcom → airfoils. The airfoil data is saved as a *.dat file. The Point data is written in 2 columns. The number of the supporting points should exceed 50. The support points are scaled from 0 till 1. Multiplied by the accordant chord length the dimension is generated. The structure of the file is shown in the text field below.

| | | | |
|--------|---------|---|---------------|
| 1.0000 | 0.0000 | } | upper surface |
| [...] | [...] | | |
| 0.0000 | 0.0000 | } | lower surface |
| 1.0000 | 0.0000 | | |
| [...] | [-...] | | |
| 0.0000 | 0.00000 | | |

All decimal points are marked by a dot. There are 4 fractional digits. One blank is in front of the first column, 3 blanks are amongst the first and the second column.

Furthermore at CEASIOM → Aerodynamics → T135-003_Export → aircraft → airfoils the data of the new airfoil has to be saved. The structure of the file is a little bit different compared to the structure above. In the first line the number of the supporting point should be set. The first number stands for the lower surface, the second for the upper surface. Hereinafter, the data is structured in the same way as above but in a different order. An example is presented in the text field below.

| | | | |
|--------|--------|---|---------------|
| 36 | 36 | | |
| 0.0000 | 0.0000 | } | upper surface |
| [...] | [...] | | |
| 1.0000 | 0.0000 | } | lower surface |
| 0.0000 | 0.0000 | | |
| [...] | [-...] | | |
| 1.0000 | 0.0000 | | |

A third data base is found under CEASIOM → Geometry → airfoil. The data is also saved as a *.dat file. Here the data is in 2 columns as well. The number of the supporting points is not asked for. In front of the first column 2 blanks are set. In the most files 6 fractional digits are given and between the two columns there are 3 blanks. An example is in the following description box.

| | | | |
|----------|----------|---|---------------|
| 1.000000 | 0.000000 | } | upper surface |
| [...] | [...] | | |
| 0.000000 | 0.000000 | } | lower surface |
| 0.000000 | 0.000000 | | |
| [...] | [-...] | | |
| 1.000000 | 0.000000 | | |

The number of the blanks and fractional digits is not mandatory binding, but to avoid problems this structure should be retained.

The integrated Weight and Balance module is relevant for the first estimation of the overall weight and inertias. The non structural masses are included, such as payload, fuel and systems. Furthermore the position of their centres of gravity is located. To put this into practice the *.xml file is read out and put into 4 scripts which are outputted in a MATLAB

structure. One is the script *wb-weight*, there the weight is computed by empirical estimation and statistical data. The *rcogs* script is responsible for the calculation of the centres of gravity. Within the script *riner* the inertia is calculated. In the last script the global centre of gravity with regard to the MTOW and MEW is deduced, it is called *rweig*. At last all results are saved in a *.xml format, shown via the Matlab window and complemented at the AcBuilder.

The Technology module is significant for the structural sizing. The user has to define the distribution of the aero mesh and the structural mesh which are needed in NeoCass. Also the material characteristics can be set and the structural concepts of the single components is chosen. All the data that is important for NeoCASS and the suitable meanings can be looked up at the NeoCASS manual (**Cavagna 2009**).

2.2.2 SUMO

SUMO is a tool developed by Larosterna¹ for surface modelling and mesh generation. It is written in C++. Within the surface modeller the geometrical components are based on the C++ library. It is designed for a simple and time saving surface modelling of different aircraft configurations. That happens through top and side views and the according cross section definitions. There are two surface types which simplify the modelling. On the one hand, the user can define a body surface, e.g. for fuselage structures or pylons. On the other hand, wing surfaces can be chosen, which are used for instance for modelling the horizontal tail and lifting surfaces. It is also possible to use an IGES file from a CAD programme for the aircraft's geometry. So SUMO is compatible with other CAD programmes.

With the help of SUMO a mesh file for CFD calculations can be generated. A surface mesh and a volume mesh are realizable. Both are unstructured. The Triangulations are based on a three dimensional in sphere criteria. The volume mesh is generated by Hug Si's tetrahedral mesh generator TetGen (**ELLER 2009**).

2.2.3 AMB

The Aerodynamic Model Builder (AMB) is a component of CEASIOM to identify the aerodynamic data. The data is prepared with the help of a tabular model. The chance to incorporate aerodynamics early into the design phase leads to a minimization of the costs. There are three possibilities for a first estimate of the aerodynamic. One is the use of handbook methods like Datcom. The second is a linear singular method, for example the Vortex Lattice method. The third method that can be used is a full non-singular method like solving the Euler equations or RANSE.

¹ Larosterna is a small software development business started in June 2009 by a researcher of the Flight Dynamics Lab at the Royal Institute of Technology in Stockholm.

Digital Datcom and Tornado are implemented in the AMB. Datcom is a handbook method and Tornado a Vortex Lattice method. Both are summed up under the Tier 1 methods and give good results for low speed aerodynamics and low angles of attack. The second fragment is based on the EDGE Euler code and belongs to Tier 1+. Here the compressible effects are captured and so it can be used for high speed aerodynamics and aeroelastic problems. Hence, aerodata for transonic flights can be produced. A third part is Tier 2, it is not yet implemented to CEASIOM. It includes a RANS flow simulation. In the AMB there is no solver for that, but a RANS solver preferred by the user can be easily linked. For that interfaces and standard formats are defined within CEASIOM (Fig. 5).

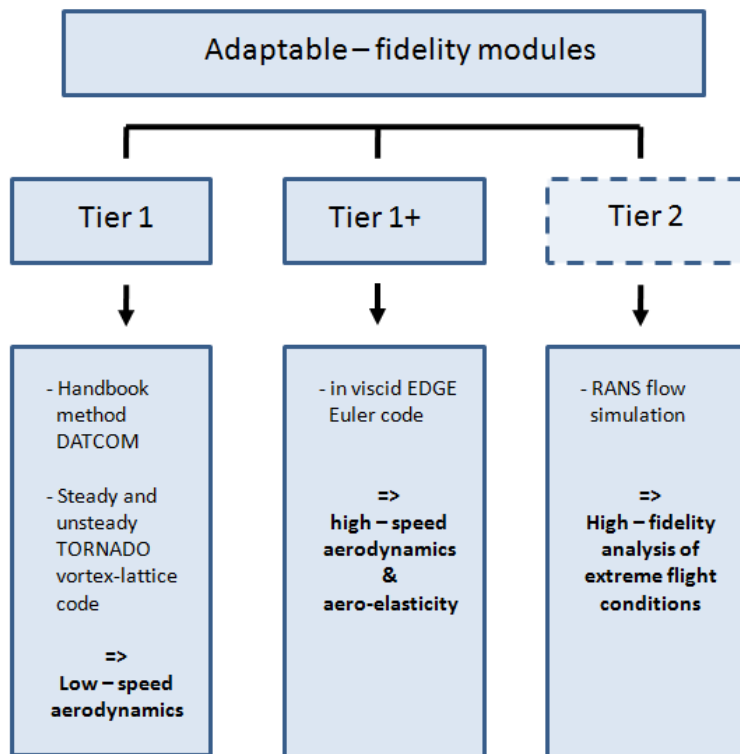


Fig. 5: Adaptable fidelity modules

The basis for all calculations in AMB is the input file. The way it is presented in Fig. 6. the input file is a *.xml file which is provided by the AcBuilder. Here the geometrical conditions are defined. With this information the Tier 1 module can be used. To run the Tier 1+ module it is necessary to give the geo.xml file to SUMO (cf. chapter 2.2.2). Here a surface mesh and a volume mesh can be generated. This is needed for the panel method and for the EDGE Euler solver. The SUMO output is also the basis for Tier 2 simulations. In this case an *.iges file has to be saved and given to an ICEM/CFD programme. After the volume mesh is generated a RANS flow simulation can be run on a separate solver.

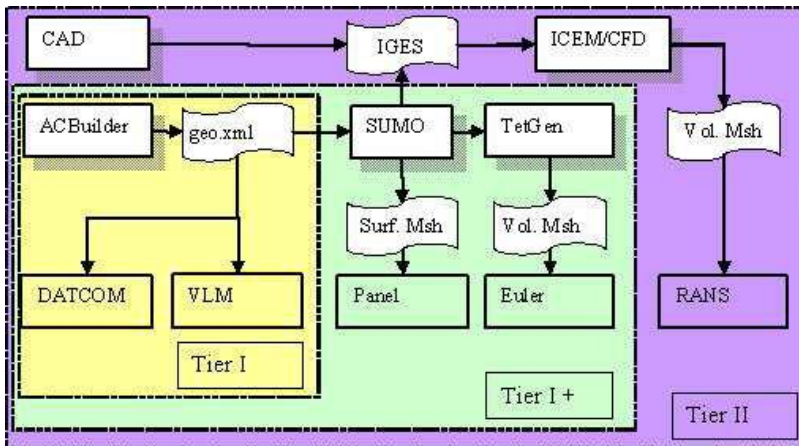


Fig. 6: Adaptive fidelity geometry modeling (Molitor 2009)

As mentioned earlier, the aerodata is generated with the help of a tabular model. The aerodynamic table in AMB has the following Format:

- α is the angle of attack,
- M is the Mach number and
- β the side slip angle
- q , p and r are the three rotations in pitch, roll and yaw
- 3 control surfaces that can be deflected: elevator δ_e , rudder δ_r and aileron δ_a

The table is linearised and is built up from 7 three-dimensional tables with α , M and a third parameter (β , q , p , r , δ_e , δ_r or δ_a). The AMB uses a body axis system coherent with the international standardised coordinate system ISO 1151-1 (ISO 1151-1). The origin is the reference point and can be specified by the user (Molitor 2009). The calculations of Tier 1 and Tier 1+ are based on Digital Datcom, Tornado and Edge Euler. In this paper the focus will lie on these three methods. A short summary of these methods follows.

Digital DATCOM is the implementation of the USAF Stability and Control Data Compendium (short Datcom) into a computer programme. Datcom was developed in the 1960s. It is a compilation of analytic and semi-empirical formulas which are collected in notebooks. In the 70s the development of Digital DATCOM started. It is based on FORTRAN and in the present a preprocessor and a postprocessor are implemented. This is why commented input files are useable and the output files produce readable data for other programmes as well. The digital Datcom calculates aerodynamic derivatives based on geometry details and flight conditions. It should be used for conventional configurations.

Unconventional configurations are no problem for Tornado. It is based on a steady Vortex - Lattice Method which is corrected by the strip theory. The viscosity is taken into account by an empirical extension. The linear results are combined with 2D viscous airfoil code XFOIL. An unsteady Version of Tornado is in work. Tornado computes forces, moments and aerodynamic coefficients. They can be calculated with respect to the angle of attack, angle of sideslip, the roll-pitch-yaw rotation and the control surface deflection. Incompressible fluid

conditions are calculated using the Prandtl-Glauert correction, which gives reasonable results up to Mach 0.6 (**Molitor 2009**).

Edge is a parallelised CFD flow solver system for solving 2D/3D viscous/inviscid, compressible flow problems on unstructured grids with arbitrary elements (**FOI 2008**). It is an edge-based formulation which uses a node-centred finite volume technique. The control volumes are not overlapping and the Edge meshes should not contain hanging nodes. In CEASIOM the Edge Euler Code is implemented via a Matlab interface, which was written in order to allow Edge calculations to be prepared and run. This call runs the pre-processing routines, launches the calculation and processes the solution for the forces and moments (**DaRonch 2009**).

2.2.4 Propulsion

The tool Propulsion generates the database of the engines for following calculations in the SDSA tool. It shows the thrust over the Mach number depending on the altitude. The input data is a *.xml file from the AMB. The output is also a *.xml file.

2.2.5 SDSA

The SDSA module is useful for dealing with stability analyses based on JAR/FAR, ICAO and MIL. Also simulations with 6 degrees of freedom are possible. A Flight Control System based on linear quadratic regulator theory is implemented. Furthermore a outlook of the performance can be made. The SDSA tool contains an eigenvalue analysis, linearised by calculating the Jacobi matrix of the derivative around the equilibrium.

There are several requirements according to the physical model. They are listed below:

- aircraft is a rigid body with 6 degrees of freedom
 - 3 translations along the axis – x, y, z
 - 3 rotations – pitch, roll, yaw
- Control surfaces are moveable but not do free vibrations
- Aerodynamics are seen as quasi steady
- Standard undisturbed atmospheric model (**SimSAC 2009**)

The coordinate system is defined as shown in Fig. 7.

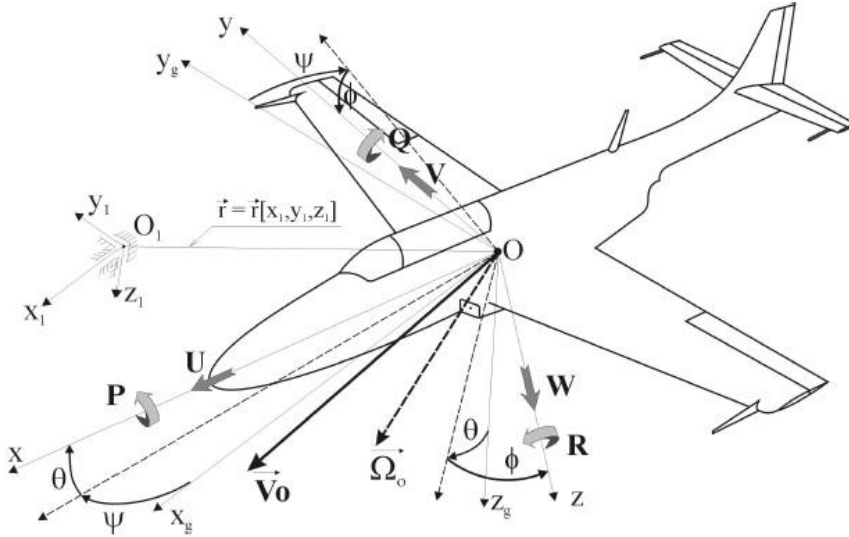


Fig. 7: SDSA coordinate system (SimSAC 2009)

$O_1-x_1y_1z_1$ is the fixed coordinate system of the earth. The movable coordinate system $O-x_gy_gz_g$ is parallel to the gravity coordinate system. The origin is a constant point on the body, mostly at 1/4 MAC. In the body axis system, OX is parallel to the MAC and points forward to the nose of the airplane. OZ is oriented down and OY is oriented towards the right wing. The origin of the body axis system is the same as the origin of the movable coordinate system.

Transformation from the $O-x_gy_gz_g$ axis system to the body axis system is defined by three rotations performed in the following order:

- *rotation around the Oz_g axis - yaw angle Ψ ,*
- *rotation around the new Oy axis (after yaw rotation) -pitch angle Θ ,*
- *rotation around the new Ox axis (after yaw and pitch rotation) - roll angle Φ .*

The components of main velocity vector V_0 (U, V, W) and main angular velocity vector Ω (P, Q, R) are defined in the body axis system (Fig. 7).” (SimSAC 2009).

Furthermore a velocity axis system is integrated. The axis OX_a is parallel to the free stream. The angle of attack α is defined by the rotation from OY to OY_a . The sideslip angle β is expressed by the rotation from the axis OZ to OZ_a . The origin can be set by the user; mostly it is at 1/4 MAC because almost all aerodynamic characteristics are referred to this point. In Fig. 8 the velocity axis system is depicted (SimSAC 2009).

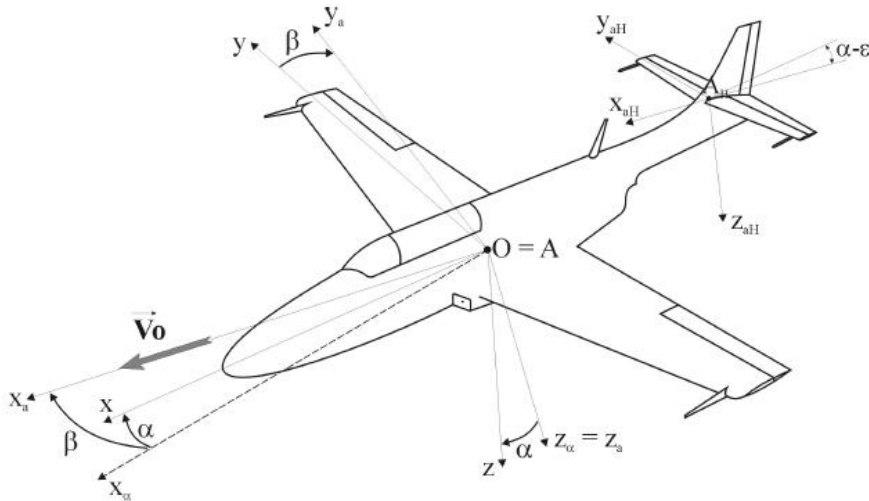


Fig. 8: Velocity axis system (SimSAC 2009)

The axis systems are necessary to get kinematic relations and create suitable equations. Therefore the relation between the coordinates of the gravity/inertia system and the linear velocity are set. Also the relation between the quasi Euler angles and the angular velocity is put into equations. Both are generated in the body axis system that is used in the AcBuilder. Besides, the dynamic equations of motion are formed on the base of the balance of forces and moments. The detailed equations can be gleaned in the paper SDSA – Theoretical basis (SimSAC 2009). The mathematical model for aerodynamics is developed for the stability analysis. Therefore aerodynamics are assumed as quasi-steady and the force along the x-y-z axis is summed up in a Taylor series.

The core module of SDSA is the stability analysis. In Fig. 9 the scheme of the stability analysis is pictured. To get the results, the mathematical model is transformed into a matrix form. SDSA includes two ways of transforming the non linear equations into a linear one. One possibility is making additional assumptions (e.g. that attitude angles are small). The second way is the direct linearization of the force vector by calculation of the Jacobin matrix for the defined state of the flight (SimSAC 2009). With the help of the Jacobin matrix the Eigenvalue problem can be formulated and out of this, the frequency and damping coefficients can be calculated. Also the motion modes can be identified. In the end the stability characteristics can be determined.

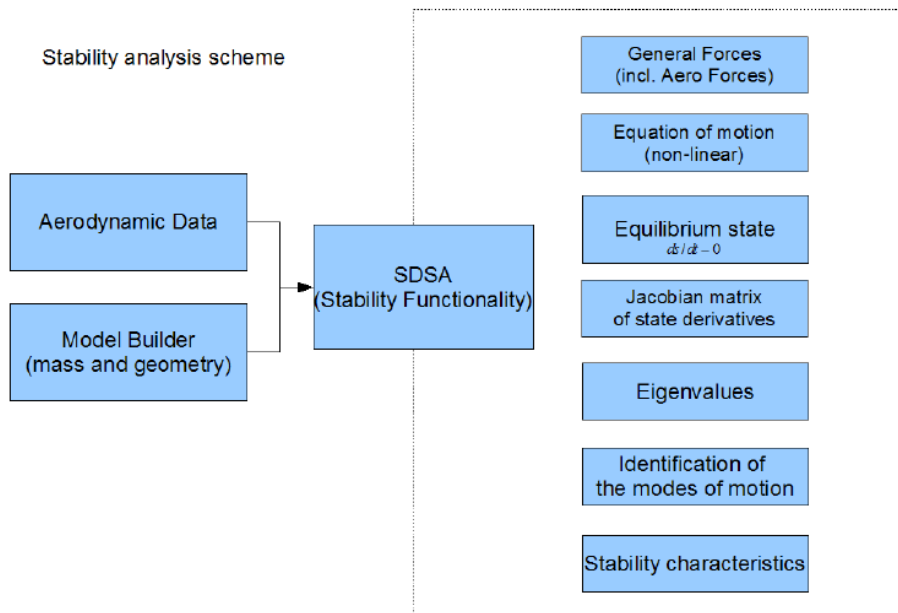


Fig. 9: Stability analysis scheme (SimSAC 2009)

For defining the states for the Eigenvalue problems (that should be solved), another module is implemented into the core module. It is called Equilibrium state computation. It is also used in the flight simulating module to compute the initial conditions. Here the time derivative of the state vector is set to zero. So the nonlinear equation, which is derived from the equation of motion, can be solved.

With the help of the flight simulating model it is possible to compute flight parameters in real time. In this way stability characteristics can be verified by using a full non-linear model. The implementation is shown in Fig. 10. Several modules that are described above are used for the computation.

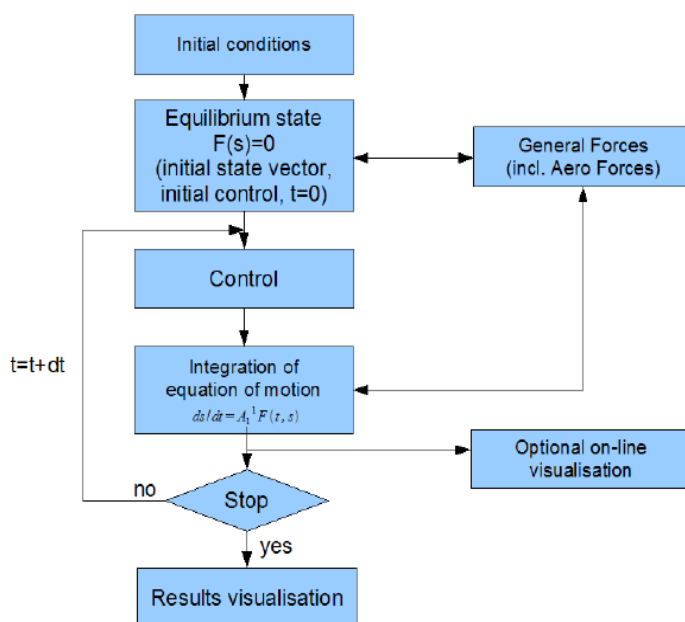


Fig. 10: Scheme of flight simulation (SimSAC 2009)

The SDSA tool also includes a flight control system, which consists of a human pilot model, a stability augmentation system, an actuators model and a stabilization system based on LQR method. A detailed description of the single tools can be found in the SDSA – Theoretical basis PDF (SimSAC 2009).

2.2.6 NeoCASS

NeoCass stands for Next generation Conceptual Aero-Structural Sizing Suit. It is the CEASIOM tool which deals with the implication of the aerodynamic forces. Static and dynamic loads are taken into account. The combination of computer related, analytical and semi-empirical methods allows a comprehensive aero- structural analysis. It includes aerodynamic, elastic and structural analysis from low to high speed. Also divergence and flutter analyses are possible. Moreover the identification of the beating of the wing can be done. Rigid and elastic airplanes can be examined. For that the aeroelastic models are linked with Tornado.

NeoCass includes the programmes GUESS and SMARTCAD. The data from the AcBuilder is given to the GUESS tool. It contains the geometrical and technical information that is needed for the structural model. Also the data of the Weight and Balance tool are implied, which is needed for a first estimation of the weight. A states.xml file has to be generated to identify the aircraft's conditions (Fig. 11).

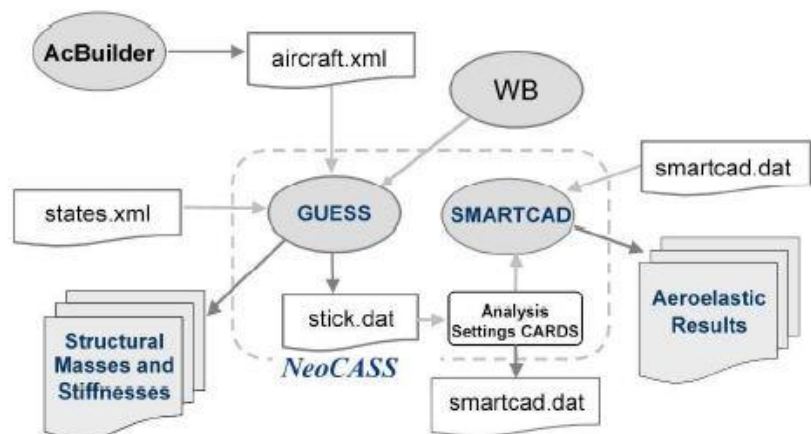


Fig. 11: NeoCASS (Cavagna 2009a)

GUESS represents a compromise between empirical and finite element methods. The load distribution concerning the geometry and aerodata serves as a base for the weight estimation. So the main components are loads and sizing. They are determinable by means of various manoeuvres. Additionally the FAR Part 25 criteria are incorporated.

The two main data for the structural sizing procedure are the geometry.xml file and the technology.xml file. Both data's contents are generated and linked within the AcBuilder. A description of the output file of the AcBuilder is given in chapter 2.2.1. As shown in Fig. 12 the geometry input file is important for the Geometry Module of GUESS. It is the base for the design weights, aerodynamics and the performance. The data of the Geometry

Module and the States input file are necessary for the Loads module. The states.xml file sets out the aircraft's conditions and the expected loads. An example for the states.xml format follows:

```
<?xml version="1.0"?>
<!-- Written on 26-Oct-2007 16:47:05 using the XML Toolbox for
Matlab -->
<root xml_tb_version="3.2.1" idx="1" type="struct" size="1 1">
  <machmin idx="1" type="double" size="1 1">0.1</machmin>
  <machmax idx="1" type="double" size="1 1">0.8</machmax>
  <alphamin idx="1" type="double" size="1 1">-5</alphamin>
  [...]
  <trim idx="1" type="struct" size="1 1">
    <alpha idx="1" type="double" size="1 1">4</alpha>
    [...]
  </trim>
</root>
```

α , M , β , the altitude, q , p , r , δ_e , δ_r and δ_a can be defined in their maximum and minimum values. Furthermore the trim conditions can be set.

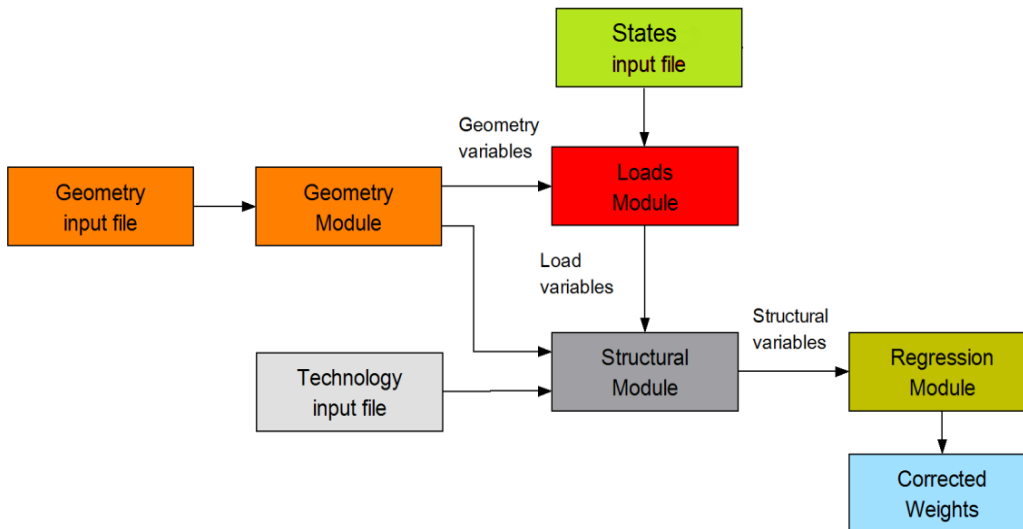


Fig. 12: GUESS (Cavagna 2009a)

At the Loads Module the loads for each component are computed. The fuselage analysis contains 3 types of loads. One type is the load resulting from the longitudinal acceleration which gets its data from the geometry.xml. Another is the tank and internal cabin pressure coming from the Weight and Balance tool and the defined pressure difference. Also the bending moment is taken into account. In this case the source is landing, tail down maneuvers, runway bump and quasi-static pull-up maneuvers. Out of these the longitudinal and circumference stress results are computed at each fuselage station along the fuselage length obtained by simulation. Furthermore, the loads of the lifting surfaces are determined by a quasi-static pull up maneuver and a fixable load factor. The load factor can be set within the AcBuilder in the technology tool. If the landing gear and the engines are located on the wings

they are considered by point loads. Also the inertia forces and the lift distribution are taken into account. The user can decide at the technology.xml whether it is a trapezoidal lift distribution or a lift distribution between an elliptical and trapezoidal shape. Based on this the lift load, centre of pressure, inertia load, centre of gravity, shear forces and bending moments are computed for each spanwise station along the elastic axis.

The loads of the horizontal tail are calculated by balanced maneuvers and maneuvers with uncontrolled elevator deflection. Required parameters are computed by a Vortex Lattice method or given as a minimum and maximum value in the geometry.xml. The correlation between the horizontal tail loads, the pitching moment and the stabilizer angle is assimilated in GUESS. For the calculation of the vertical tail loads pilot induced rudder maneuvers are used. The definition of the yawing moment is realized by asymmetrical thrust maneuvers.

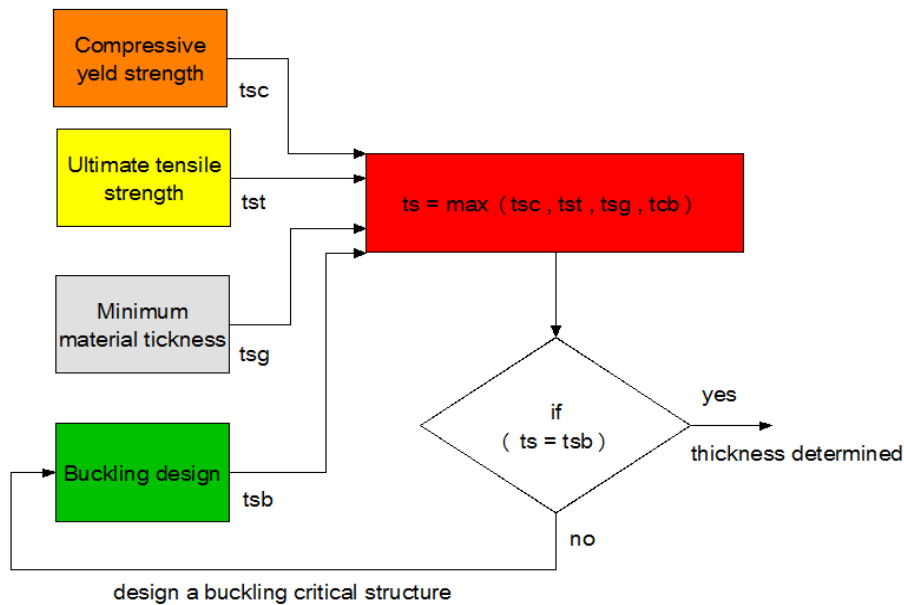


Fig. 13: Sizing tool (Cavagna 2009a)

Besides the technology input file, the results of the *Load Module* and the *Geometry Module* are important for the *Structural module*. Based on the technology.xml file different structure concepts can be chosen and defined previously. Also information about the density of the material and structural arrangement are given there. With the geometry conditions and the data of the *load Module* the minimum amount of structural material is determined. It is computed by a sizing tool. An iterative process leads to a new weight estimation. The process is depicted in Fig. 13.

With the help of the regression module a connection between the estimation of load carrying weight by GUESS, the actual weight of load bearing structure, the weight of primary structure and the total weight is defined by statistical analysis techniques. Two different applications have been developed. One the one hand, there is a linear regression equation. On the other hand, there is a power-intercept regression equation. The user can choose one of them. In the end a corrected weight is outputted by GUESS.

The output of GUESS is at the same time the input for SMARTCAD. So GUESS can be seen as a pre-processor of this aeroelastic tool. Present information become converted into an own database. Based on the input data, GUESS computes a mass distribution, generates a stick module using beam elements as well as an analytical mesh, determines stiffness distributions to define beam mechanical properties and writes an ASCII file for SMARTCAD.

SMARTCAD contains numeric aero-structural analysis based on simplified models such as a beam models and VLM/DLM aerodynamics. In this tool of NeoCass, the structure can be analysed. It also it includes stabilizer static analysis, linear buckling, vibration mode calculations and linearized flutter analysis. There are linear and non-linear static aeroelastic analysis and trimmed calculation for a free-flying rigid or deformable aircraft available. Additionally, steady and unsteady aerodynamic analysis to extract derivatives for flight mechanic applications can be done.

The basis for the structural analysis is a finite volume three node beam. The beam model consists of three nodes, at which the central node is automatically generated by the solver. The two outer nodes are defined by the AcBuilder on the technology tool and later processed by GUESS for the input of SMARTCAD. Because of the three reference points the plane of elasticity can be different from the centre of gravity (**Cavagna 2009a**). The linear static analysis is based on the state of stable equilibriums. Hence buckling phenomena can be calculated. The non linear structural solver uses follower forces to generate the results. Computational Structure Dynamics (CSD) is used to calculate the eigenvalues of the structure. Since no damping is taken into account the eigenvalue is a real value. It represents the natural frequencies, the frequency at which the structure naturally tends to vibrate. The associated eigenvector represents the mode shape, the modal shapes of the structure at a specific natural frequency. Natural frequencies and mode shapes are a function of the structural stiffness, inertia distribution and boundary conditions. They characterise the basic dynamic behaviour of the structure under small disturbances and are an indication of how the structure will respond to dynamic loads.

The aero mesh for the calculation of the aerodynamic loads is defined by the AcBuilder and given to the stick module. In SMARTCAD the Vortex Lattice Method (VLM) is used for subsonic steady aerodynamic and aeroelastic calculations. The VLM code of SMARTCAD is based on the Tornado tool, the theoretical background is described in chapter 0. The Doublet Lattice Method (DLM) is used for unsteady calculations and

is a collocation method for computing approximate solutions to the integral equation relating normalwash and aerodynamic loading for lifting surfaces oscillating harmonically in subsonic flow” (DaRonch 2007).

It is a standard method for aeroelasticity in aerospace industry and contains subsonic flutter analysis and harmonic stability derivatives prediction. Steady horseshoe vortices and oscillatory doublets along the bound vortex model the lifting surface.

At zero frequency, the doublet line corresponds to the horseshoe vortex. The vortices represent the steady-flow effects and the doublets represent the incremental effects of oscillatory motion.”(DaRonch 2007).

The doublet system can only be approximated, while the vortex system can be analysed exactly. The configuration is represented by small trapezoidal elements, which are arranged parallel to the free stream. Two edges of the trapezoidal are always in the direction of the free stream. Thus the whole surface is modeled. On each box a horseshoe vortex is placed in such a way the bound line corresponds with the quarter chord line of the box. On this way the steady flow is modeled. On the bound vortex a distribution of acceleration potential doublets of uniform strength, which have the steady-flow doublet strength subtracted, is overlaid. On this way the oscillatory increment is constituted. The control point of each box is centered spanwise on the three quarter line of the box. On this point the surface boundary condition is set up. Fig. 14 shows the general structure (DaRonch 2007).

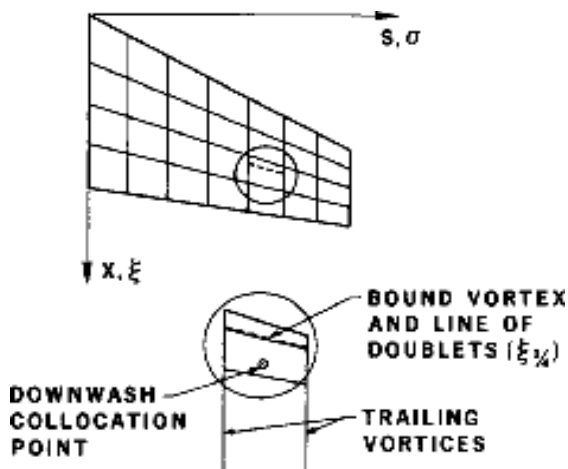


Fig. 14: DLM (DaRonch 2007)

To regard the aerodynamic load for structural belongings the finite volume three node beams are coupled with an aerodynamic lifting surface. SMARTCAD includes two spatial coupling methods. One is an innovating scheme based on mesh free Moving Least Square (MLS), the second is a Radial Basis Function (RBF) that couples the meshes. Both methods enable a data transfer between a non-matching structure and aerodynamic mesh. Also the conservation of moments and the energy transfer between the fluid and the structure is assured. The MLS and the RBF spatial coupling methods are suitable for complex configurations. The process of coupling the methods is supported by aero-nodes, which are generated by the solver.

2.2.7 FCSDT

The Flight Control System Designer Toolkit includes 5 modules.

- FCSA – Flight Control System Architecture
- SCAA – Stability & Control Analysers and Assessor
- LTIS – Linear Time Invariant Synthesis
- CLD – Control Laws Definition
- FSim – Desktop Flight Simulator

The input data of the new project is composed by data from Ceasiom, previously generated data, default data and results of other sub-codes. The interaction of the single sub-codes leads to the results and thus the output data of the FCSDT.

Under FCSA the architecture of the control systems is built up. The control system is the base for reliability analyses. On the one hand, the user can add redundancies (changing the architecture of the system) or the same architecture is used but the reliability of components forming it is increased. The FCSA tool also generates Excel sheets with the bill of material. Here all components and the number of each type are listed. Also the control surfaces that components have been used for are marked. As preparation for the subsequent tools SCAA and FSim and their failure mode study, the user can select different control surfaces and engines as failed components within FCSA. The input data can be taken from CEASIOM but it is not essential and the tool can stand on its own. Therefore under FCSDT>Defaults>DefaultFSCA>DefaultArchitectures input data for FSCA is given. This data is coded using Boolean algebra. For a closer look on this code, it is referred to in the paper FCSDT Manual_v22 (**Maheri 2008**). The results of the FCSA are given as files of the designed architecture, the bill of material and the failure mode. Also global live data for SCAA and FSim and graphical results are available.

The SCAA tool includes functionality to trim, linearising and simulating a Simulink built aircraft model. First the model is initialised, than the conditions are set for the trim and performance analyses. At last the trimming process and the simulation can be carried out.

The data from Simulink aircraft model, trim, linearisation and control system architecture is the base of the LTIS tool. In this tool flight control laws can be designed. Also the closed-loop system can be simulated and analysed. The theory behind the tool is accurately described in the paper FCSDT Manual_v22 chapter 5 (**Maheri 2008**).

The CLD module is based on the different aircraft control philosophies in various flight phases and maneuvers, built up by different parameters. It is possible to set and categorise the control laws and protections. An example for the structure and the contents of a design law is shown in Fig. 15.

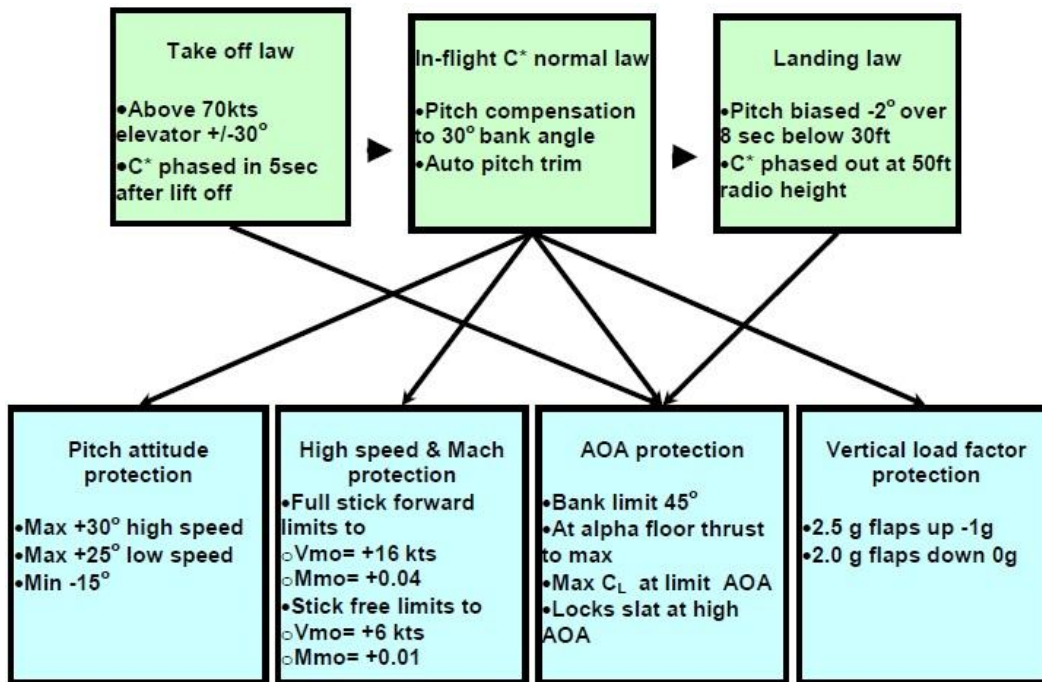


Fig. 15: Example - design law

FSim should be able to make a flight simulation according to the data from the FCSA tool.

3 Reference Aircraft A320 in CEASIOM

3.1 A320

The A320 family consists of short to medium range aircraft for commercial passenger transport. It includes the A318, A319 A320 and the A321. The A320 was the first version and first delivered in 1988. It is a narrow body low wing cantilever monoplane aircraft. It has a conventional tail with one fin. A three side drawing is seen in Fig. 16. For the familiarisation with CEASIOM the A320 – 210 is chosen as reference aircraft. This way the results of the single tools of CEASIOM can be assessed. Therefore several data is given. On the one hand, data from Airbus is given, on the other hand, the results of a PrADO calculation is used for a comparison. PrADO is a preliminary aircraft design and an optimisation program developed by the Institute of Aircraft design and Lightweight Structures of the TU Braunschweig. The program includes a set of design modules that iclude each significant discipline involved in the preliminary aircraft design process and gives detailed results of the weight (**Krammer 2010**). The A320 is additionally rebuilt with the Preliminary Sizing tool A-C from Prof. Scholz from HAW Hamburg to set the initial conditions. The initial conditions are the following, shown in Tab. 1.

Tab. 1: Initial conditions

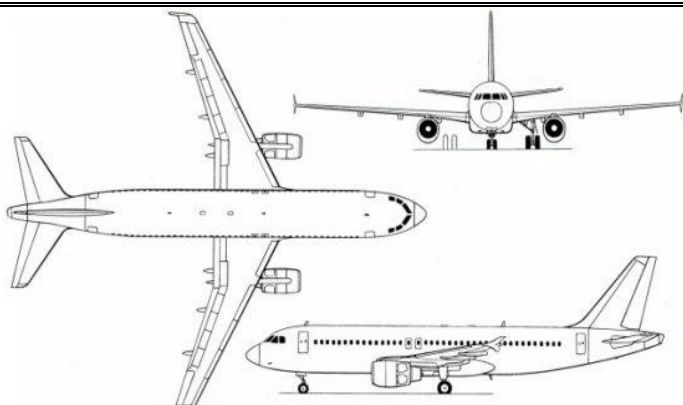
| conditions | values | three view drawing |
|-----------------------|-----------|--|
| A320 Version | A320 -210 |  |
| MTOW | 73 500 kg | |
| Engine | CFM56 | |
| Number of Passenger | 150 | |
| MPL | 20 000 kg | |
| Range at max. Payload | 1 500 NM | |
| Landing field length | 1 700 m | |

Fig. 16: Three view drawing A320 (**Aerospace 2010**)

The geometrical data that is used for the input in CEASIOM is the same that is used in the PrADO computation. All data are summarized in Appendix A.

3.2 A320 in AcBuilder

3.2.1 Implementation

The AcBuilder serves as visualisation of the geometry parameters and to set the boundary conditions for structure and aerodynamics. First of all, the components of the A320 have to be defined. A list of parameters has to be completed for each component. The data of the A320 which is taken for the parameters can be looked up in Appendix A. All input parameters for the AcBuilder are summarized there. Subsequently just a few parameters are singled out for a closer look, mainly those on which difficulties can appear.

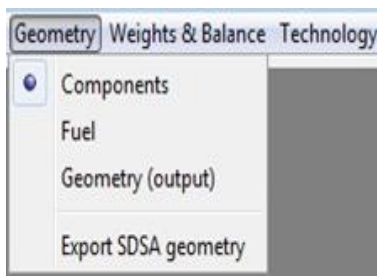


Fig. 17: Toolbar - Geometry

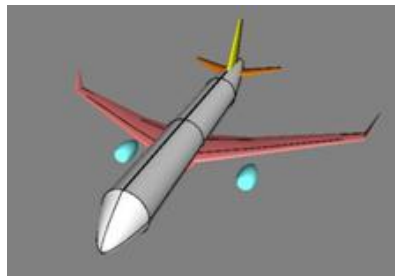


Fig. 18: Geometrical visualization

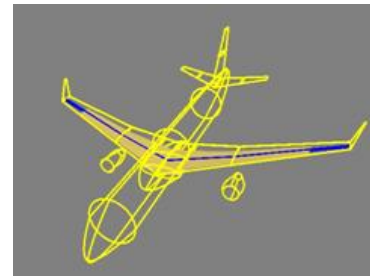


Fig. 19: Fuel visualization

Under *Geometry* the parameters for the components and the fuel are set (cf. Fig. 17). The explanations of the parameters which must be inserted at the AcBuilder are described in the paper CEASIOM XML File Definition by Andres Puelles (**Puelles 2010**). The visualisation of the geometry is pictured in Fig. 18. Fig. 19 shows a picture of the tanks. Afterwards the reference values are computed by choosing the option *Geometry (output)*. They can be output for the wing, the horizontal tail and the vertical tail. In chapter 26 the output is discussed.

One closer look at the identification number of the Layout and configuration of the engine shows, that in case of the A320 *0* has to be chosen. That stands for “slung in vicinity of the wing” (**Puelles 2010**). Here the *z* coordinate of the engine is computed by the program and cannot be added by the user. That is just possible for the identification numbers from 3 till 5. But then the engine is attached at the fuselage and not on the wing.

Another particular component is the airfoil of the lifting surfaces. In chapter 2.2.1 the implementation of a new airfoil is already discussed. For the present example the airfoil SC(2) – 0612 is taken for the wing.

Closer attention lies also on the winglets. It is only feasible to build up the winglet above the wing and not in two directions. The available model of the A320 from PRADO is computed with winglets oriented above and below the wing (cf. Fig. 20). As this is not possible a comparable winglet was created, leaned on the winglet of a newer version from the A320 winglet seen in Fig. 21. The inserted values are listed in Tab. 2.



Fig. 20: Winglet A320
(Harris 2010)



Fig. 21: Winglet A320 new version
(DWS aviation 2010)

Tab. 2: Winglet parameters

| parameter | value | parameter | value |
|-------------|----------|----------------|-------|
| Span | 1.1098 m | Cant angle | 60° |
| Taper ratio | 0.2 | Root incidence | 0° |
| LE sweep | 66° | Tip incidence | 0° |

Furthermore the definition of the cant angle is different to the description in the tutorial of the *.xml file. A short illustration is shown in Fig. 22. Data transmission to other tools is without any problems. Also it is not possible to pick a value of 90°. Otherwise the winglet grows infinitely.

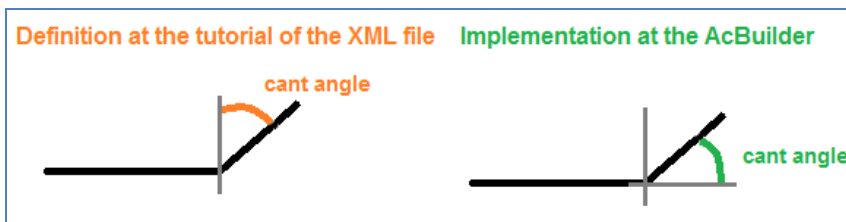


Fig. 22: Cant angle definition

Another little discrepancy appears at the parameter *Rudder.limit_deflection*. Here the user can only set a value between 0 and 1, but no ratio is asked for but an angle. To adjust this parameter the *.xml file was modified directly in the script with an editor and then given back to the AcBuilder. Thus 30° can be set for the limit deflection of the rudder.

The next part of the AcBuilder that is worked on is the *Weights & Balance* tool. Here the mandatory parameters and the values of the miscellaneous are set. An example of the visualisation of the weight and balance module is shown in Fig. 23. The input data is listed in Appendix A.

Optionally, the system weights can be added. In the present case only the landing gear's weight was added. By adding other system weight parameters some difficulties with the interface can appear. One set card automatically transmits the input data of one line to the next set card in the same line (e.g. *System weights (optional1)* to *System weights (optional 2)*). To avoid this problem it is better to insert these values directly into the *.xml file with an editor, if this application is needed.

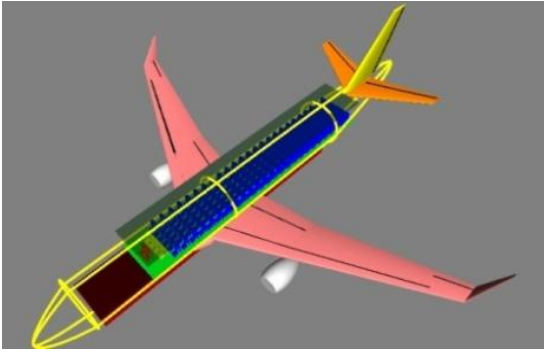


Fig. 23: Visualisation of the Weight & Balance tool

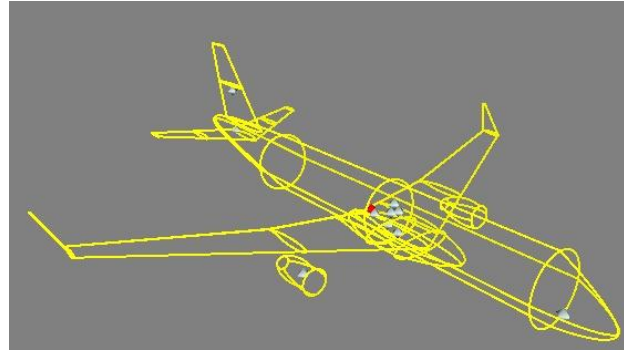


Fig. 24: Visualisation of the Centres of gravity

The computation of the weight and the single components takes place by running the option *centres of gravity*. Also the location of the centres of gravity (COG) can be out-putted and pictured (see Fig. 24). After that, the user should choose the option *Weight and Balance* again. That leads to the calculated MTOW of the A320 under the set card *System weights (optional 2)*. A detailed report is written in the Matlab command window. Here the single iteration steps can be reproduced.

The calculation of the COG of the engine is incorrect and so is the COG of the whole aircraft. Therefore a new patch, created by CFSEngineering, was implemented under CEASIOM 100-v2.0. This patch is available on the CEASIOM homepage and leads to correct results. The results are discussed in chapter 0.

After the right centres of gravities are worked out, the technology input can be checked. Under this topic supporting points of the structural and aero mesh are defined. Care must be taken to ensure that there is an even distribution. Otherwise problems can occur during the computation in NeoCASS. The display of the single distributions is seen in Fig. 25 and Fig. 26. Under *technology* also the material properties and the spar location are set. The input data can be looked up in Appendix A. Furthermore the parameters for loading, analysis and experienced values can be defined. For the A320 the default values are retained.

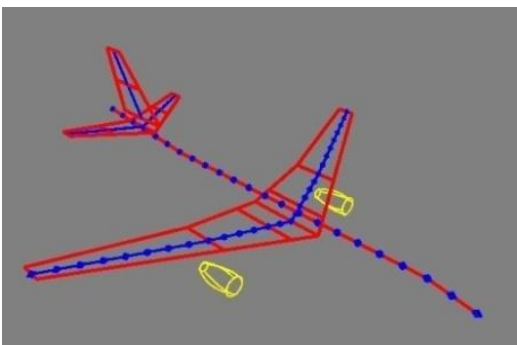


Fig. 25: Structural mesh

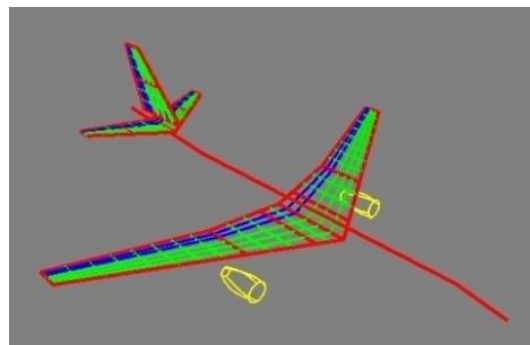


Fig. 26: Aero mesh

3.2.2 Evaluation of the Results of AcBuilder

The first output that is given by AcBuilder is the geometry output shown in Fig. 27. Here the reference data is given. These values are used for the later calculations. A sample is done with c_{MAC} . For comparison, this value is recalculated due following equations (Scholz 1999):

| Geometry (output) | | |
|-------------------------|------|----------|
| Reference wing | | |
| Horizontal tail | | |
| Vertical tail | | |
| Canard | | |
| Parameters | | |
| Parameter | Unit | Value |
| taper_ratio | | 0,28162 |
| planform_AR | | 9,59 |
| Weighted_area | m^2 | 119,9262 |
| LE_sweep | deg. | 27,418 |
| MAC | m | 3,9066 |
| relative_apex | | 0,3134 |
| Orig_root_chrd_at_ac_CL | | 6,3124 |
| Half_chord_sweep | deg. | 21,8928 |
| Quarter_chord_sweep | deg. | 24,7166 |
| non_dim_MAC_y_bar | | 0,40658 |
| Weighted_aspect_ratio | | 9,59 |
| mean_thickness | | 0,1 |

Fig. 27: Geometry output AcBuilder

$$c_{MAC, dpT} = \frac{c_{MAC_i} \cdot S_i + c_{MAC_o} \cdot S_o}{S} \quad (3.1)$$

$$c_{MAC} = \frac{2}{3} c_r \frac{1+\lambda+\lambda^2}{1+\lambda} \quad (3.1.1)$$

$$S = \frac{b}{2} c_r (1 + \lambda) \quad (3.1.2)$$

With

$$\lambda_i = 0,6186 \quad c_{ri} = 6,32 \text{ m}$$

$$\lambda_o = 0,2462 \quad c_{ro} = 3,90 \text{ m}$$

$$S_i = 64,8 \text{ m}^2 \quad c_{MAC_i} = 5,01 \text{ m}$$

$$S_o = 51,6 \text{ m}^2 \quad c_{MAC_o} = 2,73 \text{ m}$$

$$S = 116,4 \text{ m}^2 \quad \underline{c_{MAC} = 3,99 \text{ m}}$$

The deviation of c_{MAC} is about 2,7 % , the difference of the weighted area about 3% and therefore acceptable. The wing area S is different from the input area of 122,4 m². The reason, is that the area that is inside of the fuselage is not taken into account and thus smaller. The differences to CEASIOM are explainable with calculating the c_{MAC} on simplified equations, since the AcBuilder refers to the exact geometry and the exact derivatives of the values.

The next examination deals with the estimation of the weights. For this purpose the output of AcBuilder is compared with the results of a given PrADO (Prado 2010) calculation and data that is given by Airbus (Airbus 2003). In PrADO also the results for the single components are given. The Airbus data just includes the weight of the whole aircraft. The weights of the single components are implied in the thesis of Eurico J. Fernandes da Moura (Moura 2001). Here the deviations to the results of Torenbeek and data from Airbus are given for the wing, the fuselage the horizontal tail, the vertical tail and the landing gear. In the AcBuilder different models are calculated. In the end variant V3 is the one, that gives the best results. In Appendix A the comparison of all computations can be found. Moreover a short description of the single cases is given. In Tab. 3 the values of the V3 calculation, the Airbus data and the Prado results are summarized. It is obvious that the results of PrADO are very close to the Airbus data. With regard to the MTOW the AcBuilder results also match very well. But,

putting the focus on the results for maximum payload and fuel weight big differences appear and thus the OEW computed by the AcBuilder differs to the OEW of PrADO and Airbus. Finally, the OEW plus the payload plus the fuel result the MTOW. On the current version of AcBuilder the payload and fuel weight can be modified only in the *.xml file. In the future version which should appear soon, there will be a new interface for weight estimation.

Tab. 3: Weights of the A320

| | Weights in kg | | | Comparison in % | |
|----------------------|------------------|-------|-------|-----------------|-------------|
| | Airbus | PrADO | V3 | V3 - PrADO | V3 - Airbus |
| MTOW | 73500 | 73500 | 73397 | -0,14 | -0,14 |
| OEW | 40530 | 41000 | 48123 | 17,37 | 18,73 |
| max zero fuel weight | 60500 | 60188 | 63434 | 5,39 | 4,85 |
| max. payload | 20000 | 19099 | 15310 | -19,84 | -23,45 |
| GMEW | | 36230 | 40987 | 13,13 | |
| Landing gear | 2347 | 2547 | 3116 | 22,34 | 32,76 |
| Wing weight | 6279 | 8297 | 8766 | 5,65 | 40,61 |
| HT weight | 670 | 590 | 844 | 43,05 | 25,97 |
| VT weight | 464 | 434 | 490 | 12,90 | 5,60 |
| Fuselage weight | 9267 | 9119 | 7207 | -20,97 | -22,23 |
| Engine group | | 7822 | 9235 | 18,06 | |
| fuel | 12500 | 13312 | 9963 | -25,16 | -20,30 |
| | Strong deviation | | | | |

The landing gear weight was an input data. Nevertheless it was recalculated by the AcBuilder tool and is now 22% higher than the PrADO result and 33% higher than the value given by Airbus. Because of that phenomenon the model V3 was computed again without including the weight of the landing gear. The new model is called V3_b. The results are summarised and compared in Tab. 4.

Tab. 4: AcBuilder V3_b

| | Models | | | Comparison | |
|----------------------|--------|-------|--------|-------------|----------|
| | V3 | PrADO | V3 - B | V3B - Prado | V3B - V3 |
| MTOW | 73397 | 73500 | 73449 | -0,07 | 0,07 |
| OEW | 48123 | 41000 | 45485 | 10,94 | -5,48 |
| max zero fuel weight | 63434 | 60188 | 63486 | 5,48 | 0,08 |
| max. payload | 15310 | 19099 | 18000 | -5,75 | 17,57 |
| GMEW | 40987 | 36230 | 38350 | 5,85 | -6,43 |
| Landinggear | 3116 | 2547 | 3118 | 22,42 | 0,06 |
| Wing weight | 8766 | 8297 | 8771 | 5,71 | 0,06 |
| HT weight | 844 | 590 | 844 | 43,05 | 0,00 |
| VT weight | 490 | 434 | 490 | 12,90 | 0,00 |
| Fuselage weight | 7207 | 9119 | 7210 | -20,93 | 0,04 |
| Engine group | 9235 | 7822 | 9241 | 18,14 | 0,06 |
| fuel | 9963 | 13312 | 9963 | -25,16 | 0,00 |

In Tab. 4 it is obvious that the change of the landing gear input has no effect on the single components, but the weight of the payload could be adapted better and consequently, the OEW and GMEW fit better. The discrepancies regarding to the single components can be explained by the more precise material description in PrADO. The weight estimation of AcBuilder is based on Torenbeek. The deviations to the Airbus data are nearly the same. In the thesis of Moura the results calculated by Torenbeek have a deviation of -20,6% for the fuselage, 22,7% for the horizontal tail and 5,16% for the vertical tail (**Moura 2001, Moura 2000**). The deviations of the AcBuilder are nearly the same (Tab. 3). On which way the AcBuilder estimates the weight for the wing and the landing gear is not comprehensible.

For the calculations in the following tools the MTOW is the important measure and so the output of the V3 can be used in the later tools. Only in NeoCASS the input has to be proven more exact.

The AcBuilder keeps the opportunity to show the results of the x_{cg} 's for each component. These values are compared with estimated x_{cg} 's. The estimation is based on lecture notes of aircraft design at the HAW Hamburg (**Scholz 1999**). The x_{cg} of the whole structure is based on the x_{cg} of the components and the according weights m_i . The following equations are used:

$$\begin{aligned}
 \text{Fuselage:} & \quad x_{cgF} = 0,42 - 0,45 \cdot \text{fuselage length} \\
 \text{Horizontal tail:} & \quad x_{cgHT} = 0,4 \cdot \text{cord length (root HT)} \\
 \text{Vertical tail:} & \quad x_{cgVT} = 0,4 \cdot \text{cord length (root VT)} \\
 \text{Wing:} & \quad x_{cgW} = 0,4 \cdot \text{cord length (root Wing)} \\
 \text{Engines:} & \quad x_{cgE} = 0,4 \cdot \text{engine length}
 \end{aligned}$$

$$x_{cgStructure} = \frac{\sum x_i \cdot m_i}{\sum m_i} \quad (3.2)$$

The x_i values result from the location of the component and the according x_{cg} . The bases of the estimation are the weights of the Prado calculation. The results are summarized in Tab. 5.

| Values | | |
|-----------|------|-------------|
| Parameter | Unit | Value |
| x | m | 15,2827246 |
| y | m | 0,0 |
| z | m | -0,86782937 |

Fig. 28: Center of gravity – structure

Tab. 5: Centre of gravity

| Components | Ceasiom | estimated | deviation |
|-------------------------|---------|----------------------------|-----------|
| X cg of fuselage | 16,85 m | 15,78 m – <u>16,9 m</u> | - 0,30 % |
| X cg of horizontal tail | 33,80 m | 32,32 m | 4,58 % |
| X cg of vertical tail | 34,00 m | 32,10 m | 5,92 % |
| X cg of wing | 16,56 m | 16,19 m | 2,29 % |
| X cg of engines | 14,72 m | 14,41 m | 2,51 % |
| X cg of structure | 15,28 m | 16,53 m | -7,56 % |
| X cg of total aircraft | 16,85 m | 16,53 m | 1,9 % |

The results of the CEASIOM computation and the estimation due to statistical values differ no more than 10 %. It is noticeable that the CEASIOM values for the single components are smaller than the estimated one. But the x_{cg} of the total structure is smaller than the x_{cg} calculated by hand. One reason is that the weights of the single components are different. Moreover, the systems are not taken into account. Considering the x_{cg} of the total aircraft the values approximate. The reason for that can be that CEASIOM includes the flight system and the miscellaneous separately. For the estimation by equations the effects of these components are already considered. Finally, the CEASIOM results are more precise because they are based on the underlying geometry.

3.2.3 Discussion on the Practicability of AcBuilder

The handling of the AcBuilder is comprehensible and all functions are well structured. Unfortunately some problems appear when entering values and discrepancies show up after the transmission of the data to the *.xml file. But with every new version the problems decrease. Currently, the estimation of the weights is inaccurate but this problem will be rectified in the near future.

3.3 A320 in SUMO

3.3.1 Implementation

To generate a surface mesh or a volume mesh, a finer geometry rendering than given by the AcBuilder is necessary. Therefore the *.xml file of the A320 from the AcBuilder is imported in SUMO. The file serves as a basis to refine the geometry. In Fig. 29 the GUI of SUMO is shown. Under the field *Entity* the single components are listed. A right mouse click gives the possibility to delete or edit the geometry parameters. A left click on the components shows the sub-items of the components and the according parameters that can be modified. The user can also add new body or wing components by choosing the corresponding button in the task bar (see Fig. 29).

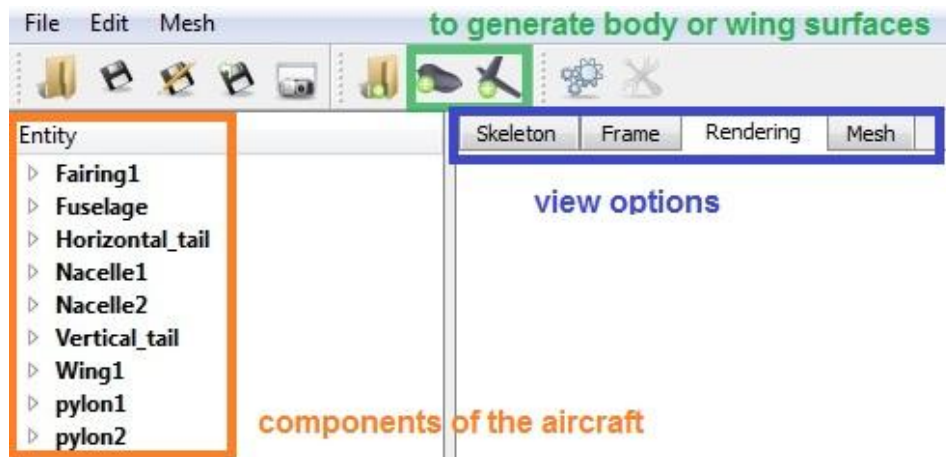


Fig. 29: GUI of SUMO

The design of the fuselage from the AcBuilder is very simple. To get better results in the subsequent calculations of EDGE Euler, the fuselage is rebuilt. But in this case the modification is not done with the help of the GUI of SUMO, but by change the *.smx file. In the first step the whole assembly is saved as an *.smx file in SUMO. Then the geometrical data in a more precise description is taken from the PRADO output. This data replaces the data of the A320 fuselage in the *.smx file. After saving this version with the new fuselage data, the *.smx file can be opened in SUMO. Under the view option Skeleton the frames and their location are pictured (see at Fig. 30). Still they can be modified in SUMO by editing the parameters or by moving the red points or the green squares with the mouse.

For the A320 also the fairing and the pylons were changed in SUMO just by combining the modification of the frames by hand and through the parameters. Furthermore the winglets were added.

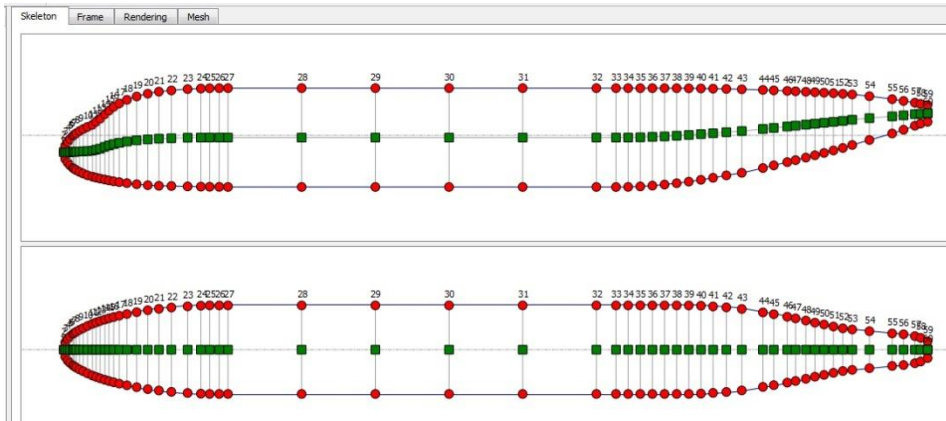


Fig. 30: Skeleton of the fuselage

In SUMO a special function is implemented which detected winglets automatically. In this case the coordinates of the winglet and its chord length can be added behind the wingtip and the surface is built by SUMO. Using this function the winglet can only be build up in one direction. In case of the A320 this variant is chosen. It is also possible to create a new wing and link it to the wing of the aircraft with the help of a body surface. Thereby any desired shape can be realized.

After refining the input data based on the *.xml file from the AcBuilder, the A320 is visualized in SUMO as shown in Fig. 31. The view can be changed with the help of the mouse. It can be rotated around the axis with the left mouse button. For zooming in/out the scroll wheel can be used. It is also possible to hold the middle button of the mouse and scroll back or forth. For sliding the view to the left, to the right, up or low, the right mouse bottom should be pushed.

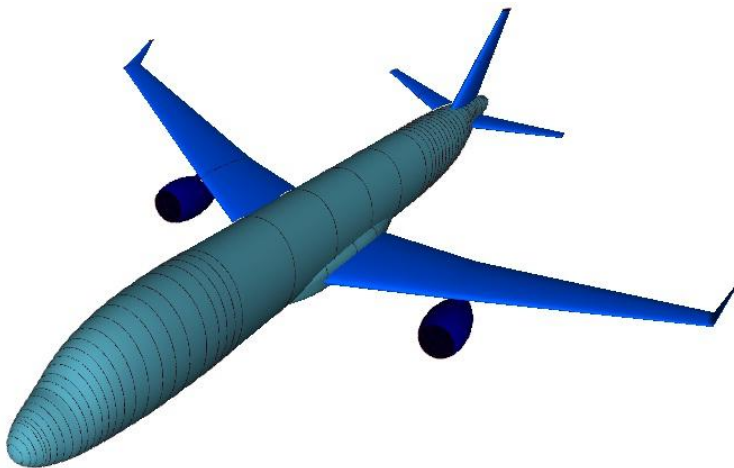


Fig. 31: Rendering of the A320

SUMO includes the possibility to check or change the control surfaces. Under *Edit* → *Edit control system* Aileron, Flaps, Elevator and Rudder are shown. The GUI gives the possibility to change the paramters and the display of the aircraft simplifies the check on the geometry of the single control surfaces (Fig. 32). It is advisable to take a closer look at the flaps and ailerons, because sometimes at this point the data from the *.xml file is processed in the wrong way and should be reworked.

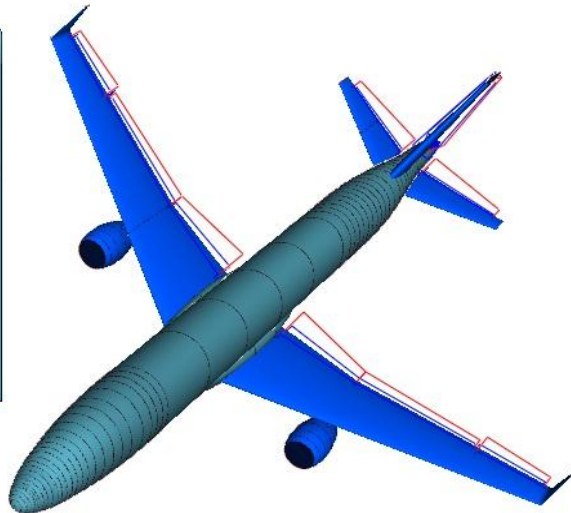
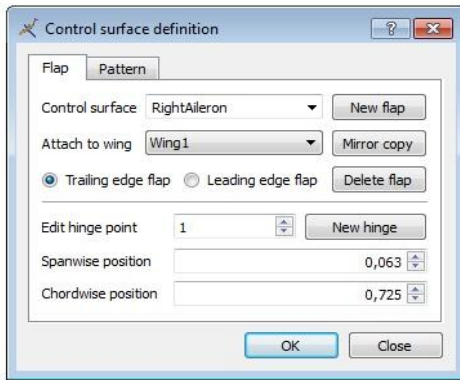


Fig. 32: Control surface definition in SUMO

Also the engine characteristics can be reworked. Selecting *Edit* → *Edit engine properties* several parameters can be defined. For example the intake region and the nozzle region can be selected. Also the user can decide whether he specifies the engine through a turbofan model and the reference mass flow or directly through the normal flow velocities. The Turbofan model on its own can be defined on parameters like By-pass ratio, turbine temperature, total pressure ratio and so on. If the user wants to create a new nacelle, he has to open the path *Edit* → *Edit nacelle geometry*. There the geometry parameters can be added.

After the modification of the geometry is finished, it should be double-checked if all surfaces are closed and the transition between the single components is not too sharp-edged. Otherwise there can be problems in generating the meshes.

To generate the surface mesh the maximum stretch ratio, the normal angle tolerance and the number of iterations has to be set. The stretch ratio can be set between 3 and 99. For the A320 model the default value 9 is taken. The normal angle tolerance is also left at 15° . The number of iterations can set from 0 to 9. In this example it was changed to 1. Apart from that the default settings are used. The surface mesh based on this data is shown in Fig. 33 and saved as *surface_mesh1.msh*. It is the basis for the volume mesh. The details of the surface mesh are shown after the calculation and listed in Tab. 6.

Tab. 6: Details of the surface mesh

| parameter | value |
|-------------|-------------------------|
| Triangles | 145 544 |
| Vertices | 72 774 |
| Wetted area | 732.279 m ² |
| Volume | 1 175.13 m ³ |

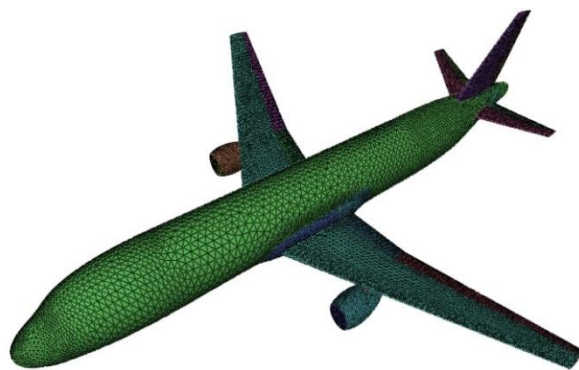


Fig. 33: Surface mesh of the A320

Before SUMO computes the volume mesh the farfield radius, the refinement and Tet radius / edge ratio have to be determined. That implies the maximum volume of the tetrahedral and the number of nodes, boundary triangles and tetrahedral. A picture of the volume mesh vol_mesh3.bmsh is shown in Fig. 34.

Four volume meshes are generated to make a convergence analysis in AMB with Edge Euler. The characteristics of these four meshes are shown in Tab. 7.

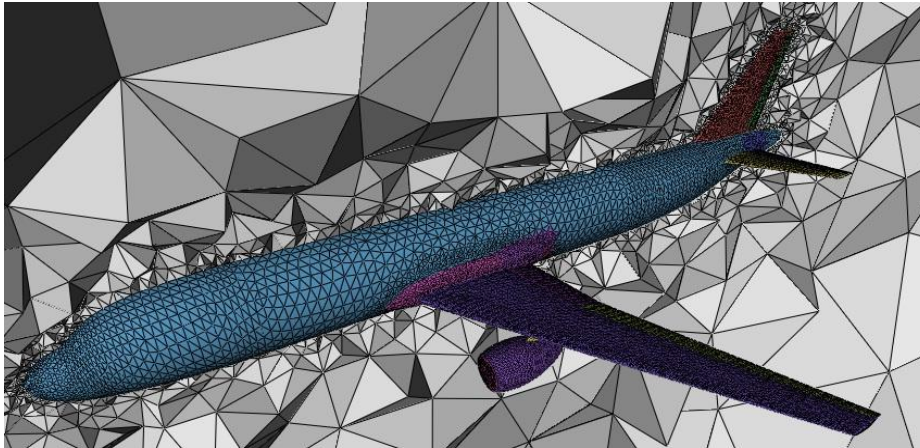


Fig. 34: Volume mesh of the A320- refinement 3

By computing the volume mesh, automatically a boundary mesh in *.aboc format is generated. This is needed later at the AMB as well.

Tab. 7: Data of the volume mesh

| Name of the file | Vol_mesh3.bmsh | Vol_mesh4.bmsh | Vol_mesh5.bmsh | Vol_mesh6.bmsh |
|-----------------------|----------------|----------------|----------------|----------------|
| Farfield radius | 218.12 | 218.12 | 218.12 | 218.12 |
| refinement | 3 | 4 | 5 | 6 |
| Tet Radius/edge ratio | 1.4 | 1.4 | 1.4 | 1.4 |
| Max. volume | 5219 | 652 | 82 | 10.2 |
| Boundary triangles | 220 848 | 224 696 | 240 046 | 301 550 |
| nodes | 228 322 | 245 071 | 378 990 | 1 461 786 |
| Tetrahedral | 1 083 910 | 1 184 920 | 2 022 104 | 8 896 842 |

3.3.2 Discussion on the Practicability of SUMO

Sumo is a well structured tool that has a clearly arranged user interface. During the work problems appear rarely. During some calculations the program crashes what could be led back to the computing power of the PC. Otherwise the tool gives good results which could be used in the following process without objection.

3.4 A320 in AMB

3.4.1 Implementation

The output file of the AcBuilder is the input file for the AMB. After opening the input file, on the left side of the window a three view drawing of the A320 shows up. Here the aircraft is pictured in a very simple way where only the proportions and configuration can be checked (Fig. 35). On the right of this drawing the Edit-Plot is located.

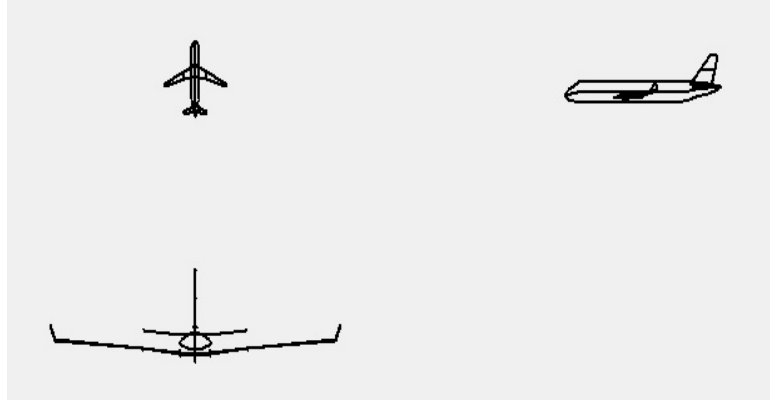
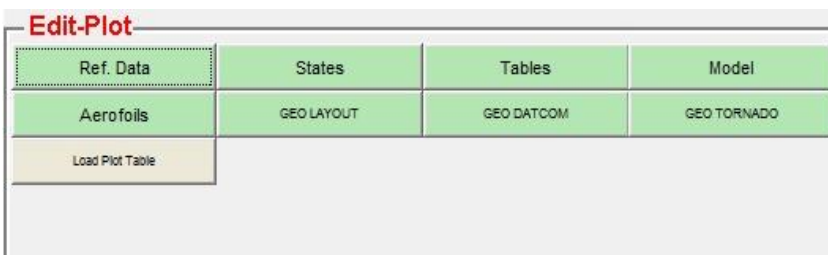


Fig. 35: Three view drawing



The Edit-Plot consists of 9 blocks. The first block *Ref. Data* refers to the input data and shows the important values (Fig. 36).

Fig. 36: Edit Plot

The second button is called: *states*. Here the range of the parameters (α , M , β , q , p , r , δ_e , δ_r or δ_a) can be appointed. Also the number of supporting points can be defined and so the aerodynamic table is built up (cf. 2.2.3.). Fig. 37 shows the states taken for the A320. To check the tables the third item: *Tables* is given. Here the table resulting from the states appears (Fig. 38).

| Parameter | Units | Min Value | Max Value | N Values |
|------------|-------|-----------|-----------|----------|
| AoA | Deg | -5 | 15 | 21 |
| Beta | Deg | -6 | 6 | 8 |
| Mach | | 0.1000 | 0.6000 | 6 |
| Elev. | Deg | -15 | 15 | 8 |
| Ail | Deg | -15 | 15 | 8 |
| Rud | Deg | -15 | 15 | 8 |
| Pitch Rate | Deg/s | -80 | 80 | 8 |
| Roll Rate | Deg/s | -80 | 80 | 8 |
| Yaw Rate | Deg/s | -80 | 80 | 8 |

Fig. 37: States AMB

| Parameter | | | | | |
|------------|--------|----------|---------|---------|------------|
| AoA | -5 | -4 | -3 | -2 | -1 ... |
| Beta | -6 | -4.5000 | -3 | -1.5000 | 1.5000 ... |
| Mach | 0.1000 | 0.2000 | 0.3000 | 0.4000 | 0.5000 ... |
| Ele. | -15 | -11.2500 | -7.5000 | -3.7500 | 3.7500 ... |
| Ail. | -15 | -11.2500 | -7.5000 | -3.7500 | 3.7500 ... |
| Rud. | -15 | -11.2500 | -7.5000 | -3.7500 | 3.7500 ... |
| Pitch Rate | -80 | -60 | -40 | -20 | 20 ... |
| Roll Rate | -80 | -60 | -40 | -20 | 20 ... |
| Yaw Rate | -80 | -60 | -40 | -20 | 20 ... |

Fig. 38: Tables AMB

When picking the button *Model*, the flight dynamic model can be chosen. Here 6 degrees of freedom or 3 degrees of freedom are given. Furthermore the user has to decide if the aircraft is symmetrically built up. The A320 is a symmetrical plane and for flight dynamics 6 degrees

of freedom are chosen. Successively the airfoil definition of the single parts can be changed under *Airfoils*. The airfoil can be chosen for each intersection (root, kink tip). Pressing *GEO LAYOUT* updates the model on the left side. After that the user has to run *GEO DATCOM*. A 3D view of the model appears and the data is prepared for *DATCOM*. Following that, the data is generated for Tornado. Running *GEO TORNADO* prepares the data for the calculation with Tornado. Four figures, representing the Tornado geometry layout, will be displayed. Two examples are shown in Fig. 39 and Fig. 40. Now all eight fields should be coloured green (cf. Fig. 36).

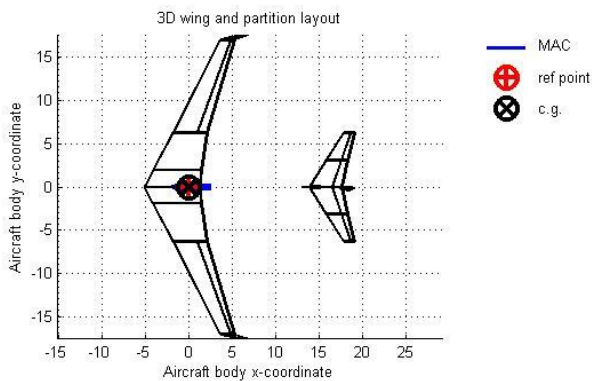


Fig. 39: Tornado 3D wing and partition layout

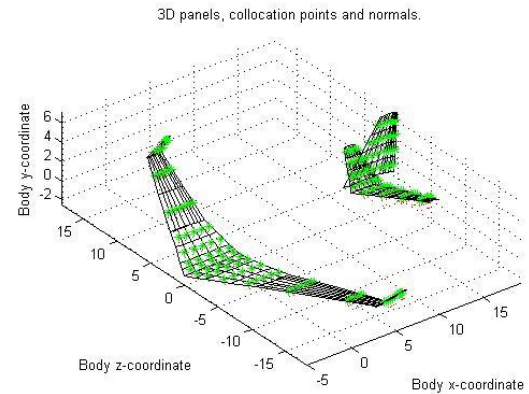


Fig. 40: Tornado 3D panels, collocation points and normals

Subsequently the user can focus on the solver (Fig. 41).



Fig. 41: Solver AMB

In the Datcom solver the type of the flaps has to be selected. For the A320 the flap of the elevator is a plain flap and the rudder flap is a plain flap. The results of the calculation of Datcom can be presented with the help of the desktop under the three-view-drawing (Fig. 42). Here it can be decided which result should be plotted.

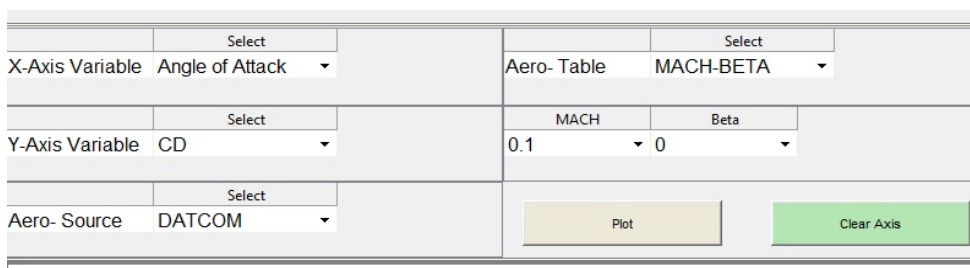


Fig. 42: Output of results

The parameters can be combined in different ways.

Selecting the potential solver leads to a Tornado calculation. First the numbers of panels in x, y direction and for flaps have to be fixed (example A320: all 5). Besides it can be selected if there are compressibility and viscous effects (example A320: both 0). In view of the calculation different possibilities are given. On the one hand, there is a *single simulation*. The user has to define a special case. In the example the incidence angle is about 5° , the Mach number 0.6 and β , q , p , r , δe , δr , δa are zero. At the end of the calculation a picture of the delta cp distribution is shown. The other results can be checked in the Matlab windows. The next option is a calculation called *Sweep Angle of Attack*. Here different states with three parameters can be chosen. One possibility is to select alpha, Mach and beta. Then Mach and beta have to be defined. After the calculation the results can be plotted in the AMB. The third facility is a Brute-Force-Calculation. In this case all feasible combinations are calculated. With this calculation the computing takes some time. The disadvantage is that the time that is needed for the calculation is not given. In the present case the calculation takes about 30 hours. This time frame depends on the computer and its computing power. The results of Tornado can be illustrated at the AMB in the same way as the results of DATCOM.

The Edge Euler Solver needs an input file from SUMO. A *.bmesh file for the volume mesh and a *.aboc file for the boundary conditions should be available. First, the type of analysis has to be selected. There are three possibilities. The user can select a single simulation for a specific Mach number, a particular angle of attack and a single side slip angle. Moreover a control surface analysis can be taken into account. The second choice is called Read *Samples*; here a table has to be generated that can be read by the AMB. In this table the special cases of the computation can be defined. The third analysis type gives the opportunity to run a calculation with a sampling of all possible combination of the Mach number, angle of attack and elevator deflection.

In the current example of the A320 several single simulations are done. From an AoA of -5° to an AoA 10° at a side slip angle of 0° and a Mach number of 0,75 the calculation is run. In this way a graph of CL over AoA can be produced. Additionally a grid convergence study is done for four meshes, to prove the quality of the mesh produced by SUMO. This study is for an AoA of 0° , at Mach number 0,75 and a sideslip angle of 0° .

3.4.2 Evaluation of the Results of AMB

To evaluate the results of the AMB, first of all a simple method was taken to compare CL over the Angle of Attack. The basic equation is (Schulz 2007):

$$C_L = \frac{dC_L}{d\alpha} \cdot (\alpha - \alpha_0) \quad (3.3)$$

it is

$$\frac{dC_L}{d\alpha} = 2\pi \cdot \frac{\Lambda}{\Lambda+2} = 5,81 \quad (3.3.1)$$

for an elliptical lift distribution and $\alpha_0 = -4,0^\circ = -0,08 \text{ rad}$; $\Lambda = 9,4$.

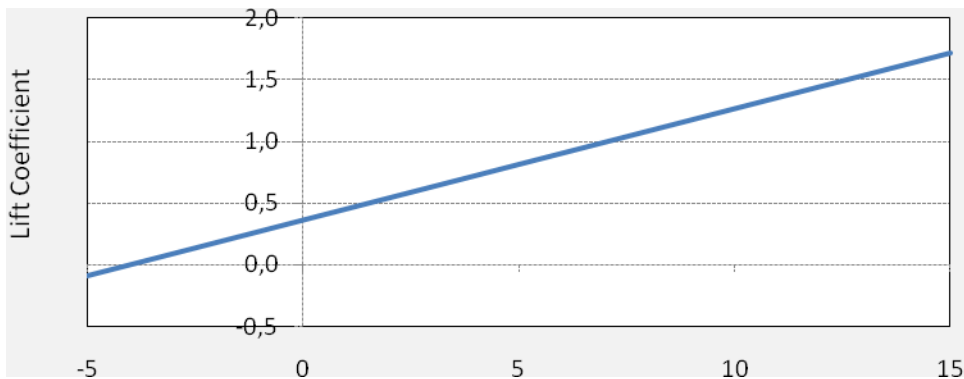


Fig. 43: Results calculated on equations

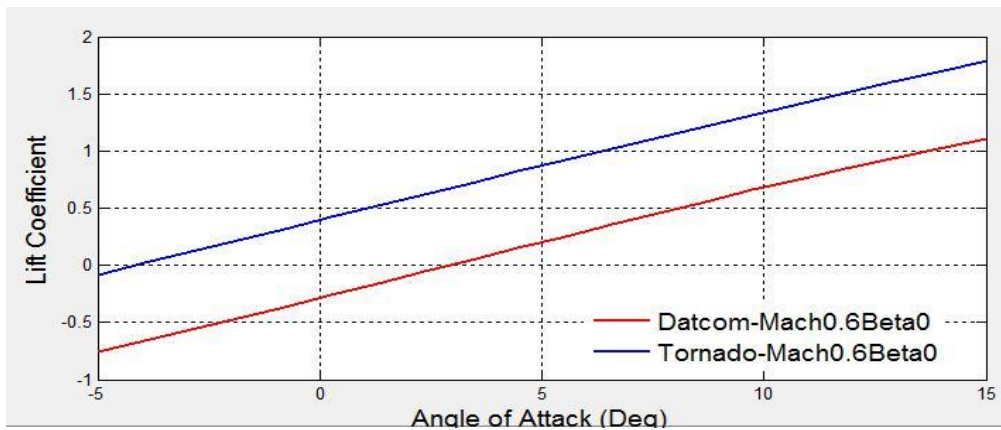


Fig. 44: Results C_L over AoA Tornado and DATCOM

In Fig. 43 the results of the simple method are depicted, Fig. 44 shows the results of Tornado and DATCOM. It is evident that the Tornado result fits with the result calculated in the equations. The DATCOM result deviates from the other calculations. Normally it is understandable that the DATCOM output is more imprecise than the Tornado calculation, but here it gives results that are worse than the results of a simplified calculation. Furthermore α_0 is at 3° which is also unrealistic. The reason for that can be the choice of the airfoil. It is no NACA airfoil and so eventually the library of Digital DATCOM, where the calculation falls back to, includes no fitting data for this airfoil. When using the NACA 4412 the deviates of Tornado and DATCOM are small (see Fig. 45).

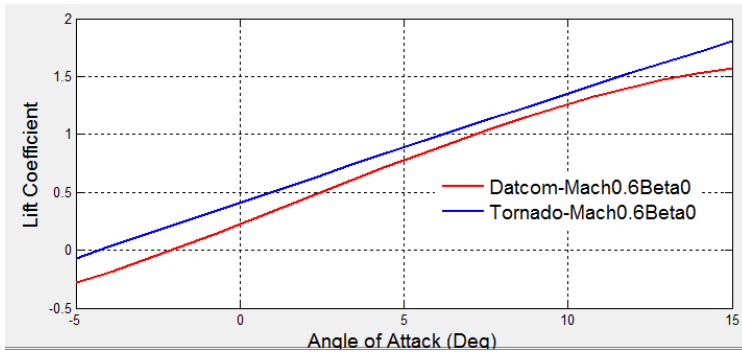


Fig. 45: NACA 4412 C_L over AoA

Focusing on the drag the DATCOM result looks better. Here the drag coefficient is checked by the following equations:

$$C_D = C_{Di} + C_{D0} \quad \text{with} \quad (3.4)$$

$$C_{Di} = \frac{C_L^2}{\pi \cdot e \cdot \Lambda}, \quad e = 0,92, \quad \Lambda = 9,4 \quad (3.4.1)$$

$$\text{and } C_{D0} = C_{fe} \cdot \frac{S_{wet}}{S_W}, \quad C_{fe} = 0,003; \quad \frac{S_{wet}}{S_W} = 6,1 \quad (3.4.2)$$

C_{Di} is the induced drag coefficient. C_{D0} is the zero - drag coefficient which takes the viscosity into account. In Fig. 46 the induced drag coefficient above the AoA are shown. It is almost the same as the result of Tornado (Fig. 48). So it is obvious that the viscosity is not considered in the Tornado calculation. This feature will be added in one of the next versions of CEASIOM.

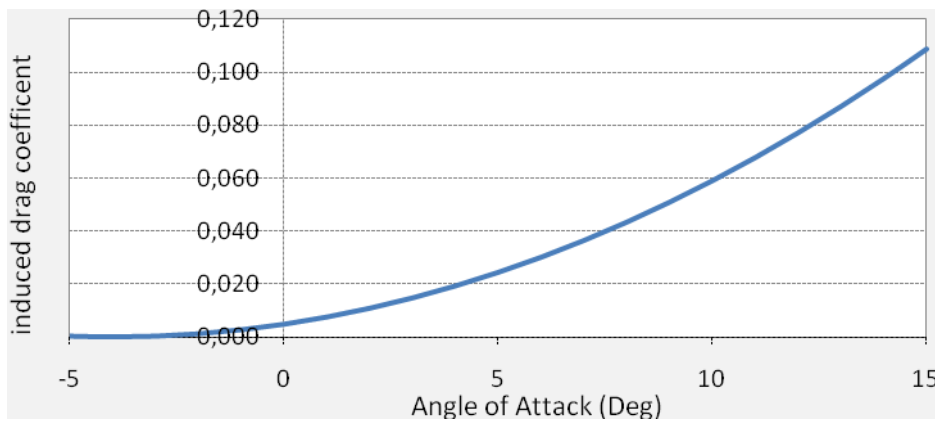


Fig. 46: C_{Di} calculated on the equations

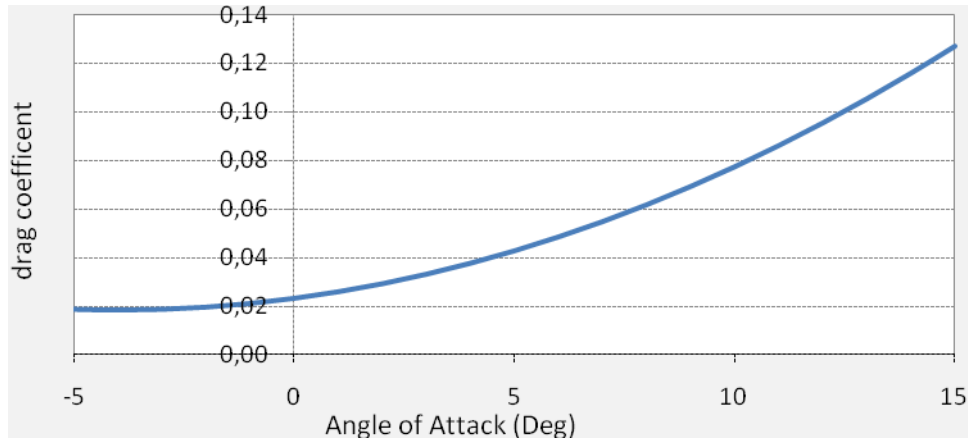


Fig. 47: C_D calculated on the equations

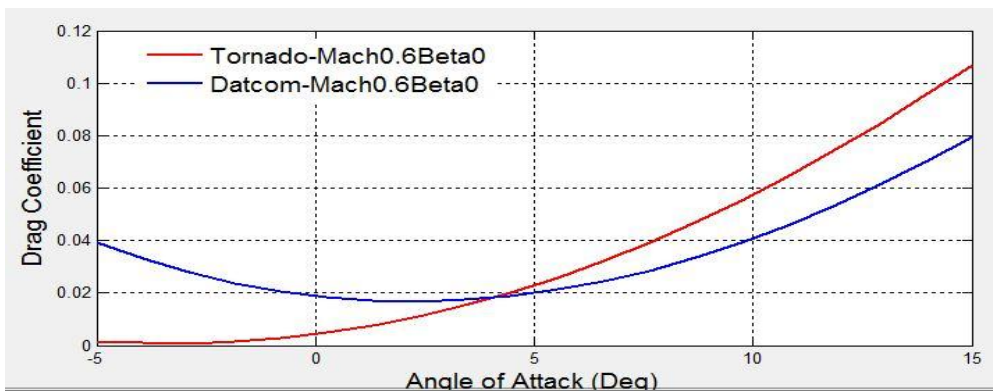


Fig. 48: C_D Tornado and DATCOM

Fig. 47 depicts the drag coefficient calculated by hand. Here the viscosity is taken into account on a statistical way. Fig. 48 contains the result of DATCOM. It is shown that the DATCOM output includes the effect of viscosity. Here the estimation of the drag coefficient falls back to a more complex procedure than the one calculated by hand. Therefore it should be more precise. As the determination of the lift coefficient for that airfoil is not so exact, these values should be considered critically.

Before evaluating the results of Edge Euler a grid convergence study is done. The different meshes that are used are depicted in chapter 3.3.1. The requirements are a Mach number of 0,75 at an angle of attack of 0° .

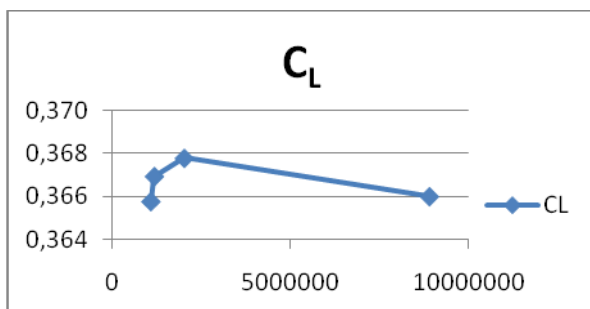


Fig. 49: Grid convergence C_L

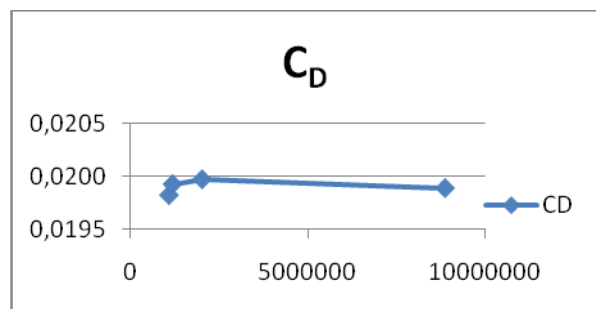


Fig. 50: Grid convergence C_D

Fig. 49 and Fig. 50 show the results of the grid convergence study. By those two graphs of the lift coefficient and the drag coefficient it is proved whether the fineness of the mesh significantly influences the results. By means of the two graphs it is recognizable that the results do not deviate much. The biggest divergences are between mesh 1 and mesh 3. For the lift coefficients it is 0,55% for the drag coefficient it is about 1,73 %.

The results of the Edge Euler calculation are first plotted in the Matlab desktop. Furthermore they are saved in a separate folder with a corresponding *.log file, *.ainp file, *.bout file, *.bres file and *.plt file. In Fig. 51 and Fig. 52 the output of Matlab is depicted. Fig. 53 and Fig. 54 present the output of the *.log files.

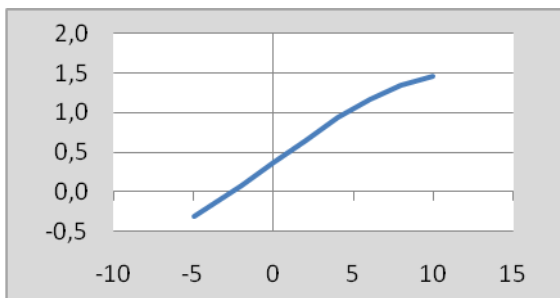


Fig. 51: C_L over AoA Matlab output Edge Euler

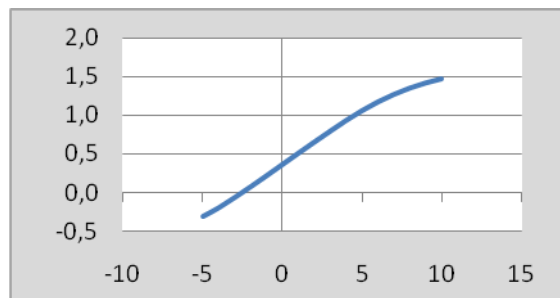


Fig. 52: C_L over AoA logfile output

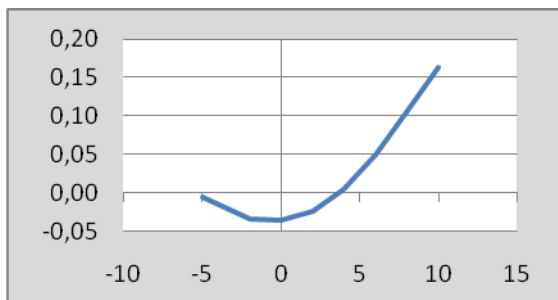


Fig. 53: C_D over AoA Matlab output Edge Euler

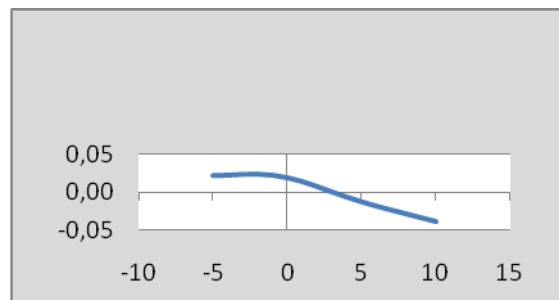


Fig. 54: C_D over AoA logfile output

If one considers the lift coefficient both outputs are the same. The results are close to the Tornado output. As all surfaces are considered, the lift coefficient computed by Edge Euler is a bit greater than the one of Tornado. Thus the results are comprehensible.

Focusing on the drag coefficient the divergences are significant. From the course of the graph the Matlab output looks better (Fig. 53), but for an angle of attack from -5° to 4° the drag is negative. That is unrealistic. Considering the results saved in the *.log file the course of the graph is not typical. But, from -5° to 2° the magnitude of the values look realistic. A closer look at the *.log file reveals that viscosity effects are included towards the x axis. For high angles of attack the aspect of the viscosity in x direction becomes smaller and therefore the values of the drag coefficient do as well. Potentially, the postprocessor of AMB compensates for this aspect but also gives inaccurate results.

It is necessary to have accurate values for the drag coefficient to evaluate the Edge Euler data. Therefore the drag polar of the NASA SC(2)-0612 depicted in Fig. 55 is used. According to the lift coefficient calculated by equation (3.2) the drag coefficient is determined. C_D over the angle of attack is then shown in Fig. 56 for a Reynolds number of 25000.

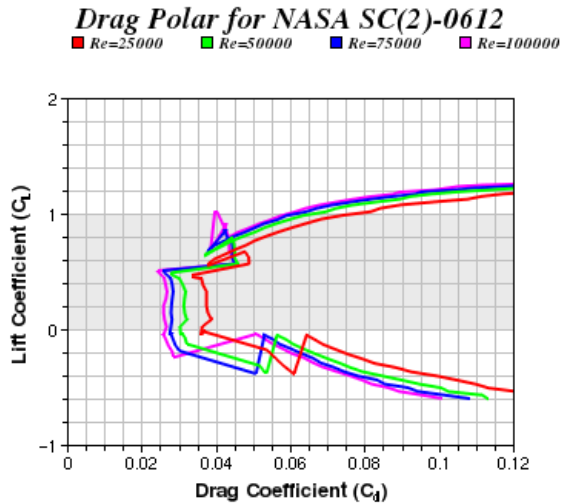


Fig. 55: Drag polar SC(2)-0612 (Krauss 2010)

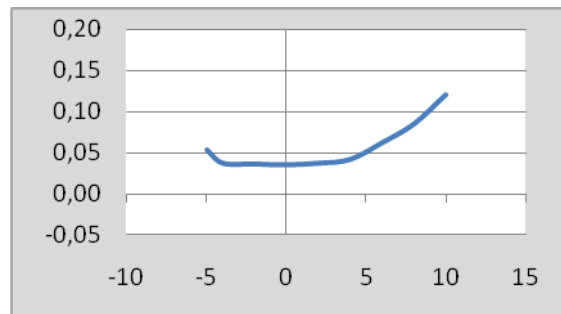


Fig. 56: C_D for a NASA SC(2)-0612

The results of Edge Euler do not correspond with the C_D value given by the drag polar. Both the Matlab output and the *.log file results deviate from the values given in Fig. 56.

It is possible to post-process the results of Edge Euler with the help of Tecplot. Tecplot is a software for plotting or animating simulation and experimental data. Opening the *.plt file with Tecplot it is possible to depict the pressure distribution or the Mach distribution. There are other features that can help analysing a calculation, but in this instance just the Mach and pressure distribution is plotted. This way the principle correctness of the computation can be assessed. In Fig. 57 the C_p distribution at a Mach number of 0,75 and an angle of attack of 0° for the whole aircraft is depicted. Fig. 58 shows the A320 at an angle of attack of 5° at the same velocity. The negative pressure coefficient on the upper wing surface increases with the higher angle of attack and thus the lift at AoA 5° is bigger than at an AoA of 0° . The position of the stagnation point looks good in both figures. It runs on the leading edge of the wing and is on the top of the fuselage nose. The stagnation point is defined by a C_p of 1 (deep red).

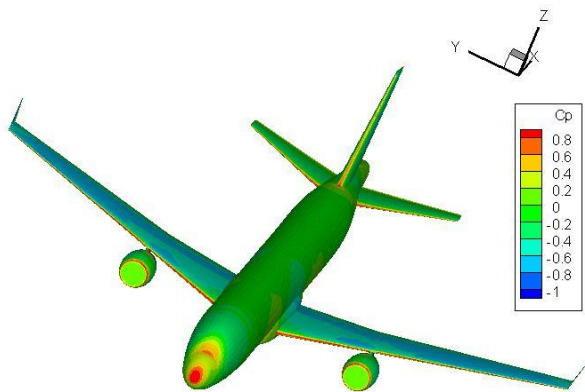


Fig. 57: Mach 0.75 AoA 0° c_p distribution

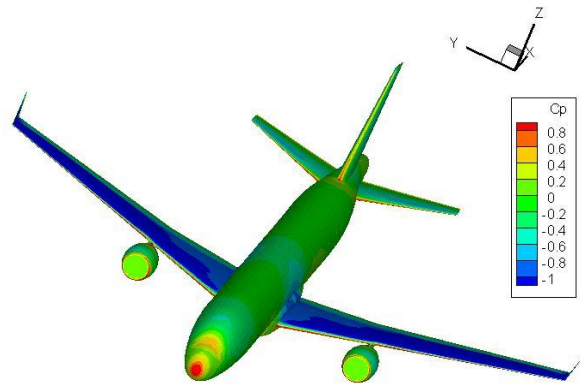


Fig. 58: Mach 0.75 AoA 5° c_p distribution

Fig. 59 shows the Mach distribution at an angle of attack of 0° and a cruise velocity of 0,75 Mach. For these conditions the velocity on the wing is sometimes bigger than Mach 1. So a wave drag will occur. The Mach number becomes 0 at the stagnation points.

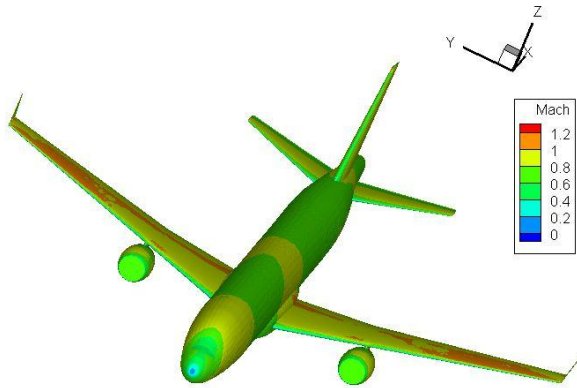


Fig. 59: Mach 0.75 alpha 0° Mach distribution

3.4.3 Discussion on the Practicability of AMB

The CEASIOM tool AMB is well structured and the workflow self-explanatory. At the moment it is not possible to display all results that are computed via the AMB user interface. That work is under way. During the computation the system crashes sometimes and the computer has to be restarted. This problem cannot be assigned to AMB, but it his helpful to verify the computer performance before starting extensive calculations. Moreover it might be helpful to have an estimation of the required time. The results have to be critically examined. For a first estimation of the coefficients the tool gives good results and can be used without hesitation. As long as the viscosity is not taken into account the values for the drag coefficient are okay. When the analysis goes deeper, the results are not accurate enough. There are still uncertainties about the accuracy of the drag coefficient, which could not be overcome even with the help of CSF Engineering.

3.5 A320 in Propulsion

3.5.1 Implementation

To run the Propulsion module, the *.xml file from the AMB has to be opened. There are two parameters, the altitude and the Mach number. These parameters do not have to be changed. Clicking the button *Run* starts the calculation (Fig. 60).

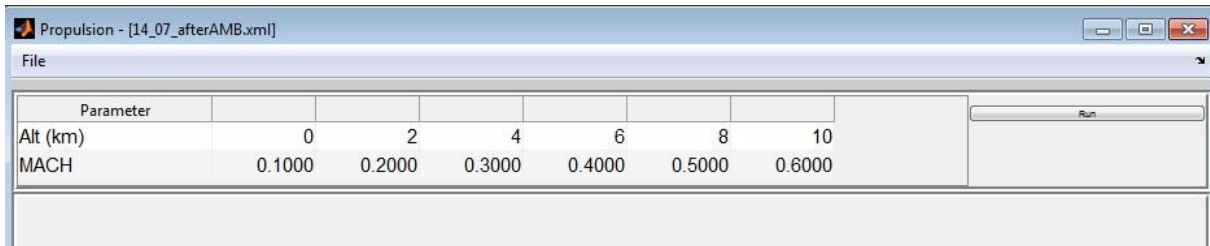


Fig. 60: Propulsion GUI

3.5.2 Results

The result of the Propulsion tool is the data for the engines that is necessary for the SDSA tool and shows the thrust above the Mach number depending on the altitude.

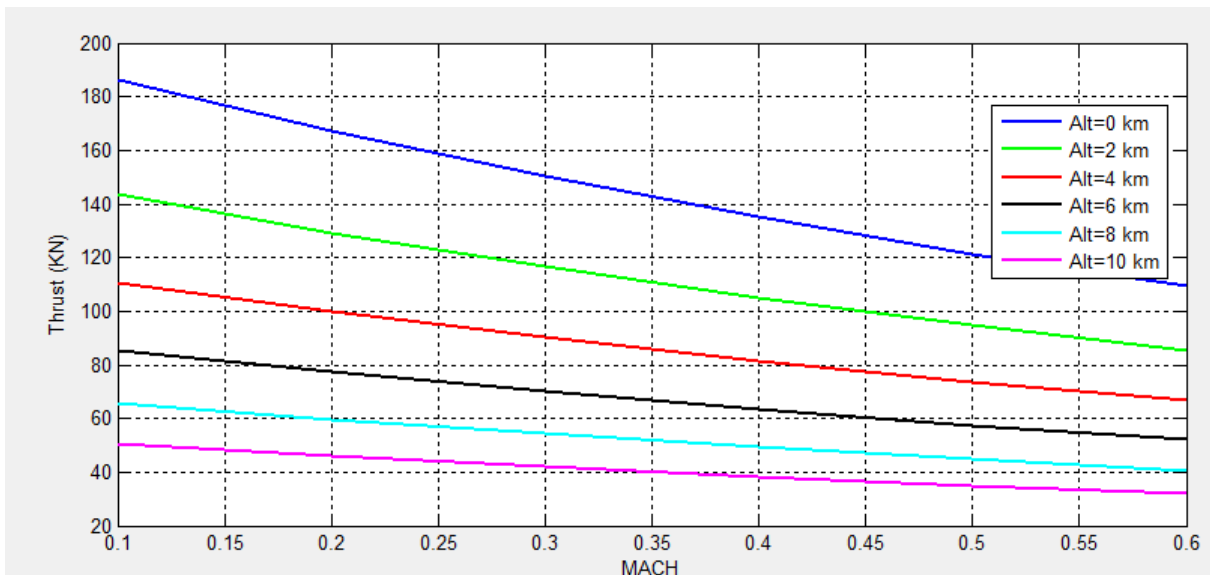


Fig. 61: Propulsion output

The results (Fig. 61) serve the calculation of stability and control and should be saved under a new name in *.xml format.

3.6 A320 in SDSA

3.6.1 Implementation

The input data of the SDSA tool is the output of the propulsion module. It includes data from the AMB, in the present example from Tornado and Datcom. Opening SDSA via CEASIOM, it is asked if it is an AMB based or Stand alone computation. In the present case the AMB-SDSA variant is chosen and for the aerodynamic data Tornado is selected. The reason for that is, that Datcom does not produce the right aerodata and while reading its input data an error message appears in SDSA.

The first thing that appears is the *xml data report*. Here warnings, errors and messages are listed. If there are some problems in later calculations the possible cause can be found here. Furthermore the *data analysis report* is helpful, that is found under the submenu *Aircraft*. To define the parameters for the aerodynamic data report the field *Check data options* should be chosen. Here the minimum and maximum values can be changed to the preferred values. Under *Data interpolation option* the conditions for the interpolations can be set. For the example of the A320 the default values of the above mentioned options are set. Under *Aircraft* → *aerodynamic data* the aerodynamic values are depicted corresponding to Tornado. Here one finds several components that can be selected. In Appendix B the selection features are listed. They can be mapped over the angle of attack, Mach or the according control surface deflection.

The next sub module is *Performance*. Selecting the set card *Envelope* the minimum and maximum airspeed for TAS, IAS and Mach can be computed. Also a curve for the altitude over the speed can be computed and the theoretical ceiling in meter. Under *Range and Endurance* the maximum and minimum speed and altitude can be added and the results are given in a graphical way. The engine type and the mass can also be adjusted. For the A320 the data taken from the input file is kept. The insert data for the computation of range is found on the right side in Fig. 62. For the endurance calculation just the y variable and the method are changed. The other parameters are kept. The input box is pictured in Fig. 63. The computed results of range and endurance are presented in chapter 3.6.2.

X variable: Mach | km/h
 Y variable: Range [km]
 Method: CL = const

Altitude range
 H min [m]: 2000
 H max [m]: 10000
 H step [m]: 2000

Airspeed range
 Vmin [m/s]: 100.0
 Vmax [m/s]: 240.0
 V step [m/s]: 20

airspeed range from envelope

Compute

Engine type: TURBO JET

Specific fuel consumption (SFC)
 Use typical SFC:
 Current SFC: 0.50 [kg/daNh]
 Typical SFC: 0.50 [kg/daNh]

Masses [kg]:
 Max TO mass: 73396.9
 Fuel mass: 11009.5
 Fuel reserve [%]: 10

Fig. 62: Input range SDSA

The next field is *manoeuvres*. Here the turn parameters can be determined; on the one hand for a special case with defined altitude, airspeed and roll angle. Consequently the turn radius, half turn time, Gz force EAS and Mach number are computed. On the other hand, also a multivariable set can be computed. The results are given in a graphical way with the asked parameters of the turn on the Y axis and the Mach number, TAS, EAS or IAS on the X axis. For the A320 the x variable is the Mach number and the Y variable the Radius in meters. For the altitude and airspeed range the same data as in Fig. 62 is used. The limit Gz is 2,5. With this data the minimum radius is computed. For a constant roll angle regular turn three roll angles of 30°, 45° and 60° are chosen at an altitude of 1000 m. The result is mapped in chapter 3.6.2.

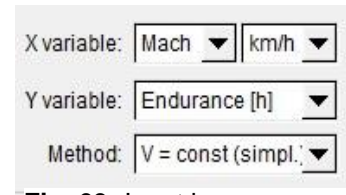


Fig. 63: Input box performance

The last performance option is an external module for the performance. In Fig. 64 the interface of this tool is depicted. The sub items are *Characteristics*, *Power plant*, *Climb*, *Operating envelope*, *Range and Endurance* and *Take-Off and landing*. In this thesis the range and endurance results will be compared to the results coming directly from the SDSA.

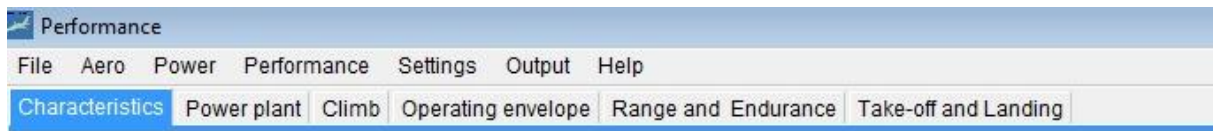


Fig. 64: External performance module

FCS is the Flight Control Submenu. Under this item the *Basic FCS parameters*, *Pilot model* and the *Stability Augmentation System* (SAS) can be defined. Also a Linear Quadratic Regulator matrix can be computed. The Basic FCS parameters are depicted besides the input field. The maximal control surface deflection of the elevator, aileron and rudder is taken from the *.xml file of the A320 and automatically read from the SDSA module. The parameters lag time, B and sin correction are kept in the default setting. A sketchy depiction of these values is shown in Fig. 65. At the pilot model the motoric, adaptive and remnant parameters are asked for. These parameters are assigned to the pilot pitch, roll and yaw control channel. At the SAS submenu the parameters of the actuators from the control surfaces and the SAS parameters explained in chapter 2.2.5 can be set. For the computation at SDSA the default values are chosen. At last the linear quadratic regulator matrix can be generated. The matrix and the according input data is shown in Appendix B. All data of the FSC is used at the Simulation submenu.

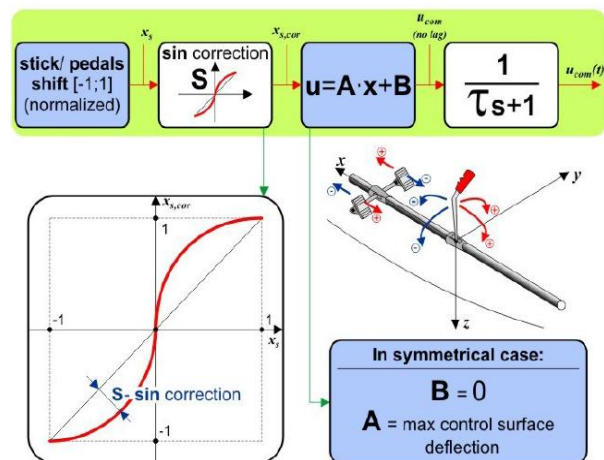


Fig. 65: Basic FCS parameters

At first the *Simulation* submenu gives the possibility to set the *initial conditions* and the *environment conditions*. At the GUI of the initial condition the values for the altitude, airspeed, path angle, roll angle, heading and location can be set. Two simulations will be run. One with the default values of SDSA exclude from altitude and airspeed. The other with side wind located in Hamburg and with the effects of a ground start. The computation with the default values is based on an altitude of 10000 m and an airspeed of 224 m/s. The predefined coordinates are the one of the South Pole and the engines are on. These parameters are set under *Simulation* → *Initial conditions*.. Under *Simulation* → *Environment* the values for temperature, wind, pressure, air density and speed of sound can be defined. For the first simulation the default settings are chosen. The results of the simulation are described in chapter 3.6.2. The second simulation S2 is located in Hamburg. The initial position is changed and the ground start button is activated. Also a path angle of 15° is set. Moreover a side wind is defined. The wind course is about 5° , the horizontal wind speed related to a fresh breeze is set to 8 m/s and the vertical wind speed is set to 0 m/s. The runway conditions are dry and the wind shear turbulence is light. The parameters for the windshear root are on default values. The results are also shown in chapter 3.6.2.

Under SDSA there is also a tool for the stability analysis. Under *stability* → *Eigenvalues* the *Stability Criteria*, *Stability characteristics* and the *Trim results* can be computed and depicted. First the conditions for the calculation has to be defined.

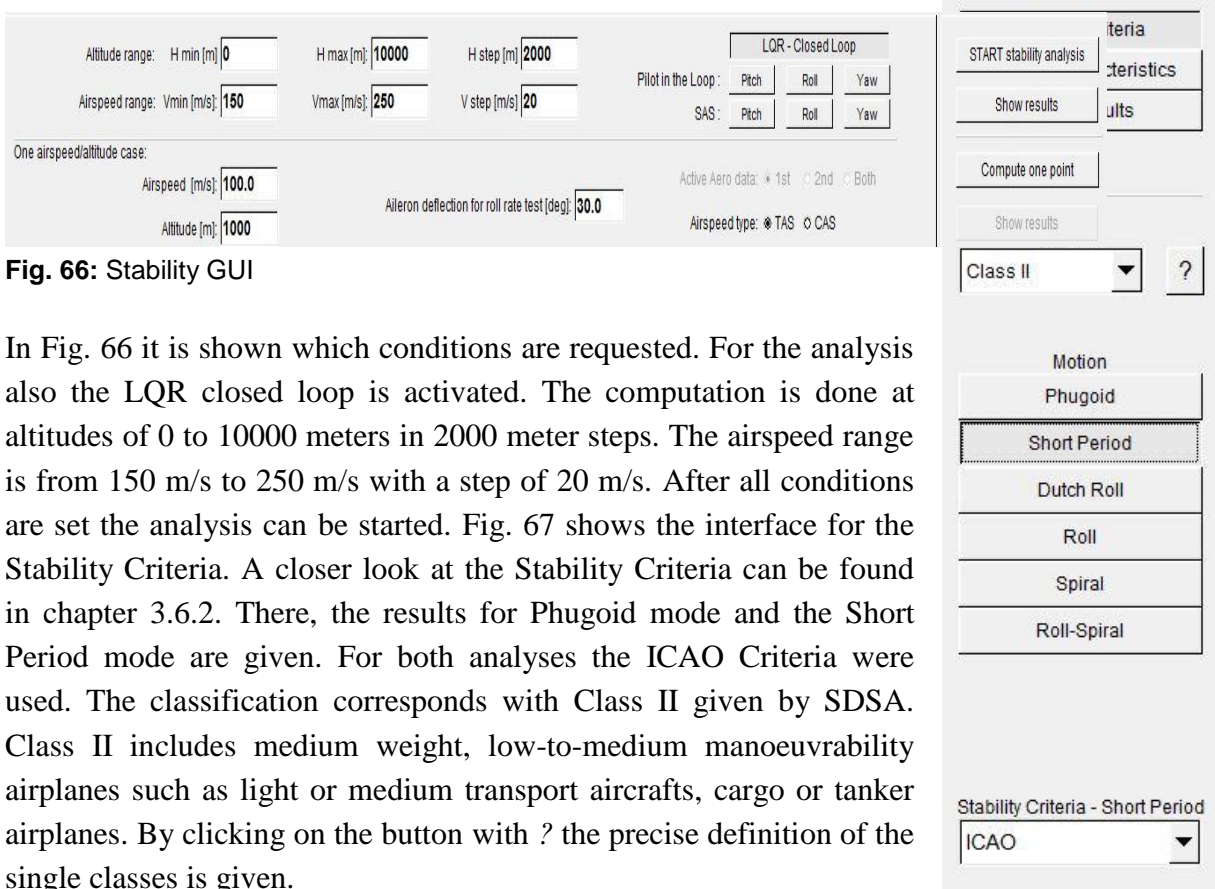


Fig. 66: Stability GUI

In Fig. 66 it is shown which conditions are requested. For the analysis also the LQR closed loop is activated. The computation is done at altitudes of 0 to 10000 meters in 2000 meter steps. The airspeed range is from 150 m/s to 250 m/s with a step of 20 m/s. After all conditions are set the analysis can be started. Fig. 67 shows the interface for the Stability Criteria. A closer look at the Stability Criteria can be found in chapter 3.6.2. There, the results for Phugoid mode and the Short Period mode are given. For both analyses the ICAO Criteria were used. The classification corresponds with Class II given by SDSA. Class II includes medium weight, low-to-medium manoeuvrability airplanes such as light or medium transport aircrafts, cargo or tanker airplanes. By clicking on the button with ? the precise definition of the single classes is given.

Fig. 67: Results GUI

Another sub-item of the stability tool is called Time history. Here, the results of the simulation can be presented. The prerequisite is that a simulation has already been run and saved as a *.txt file under *SDSA→out*. After opening the simulation file different variables can be plotted regarding time. The description of the single variables is not that exact and just marked by single letters, but most meanings can be deduced from previous definitions and generally valid terms. The results of this tool will be compared with the results directly put out by the simulation tool (chapter 3.6.2). The last sub-item of the stability tool is *Static margins*. Here the static and controllability margins can be calculated.

3.6.2 Evaluation of the Results of SDSA

The aerodynamic data can be displayed. The output depends on the data of Tornado and is not computed again. For example, the pitching moment derivative subjected to the elevator deflection can be displayed. Also the roll moment derivative can be plotted against the aileron deflection or the yaw moment derivative against the rudder deflection.

The first thing that is proven is the output of the performance. Here SDSA gives results and additionally an external performance tool is available. In Tab. 8 the results are summarized. The according graphics are shown in Appendix B. For checking purpose, range and endurance are calculated according to common equations (**Young 2001**). The equations are divided in three different flight schedules:

- 1. Flight at constant altitude and constant lift coefficient
- 2. Flight at constant airspeed and constant lift coefficient
- 3. Flight at constant altitude and constant airspeed

These result in the following equations for a turbofan/turbojet:

$$(1.) R = \frac{2 E v}{spc \cdot g} \left[1 - \sqrt{\frac{m_1}{m_2}} \right] \quad (3.5.1)$$

$$(2.) R = \frac{E v}{spc \cdot g} \ln \left[\frac{m_1}{m_2} \right] \quad ; \quad t(2) = R(2) \div v \quad (3.5.2)$$

$$(3.) R = \frac{2 E v}{spc \cdot g} \arctan \left[\frac{\sqrt{B_3} (m_1 - m_2)}{B_3 + m_1 m_2} \right] \quad ; \quad t(3) = R(3) \div v \quad (3.5.3)$$

While

$$B_3 = \frac{C_{D0} \cdot \rho^2 \cdot S^2 \cdot v^2 \cdot \pi \cdot A \cdot e}{4 g^2} \quad (3.5.3a)$$

$$\begin{array}{llllll} \text{sfc} = 1,674 \cdot 10^{-5} & v = 224 \text{ m/s} & E = 17,88 & g = 9,91 \text{ m/s}^2 & e = 0,85 \\ \rho = 0,2969 & m_1 = 73\,500 \text{ kg} & m_1 = 60\,500 \text{ kg} & C_{DO} = 0,018 & A = 9,5 \end{array}$$

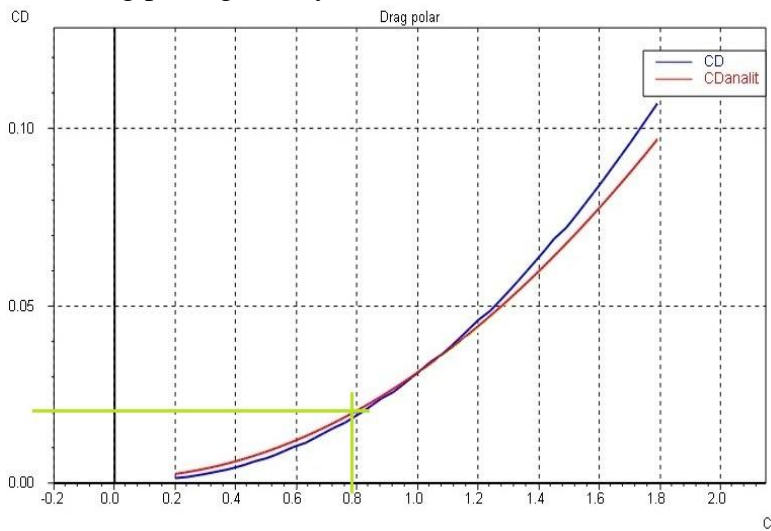
Tab. 8: Endurance and range

| | Given data | | calculated | | |
|-----------|--------------|------------|------------|----------|----------|
| | Max. payload | Max. range | 1 | 2 | 3 |
| Endurance | 3,5 h | 6,7 h | 5,6 h | 5,9 h | 5,8 h |
| Range | 2 780 km | 5 350 km | 4 520 km | 4 750 km | 4 730 km |

| | External SDSA tool | | | SDSA | | |
|-----------|--------------------|----------|----------|---------|----------|----------|
| | 1 | 2 | 3 | 1 | 2 | 3 |
| Endurance | 7 h | 6 h | 8 h | 5,8 h | 4,5 h | 6,5 h |
| Range | 5 000 km | 5 000 km | 5 000 km | 4500 km | 4 100 km | 5 000 km |

The difference between the results of the performance tools of CEASIOM and the calculated one by hand is not so big. The difference is explainable with the fuel mass computed in the AcBuilder. This value is not accurate and is about 11 tonnes while the fuel mass for the calculation by hand is 13 tonnes. The precision is impaired by reading errors.

It is interesting that the difference between the calculated results and the output of the external SDSA tools is not much bigger, as the value of the glide ratio is not the same. A closer look on the drag polar given by the external tool shows that the cruise glide ratio is about 36. If this

**Fig. 68:** Glide ratio SDSA

glide ratio is considered, a range of 9 100 km would be the result of the calculation by hand. The high glide ratio is explainable by the inaccurate reproduction of the drag coefficient. Like shown in chapter 3.4.2, the viscosity is not considered. Because of that the glide ratio differs. To determine the glide ratio of the SDSA tools, the CL for the flight is needed.

It is calculated using the following equation and depicted in Fig. 68:

$$CL = \frac{L}{0,5 \rho \cdot v^2 \cdot S} \quad (3.5.1)$$

While $L = 73500 \text{ kg} \cdot 9,81 \frac{\text{m}}{\text{s}^2}$; $\rho = 0,2969$; $v = 224 \text{ m/s}$ and $S = 122,4 \text{ m}^2$.

For manoeuvres the turn radius is in the focus. With the help of SDSA a single value is calculated. The input data is an altitude of 10 000 m, an airspeed of 225 m/s and a roll angle of 30°. For that the regular turn radius is 8 950 m. With the equation (Young 2001)

$$r = \frac{v^2}{9,81 \frac{m}{s^2} \cdot \tan \phi} \quad (3.6.1)$$

and

$$r = \frac{v^2}{9,81 \frac{m}{s^2} \cdot \sqrt{Gz^2 - 1}} \quad (3.6.2)$$

the results are checked. Using the given formula a radius of 8 860 m is calculated which is close to the SDSA output. In Appendix B the minimum radius depending on altitude and Mach number is depicted. At an altitude of 10 000 m and a Mach number of 0,76 the minimum radius for a regular turn is 7 100 m. That leads to a roll angle of 54 ° and a Gz of 1,71. Another possibility of this tool is to present the radius of the regular turn for different roll angles (Fig. 69). In comparison of the results due to the equation it is shown that there are no differences (Fig. 70).

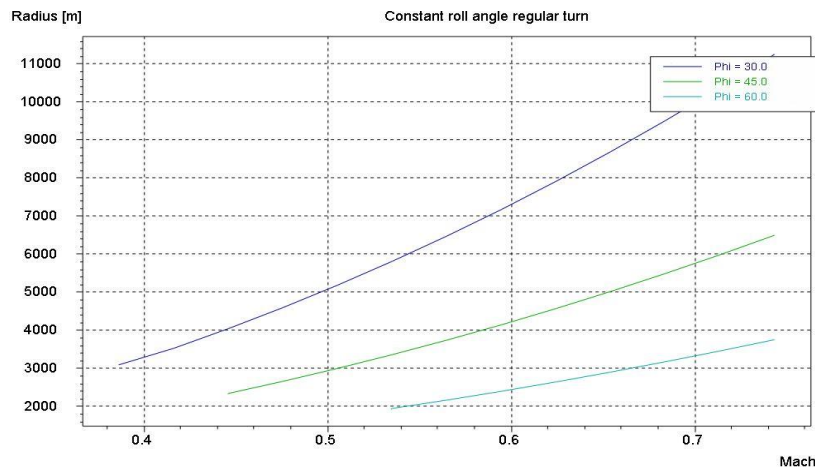


Fig. 69: Constant roll angle regular turn

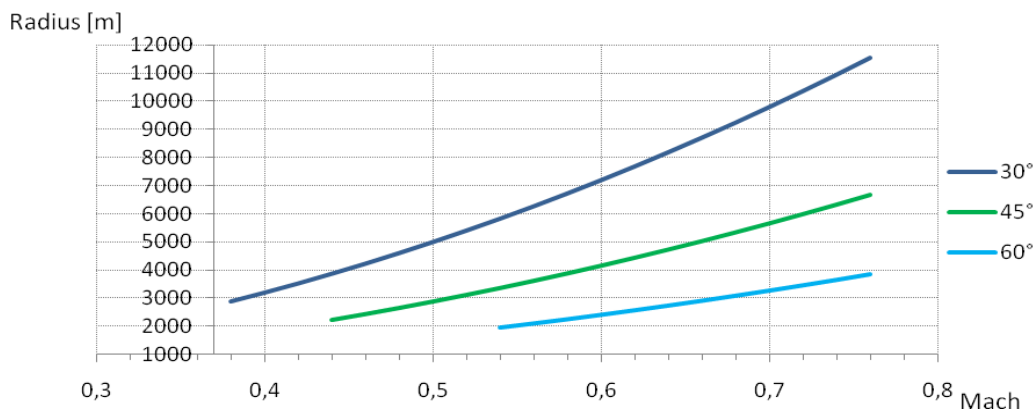


Fig. 70: Constant roll angle calculated by equations

The submenu *Simulation* gives the possibility to try several maneuvers. In Fig. 71 the GUI of the tool is depicted. Below this interface a message is inserted, that says weather the flight is ok or not.

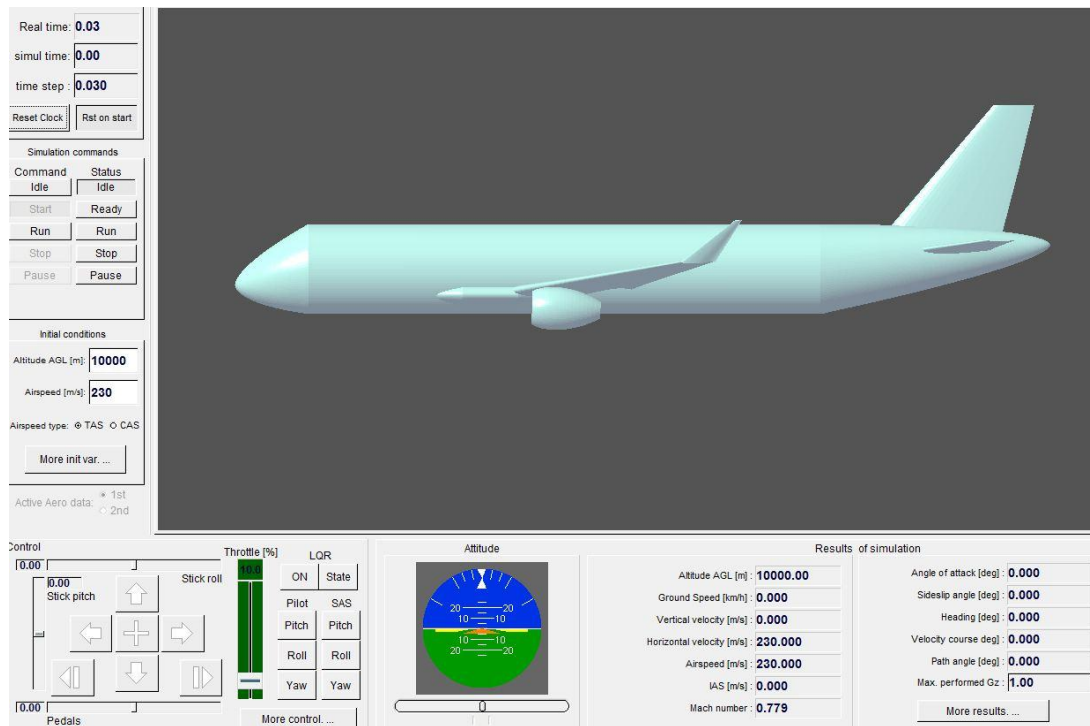


Fig. 71: Simulating tool

The first simulation is done with the default values of the program. The effect of an abrupt control stick movement is reproduced. In Fig. 72 the path angle depending on this modification is shown. The orange mark labels the intervention in the steady flight phase, after that the path angle changes depending on the time in a sinusoidal oscillation. It is visible that the oscillation does not increase. The aircraft is stable and goes back to its initial position. After 320 seconds the LQR is turned on. As a result the aircraft goes immediately into a steady flight. The speed and the altitude set for the conditions are controlled.

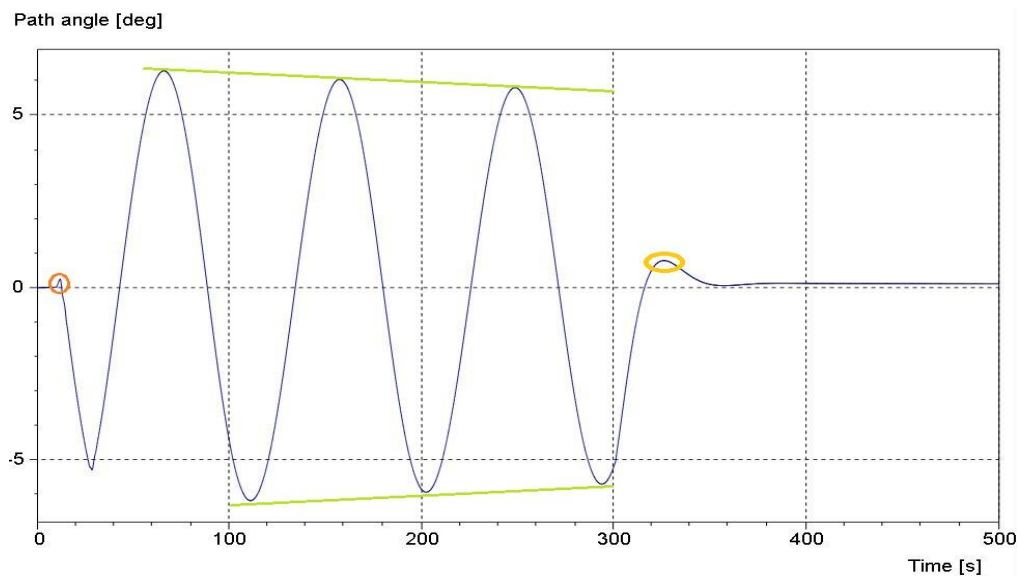


Fig. 72: Path angle for simulation

In the second simulation the ground effect and the wind are considered. The second simulation should run a little bit longer. Therefore the recording time can be changed under *Options* → *recording time*. It is attempted to simulate a climb. This simulation is once tried with the LQR on and a second time without the LQR at the beginning. For the first run the altitude over sea level and the velocity in km/h are plotted above the distance in x direction flown by the aircraft (Fig. 73). Fig. 74 shows the second run. Here the altitude above sea level and the velocity are plotted over the time in seconds.

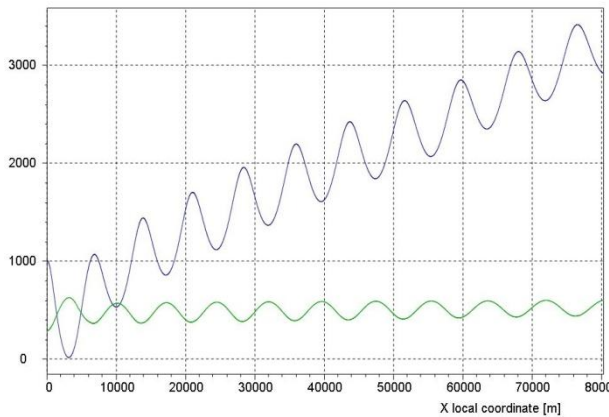


Fig. 73: Simulation 2 run 1

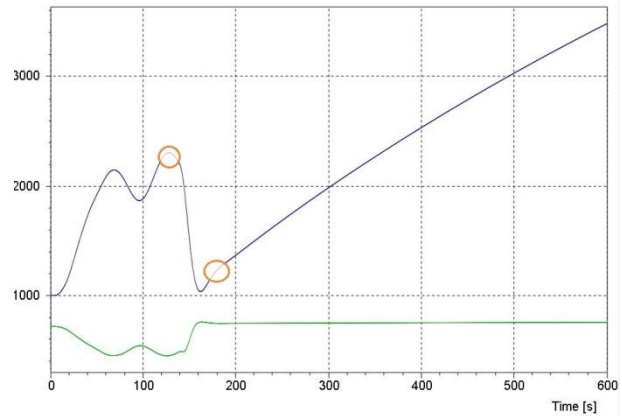


Fig. 74: Simulation 2 run 2

In Fig. 73 the blue line represents the altitude and the green line the velocity. The same allocation of colors is chosen for Fig. 74. At the first run of simulation 2 the climb happened in sinusoidal waveform. The course of the velocity graph follows the path angle of the airplane. When the airplane climbs the velocity decreases, for the phases of descent the velocity rises. All in all the velocity wavers around a fixed value. The reason for that is that if the LQR is put on the aircraft tries to reach the initial condition of a given altitude and velocity set before. That is not possible because the user controls the stick and its position that gives the command for climb. It is fixed and therefore the phugoid mode is visible. In the second run the user controls the aircraft without helping systems. For the first minute the aircraft climbed, but after an angle of attack 15° is exceeded the altitude above sea level decreases again. At this moment (first orange circle Fig. 74) the LQR was put on. The aircraft immediately controls towards the altitude set in the initial conditions. During the simulation the initial conditions can be changed. That happened after 180 seconds, marked by the second orange circle in Fig. 74. The new altitude is set to 10 000 meters. Now the aircraft transfers to a constant climb. After 600 seconds the simulation was stopped. During the time the LQR is active the effects on the control surfaces can be observed during the simulation on the control windows. In Fig. 75 and Fig. 76 the settings of the control windows at the beginning of the simulation and during the simulation are depicted. The user can decide which flaps are active or if the landing gear is taken into account. At the beginning only the elevator is deflected and the thrust is at zero. Looking at the control window during the flight the automatic change of the control surfaces and the thrust can be seen.

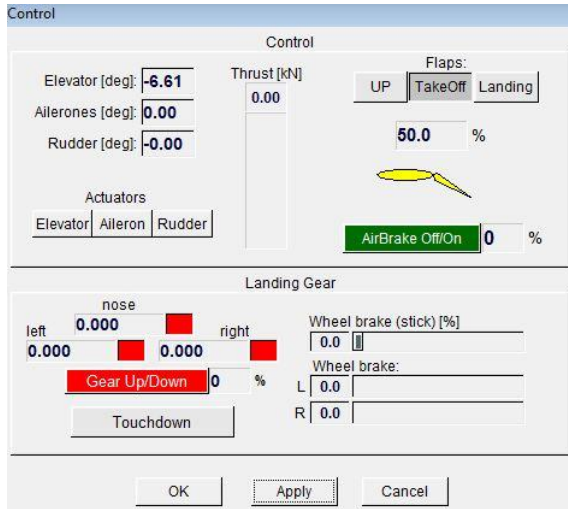


Fig. 75: Control window at the beginning of the simulation

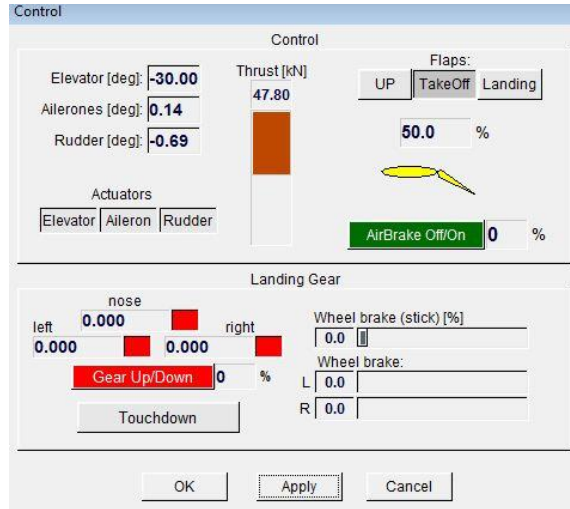


Fig. 76: Control window at the simulation

The last topic of SDSA that is examined is the stability. Here the phugoid and the short period are recalculated using the equation of the flight mechanic 2 script of Dr.D.Nguewo (Nguewo 2009) and compared with the output of the SDSA tool. For the analysis the ICAO criteria serve as bases.

The phugoid is a slow oscillation where the angle of attack is constant and also the change in time for the angle of attack. It is a long period oscillation in speed and altitude.

As long as the stick is held fixed, the aircraft will not maintain straight and level flight, but will start to dive, level out and climb again. It will repeat this cycle until the pilot intervenes. (Wiki 2010)

The equations for the phugoid are the following (Nguewo 2009):

The mode shape of the phugoid is

$$s^2 + a_1 s + a_0 = 0 \quad (3.7)$$

Where

$$a_0 = -x_u \cdot Z_\theta + Z_u \cdot x_\theta \quad (3.7.1)$$

$$Z_u = \frac{\rho \cdot S}{m} (-CL) \quad (3.7.1a)$$

$$a_1 = -x_u + Z_\theta \quad (3.7.2)$$

$$x_u = \frac{\rho \cdot S \cdot v}{m} (-CD) \quad (3.7.2a)$$

$$x_{\theta} = -g = -9,81 \frac{m}{s^2}; \quad Z_{\theta} = 0; \quad CL = 0,27; \quad CD = 0,0231;$$

$$S = 122,4 \text{ m}^2; \quad \rho = 0,3367 \frac{kg}{m^3}; \quad v = 240 \frac{m}{s}; \quad m = 73500 \text{ kg}$$

The data for the aerodynamic coefficients is taken from the Tornado output. The conditions are for a flight in 10 000 meters above sea level at a speed of 240 m/s. Inserting the data into the equations a_1 becomes 0,0154 1/s and a_0 becomes $9,76 \cdot 10^{-3}$ 1/s. According to these values the frequency, damping and period can be defined. The characteristic equation for oscillation is:

$$\lambda^2 + 2\zeta w_0 \lambda + w_0^2 = 0 \quad (3.8)$$

Therefore $w_0 = \sqrt{a_0}$ and $2\zeta w_0 = a_1$. To calculate the period the following transformation is used:

$$w = w_0 \sqrt{1 - \zeta^2} \quad (3.8.1)$$

and

$$f = \frac{w}{2\pi}; \quad T = \frac{1}{f} \quad (3.8.2)$$

The determined values are inserted into the output of the SDSA tool (Fig. 77). So it is easier to compare them.

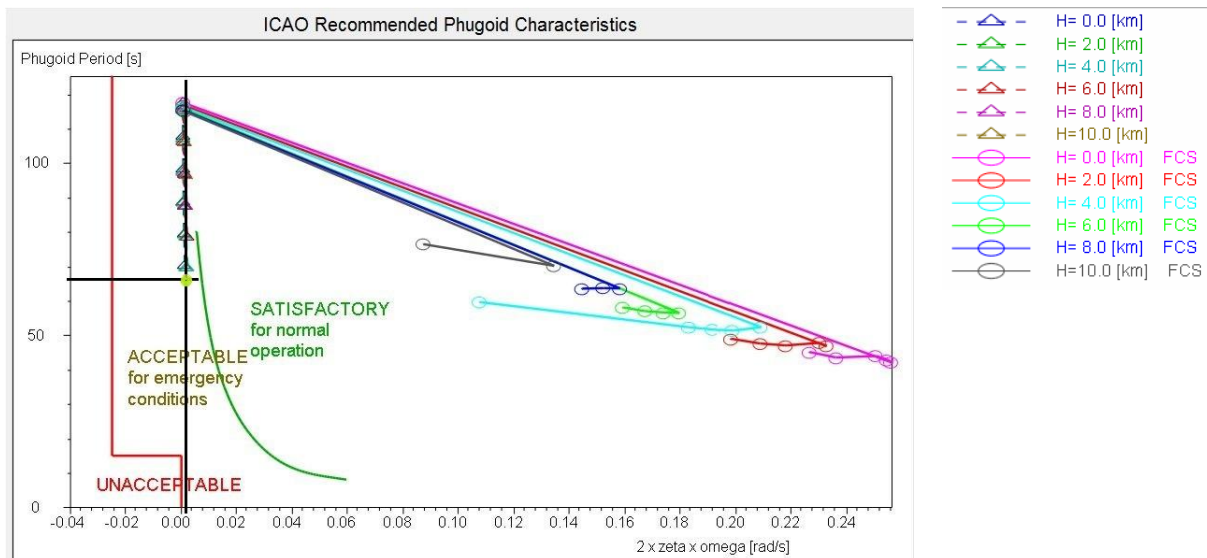


Fig. 77: Phugoid

The green dot presents the result of the calculation based on the lecture notes. It is not close to the results calculated by SDSA (brown triangle) for a 10 km altitude, but the value of a_1 fits. The deviation can only lead back to the simplified method of the equation or the transmitted geometrical values at SDSA. The aerodynamic coefficients were the same in both calculations. Furthermore it is depicted that without a supporting flight control system the aircraft did not lie in the satisfactory area, as defined by the ICAO criteria. In the stability tool

of SDSA it is possible to compute the values with a support system. Then the values for all different altitudes are in the satisfactory area.

The short period is the fast oscillation of the angle of attack. It is the time respond directly after a disturbance, for example a pull at the stick by the pilot. Θ and the angle of attack α change very fast while the velocity is nearly the same. The equations for the short period are the following:

The mode shape of the short period is

$$s[s^2 + a_1 s + a_0] = 0 \quad (3.9)$$

Where

$$a_0 = Z_\alpha \cdot M_q - M_\alpha \quad (3.9.1)$$

$$Z_\alpha = \frac{\rho \cdot S \cdot v}{2m} (CL_\alpha + CD) \quad (3.9.1a)$$

$$M_\alpha = \frac{\rho \cdot S \cdot v^2 \cdot c_{MAC}}{2I_y} (Cm_\alpha) \quad (3.9.1b)$$

$$M_q = \frac{\rho \cdot S \cdot v \cdot c_{MAC}^2}{2I_y} (Cm_q) \quad (3.9.1c)$$

$$a_1 = -M_q - Z_\alpha - M_{\dot{\alpha}} \quad (3.9.2)$$

$$M_{\dot{\alpha}} = \frac{\rho \cdot S \cdot v \cdot c_{MAC}^2}{2I_y} (Cm_{\dot{\alpha}}) \quad (3.9.2a)$$

$$CL_\alpha = 5,113 ; CD = 0,114 ; Cm_{\dot{\alpha}} = -50,232 ; Cm_\alpha = -2,649 ; Cm_q = -0,14976$$

$$S = 122,4 \text{ m}^2 ; \rho = 0,3367 \frac{\text{kg}}{\text{m}^3} ; v = 240 \frac{\text{m}}{\text{s}} ; m = 73500 \text{ kg} ; I_y = 2441460 \frac{\text{kg}}{\text{m}^2} ;$$

$$c_{MAC} = 3,9066 \text{ m}$$

Based on these equations $a_1 = 1,211 \text{ 1/s}$ and $a_0 = 10,063 \text{ 1/s}$. Like in equations (3.8), (3.81) and (3.82) the frequency, damping and period can be determined and is depicted in Fig. 78. The time to half amplitude was calculated based on the following equations:

$$u(t) = \hat{u} \cdot e^{-\delta t} \cdot \cos(\omega t) \quad (3.10)$$

It is asked for the half amplitude. Therefore $u(t)/\hat{u}$ has to be 0,5. So the following equation has to be dissolved to the time t .

$$0,5 = e^{-\delta t} \cdot \cos(\omega t) \quad (3.10.1)$$

Thus the time to the half amplitude is 0,618 seconds. The results are also marked in the figure given by the SDSA stability tool (Fig. 78) with a green dot. Here the same problem appears like in the analysis of the phugoid. The symbol for the flight at 10 000 meter height at a velocity of 240m/s is the brown triangle. The results of the SDSA tool should always be checked very precisely. The better the input, the better are the results of the SDSA stability tool.

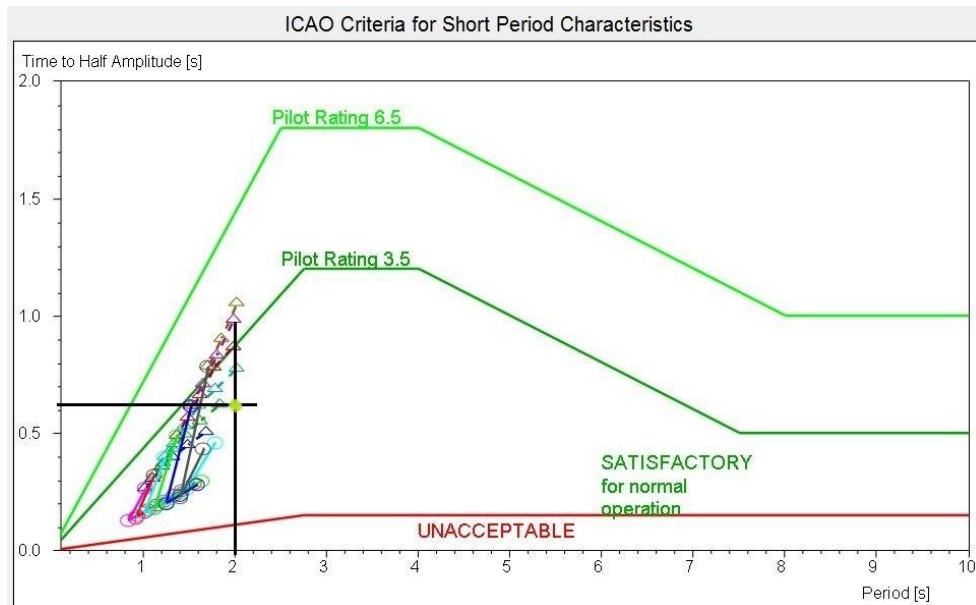


Fig. 78: Short period

3.6.3 Discussion on the practicability of SDSA

SDSA is a very complex tool. It gives the user the possibility to cover many fields of the aircraft design process in a comfortable way. For the features like the simulation tool or the stability tool it is necessary to have enough basic knowledge to evaluate the results before using them in further steps. The handling of the tool is also very easy. During the work with this tool just a few problems appear and these problems could lead back to failures in the input data. Therefore it is very important to check the output of the AcBuilder and the AMB to get good results.

3.7 A320 in NeoCASS

3.7.1 Implementation in GUESS

Upon opening NeoCASS a Graphical User Interface (GUI) appears. The GUI is shown in Fig. 79. On the work surface which is named *File* the different parameters for the calculation can be set.

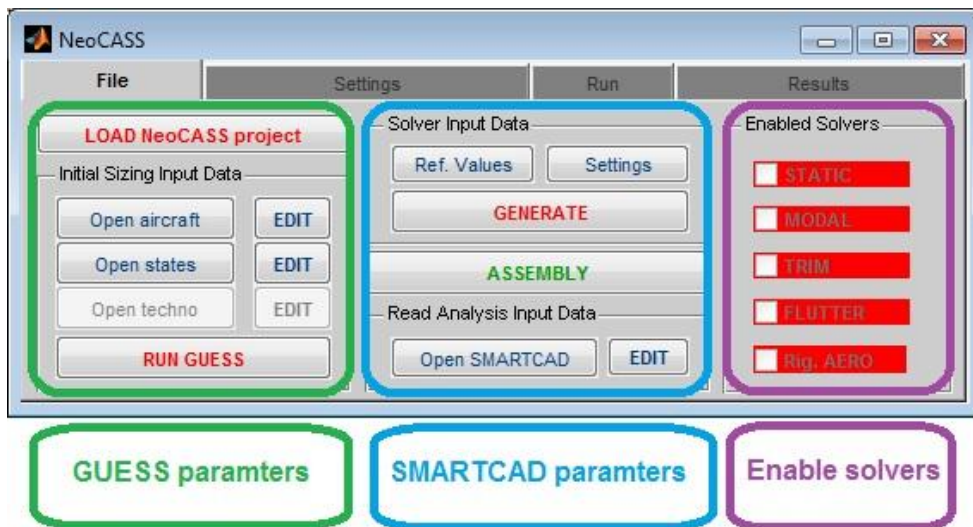


Fig. 79: GUI NeoCASS

To work with GUESS the *aircraft.xml* file is needed. It is build up with the AcBuilder and includes the data of the Weight & Balance tool and the content of the *techno.xml* file. Pressing the button *Open aircraft* a folder shows up and the accordant file can be loaded. In the same way the state file can be edited. The structure of the state file is described in chapter 2.2.6. To generate this file, examples from the CEASIOM folder can be used. In the folder: CEASIOM → Structure → NeoCASS_V1.4 → examples → GUESS samples of different aircrafts and their state files are given. The *open techno* button is not needed when getting the *aircraft.xml* file from the AcBuilder, because all necessary data is included. Using the NeoCASS tool as a standalone program is also possible. Therefore the user should go through the NeoCass manual (Cavagna 2009) carefully to generate the input data in the right way. After uploading the input files GUESS can be started. By pressing the button *RUN GUESS* the calculation of GUESS starts and the results are written into an *.ascii file. While running GUESS some problems occur. One error source is the distribution of the nodes. The nodes that are important for the aero mesh and the structure mesh should be evenly spread along the axes, so that the ratio of the single cells to each other is not too big. Another problem that may arise is, that Matlab calls the wrong Tornado programme. The AMB tool also reverts to Tornado but two different versions are used. If there are problems with regard to the VLM it is the best to start NeoCass on Matlab on its own and do not open it with the help of CEASIOM. Therefore the *set_neocass_path.m* should be opened from the folder: CEASIOM → Structure → NeoCASS_V1.4. When Matlab is opened the GUI has to be started. Under the

Matlab window *current folder* the directory GUI has to be opened and NEOCASS.p should be run. Opening NeoCASS on this way no further problems appear.

The results of GUESS can be plotted under the work surface *Results* and are also written into the MATLAB script. The GUI of the results is shown in Fig. 80.

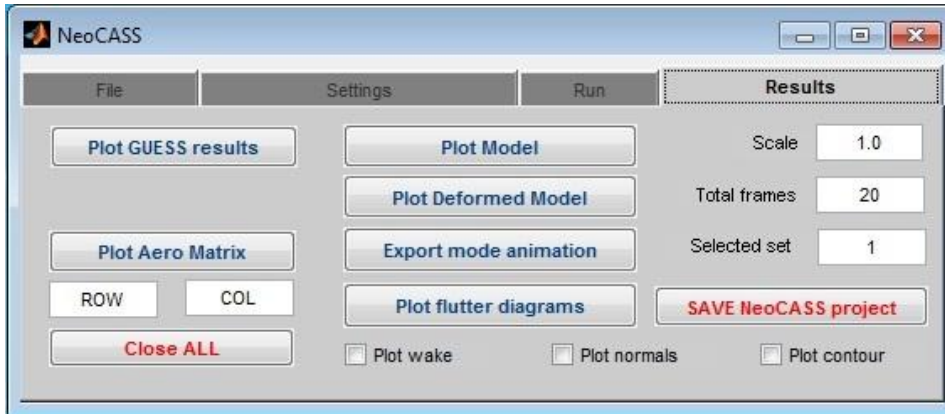


Fig. 80: GUI Results

To plot the different results the window selected set can be changed from 1 to 10. The accordant contents are listed below:

- 1 – fuel volume
- 2 – fuel centroid
- 3 – lift load area
- 4 – centre of pressure
- 5 – shear force
- 6 – Bending Moment
- 7 – Thickness estimation
- 8 – weight estimation (bending shear total)
- 9 – weight estimation (Guess structural weight – primary weight)
- 10 – GUESS vs. stick module properties

3.7.2 Evaluations of the Results of GUESS

The first calculated value of GUESS is the weight. The input is coming from the AcBuilder output and here the material is taken into account. The data is plotted in the Matlab command window and is used for later aeroelastic calculation. In Tab. 9 the results of GUESS are contrasted with the results of the AcBuilder V3 version and Prado. It is traceable that the value for maximum payload, the landing gear and the engine group are taken from the AcBuilder output. The other values are computed by GUESS again. As the input of the

payload is important for the GUESS calculation, variant V3_b serves as input, too. In Tab. 10 the results are depicted for the computation with V3_b. The payload changes in this version.

Tab. 9: GUESS weight estimation

| | Models | | | differences | |
|----------------------|----------|-------|-------|----------------|-------------|
| | GUESS V3 | Prado | V3 | Prado-GUESS V3 | V3-GUESS V3 |
| MTOW | 69910 | 73500 | 73397 | -4,88 | -4,75 |
| OEW | | 41000 | 48123 | | |
| max zero fuel weight | 57410 | 60188 | 63434 | -4,62 | -9,50 |
| max. payload | 15310 | 19099 | 15310 | -19,84 | 0,00 |
| Landing gear | 3116 | 2547 | 3116 | 22,34 | 0,00 |
| Wing weight | 6160 | 8297 | 8766 | -25,76 | -29,73 |
| HT weight | 696 | 590 | 844 | 17,97 | -17,54 |
| VT weight | 963 | 434 | 490 | 121,89 | 96,53 |
| Fuselage weight | 10828 | 9119 | 7207 | 18,74 | 50,24 |
| Engine group | 9235 | 7822 | 9235 | 18,06 | 0,00 |
| fuel | 12500 | 13312 | 9963 | -6,10 | 25,46 |

Tab. 10: GUESS weight estimation input V3_b

| | Models | | | differences | |
|----------------------|------------|-------|-------|------------------|------------------|
| | GUESS V3_b | Prado | V3_b | Prado-GUESS V3_b | V3_b- GUESS V3_b |
| MTOW | 72789 | 73500 | 73449 | -0,97 | -0,90 |
| OEW | | 41000 | 45485 | | |
| max zero fuel weight | 60289 | 60188 | 63486 | 0,17 | -5,04 |
| max. payload | 18000 | 19099 | 18000 | -5,75 | 0,00 |
| Landing gear | 3119 | 2547 | 3119 | 22,46 | 0,00 |
| Wing weight | 6172 | 8297 | 8771 | -25,61 | -29,63 |
| HT weight | 816 | 590 | 844 | 38,31 | -3,32 |
| VT weight | 999 | 434 | 490 | 130,18 | 103,88 |
| Fuselage weight | 10829 | 9119 | 7210 | 18,75 | 50,19 |
| Engine group | 9242 | 7822 | 9242 | 18,15 | 0,00 |
| fuel | 12500 | 13312 | 9963 | -6,10 | 25,46 |

It is obvious that GUESS gives better results for the MTOW and the maximum zero fuel weight when the payload is closer to the realistic data. The deviation for the components like the vertical tail and the horizontal tail are still big or even become bigger. One reason is the definition of the material. For a first run the material values are left at the default settings. This can be optimised in later runs. Moreover the inaccurate input for the engine group and the landing gear leads to major differences. The deviations will become smaller when the weight estimation of the AcBuilder tool is improved.

The next step of GUESS is the computation for the structural parameters. For comparison, the values of the shear forces and the bending moment are calculated using equations from the lecture on structural design (**Seibel 2008**). The fundamental equation used to determine the transverse force of an unswept wing is:

$$Q_y(\eta) = \left[\left(\frac{G \cdot nz}{S} \cdot \int_0^\eta c(\eta) d\eta \right) - \left(\frac{m_{FL} \cdot g \cdot nz}{S} \cdot \int_0^\eta c(\eta) d\eta \right) - \left(\frac{m_K \cdot g \cdot nz}{S} \cdot \int_0^\eta c(\eta) d\eta \right) - m_T \cdot g \cdot nz \right] \quad (3.11)$$

The sweep of the wing has no influence on the transverse force.

The torsional moment is calculated as below:

$$M_y(\eta) = \left[\left(\frac{G \cdot nz}{S} \cdot e \cdot \int_0^\eta c(\eta)^2 d\eta \right) + \left(cm_0 \cdot q \cdot \int_0^\eta c(\eta)^2 d\eta \right) + (Th \cdot h_T - m_T \cdot g \cdot nz \cdot h_T) \right] \quad (3.12)$$

The following applies to swept wings:

$$M_{y\varphi}(\eta) = M_y(\eta) \cdot \cos(\varphi) \quad (3.12.1)$$

The equation for the bending moment of an unswept wing is as follows

$$M_x(\eta) = \int_0^\eta Q_y(\eta) d\eta \quad (3.13)$$

$$M_x(\eta) = \left[\left(\frac{G \cdot nz}{S} \cdot \int_0^\eta \int_0^\eta c(\eta) d\eta \right) - \left(\frac{m_{FL} \cdot g \cdot nz}{S} \cdot \int_0^\eta \int_0^\eta c(\eta) d\eta \right) - \left(\frac{m_K \cdot g \cdot nz}{S} \cdot \int_0^\eta \int_0^\eta c(\eta) d\eta \right) + m_T \cdot g \cdot nz \right] \quad (3.13.1)$$

Conversion for a swept wing:

$$M_{x\varphi}(\eta) = M_x(\eta) \cdot \frac{1}{\cos(\varphi)} - M_y(\eta) \cdot \sin(\varphi) \quad (3.13.2)$$

The equation for the chord length $c(\eta)$ on the according cut η is:

$$c(\eta) = c_t + \frac{c_r - c_t}{b} \cdot \eta \quad (3.14)$$

The integrations for $c(\eta)$ that are needed are:

$$\int_0^\eta c(\eta) = c_t \cdot \eta + \frac{c_r - c_t}{b} \cdot 0,5 \cdot \eta^2 \quad (3.14.1)$$

$$\iint_0^{\eta} c(\eta) = 0,5 \cdot c_t \cdot \eta^2 + \frac{c_r - c_t}{b} \cdot \frac{1}{6} \cdot \eta^3 \quad (3.14.2)$$

For the torsional moment $c(\eta)^2$ is needed:

$$c(\eta)^2 = c_t^2 + 2 \cdot c_t \cdot \frac{c_r - c_t}{b} \cdot \eta + \left(\frac{c_r - c_t}{b}\right)^2 \cdot \eta^2 \quad (3.14.3)$$

All equations from (3.7) to (3.10.3) are inserted into an Excel sheet and this way the bending moment and the shear force is calculated. The input data is summarized in Appendix C. Fig. 83 and Fig. 84 indicate the results.

The output of GUESS is depicted by choosing number 5 and 6 at *selected set* in the interface of NeoCASS. The presentation is shown in Fig. 81 and Fig. 82.

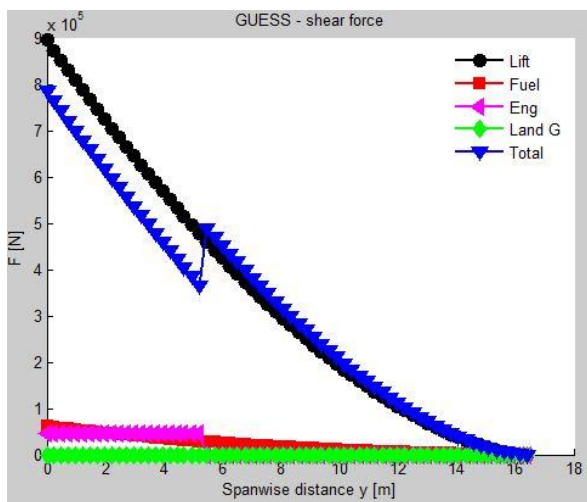


Fig. 81: Shear force over b/2 V3b

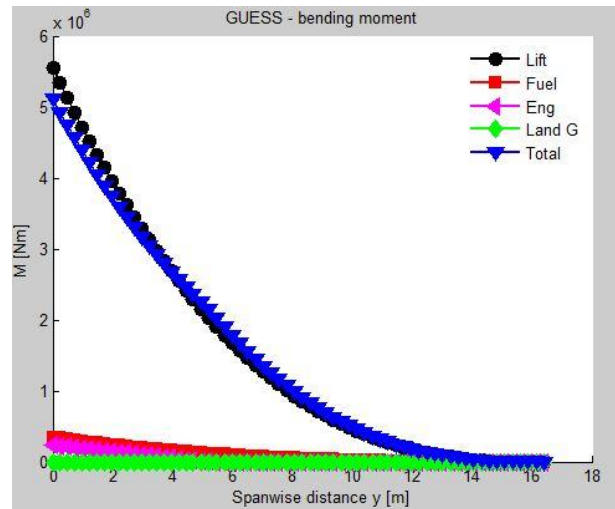


Fig. 82: Bending moment over b/2 V3b

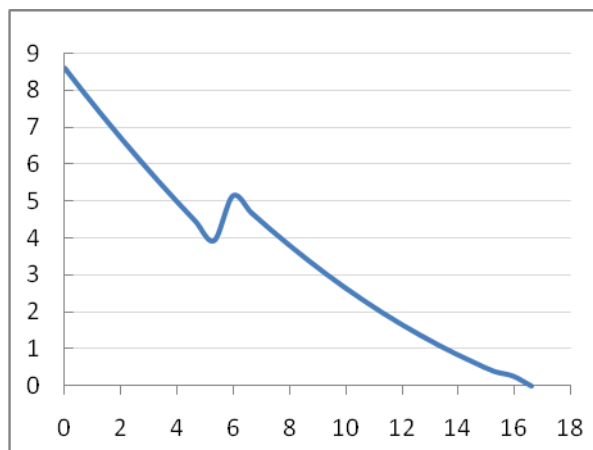


Fig. 83: Shear force on equations

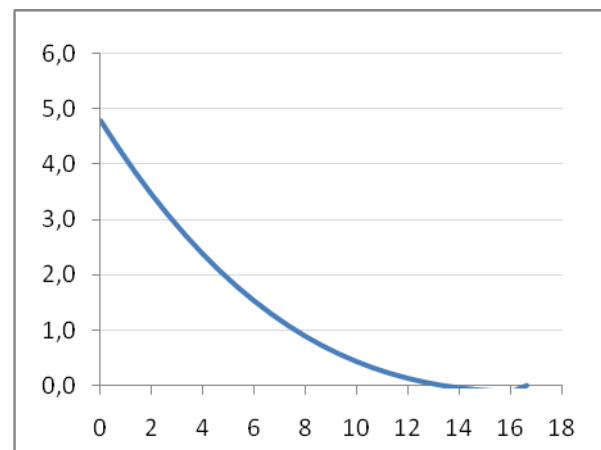


Fig. 84: Bending moment on equations

Via the given equations the whole wing is considered. The results did not deviate much. That is because the input for the weights is similar to the data of GUESS. The small difference can be traced back to the imprecise reproduction of the wing. In the equations the kink is not taken into account.

3.7.3 Implementation in SMARTCAD

After the calculation of GUESS the data for the preparation of the SMARTCAD file can be set. The input for the SMARTCAD tool should be defined via the GUI presented in Fig. 85. First the *Ref. Values* can be defined. This includes the reference chord, the reference span and the reference surface. The values can be found in AMB or via the AcBuilder (*geometry output*). In the present case the reference chord is 3.9066 m, the reference surface 119.9262 m² and the reference span is 33.913 m. In the AcBuilder just the aspect ratio and the reference surface are given. Because of that the reference span has is calculated by the equation:

$$A = \frac{b^2}{S} \rightarrow b = \sqrt{S \cdot \lambda}$$

(3.15)

$$9.59 = \frac{b^2}{119.9262 \text{ m}^2} \rightarrow b = \sqrt{119.9262 \text{ m}^2 \cdot 9.59} = 33.913 \text{ m}$$

An important matter is that all decimal places of the input data are indicated by a point. Under the button *Ref. Values* the aerodynamic settings can be determined as well. In this example for the *vertical symmetry* the ID number 0 is chosen what stands for the full aircraft model. There are two other choices. The ID 1 is for a calculation with the half model which is completely symmetrical. -1 stands for an anti symmetrical calculation. Under the topic *horizontal symmetry* the ground effect can be considered. 0 means no ground effect is taken into account and 1 that it will be regarded. In this case the altitude of the airplane has to be defined. At the last sub-item the user can specify if the calculation is linear or quadratic. 1 stands for linear and 2 for quadratic. For the calculation of the A320 the quadratic calculation is used. To determine the single analysis and their parameters the button *Settings* has to be chosen. For static aeroelastic analysis a number of different flight conditions can be defined. It is necessary for the trim conditions. First the Control Surfaces should be set. Then the number of flight conditions can be fixed. Selecting the values the conditions can be defined. One example is shown on the left side (Fig. 86). Here the second flight condition of three is pictured. The three cases regarded are summarized in the table below (Tab. 11). Only symmetric manoeuvres are calculated in the example of the A320 for getting a first general view of the possibility and handling of NeoCASS.

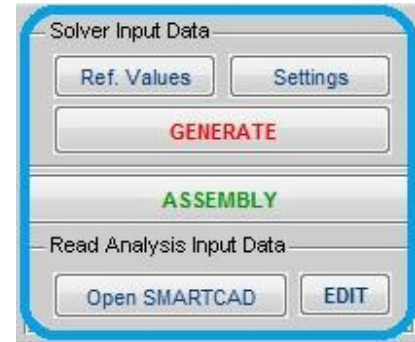


Fig. 85: SMARTCAD Input

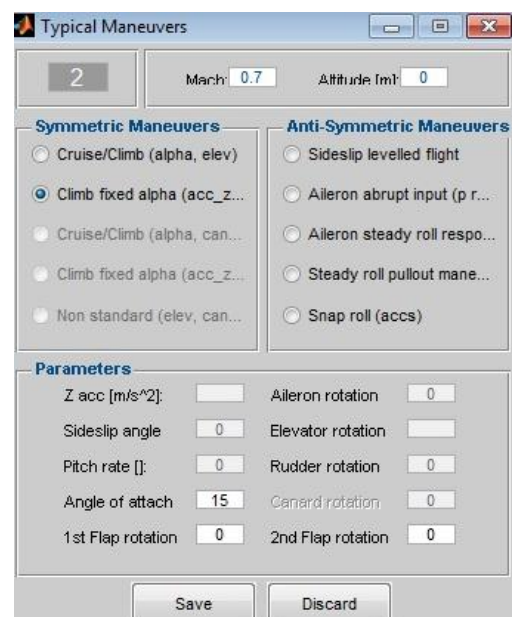


Fig. 86: Flight condition

Tab. 11: Flight conditions

| number | condition | Mach | Altitude in m | AoA in ° | Z acc | Manoeuvre |
|--------|------------------------|------|---------------|----------|-------|--------------|
| 1 | flight | 0.8 | 10000 | 0 | 9.81 | Cruise/Climb |
| 2 | Take off | 0.7 | 0 | 10 | 9.81 | Climb fixed |
| 3 | User defined situation | 0.6 | 5000 | 0 | 25 | Cruise/Climb |

Looking at the *modal analysis* first the *Normalization* (1 MASS, 2 MAX, 3 POINT) has to be defined. If a POINT normalization is chosen the user must provide the Grid Point ID and DOF. ID means Grid Identification Number and DOF the degrees of freedom from 1 to 6. For the example the MASS normalization is used. The number of mode shapes is set at 20 out of 0 to 999999, to get the first 20 mode shapes.

For flutter analysis it is possible to decide between a V-g plot for a single flight condition or a flutter envelope for a defined number of Mach values. In both cases the number of mode shapes and the number of reduced frequencies should be set. Also the modal base and the mode tracking frequencies should be selected. For the A320 the same number of mode shapes as at the modal analyses is taken. The number of reduced frequencies is set to 8 (0.001; 0.01; 0.05; 0.1; 0.5; 1; 1.5; 2). For the modal base all frequencies are selected, for the mode tracking the first six are omitted.

When selecting the *V-g plot* analysis the programme asks for the maximum speed for the flutter calculation, the maximum V step (number of steps used during iterative mode tracking), the air density and the Mach number of the aircraft. The values are shown in the following table (Tab. 12):

Tab. 12: Parameters V-g plot

| parameter | value |
|-------------|--------------------------|
| Max. speed | 350 m/s |
| Max. V step | 50 m/s |
| Density | 0.3367 kg/m ³ |
| Mach number | 0.76 |

Choosing the *flutter envelope* the user just has to set the number of Mach values for which the flutter envelope is computed. The values can be defined in a table which shows up.

When all input data for the settings are given, together with the *Ref. Values* a file of the SMARTCAD parameters can be generated. Creating the final SMARTCAD input an assembly of the GUESS file and the just generated parameter file is needed. Before starting the calculation the settings of the structural solver can also be defined. In the present case the default settings are left. Otherwise it is possible to choose between a linear beam model, a non-linear beam model and an equivalent plate model for the structure. Taking the equivalent plate model an aspect ratio has to be added. Choosing the non-linear beam model the convergence tolerance, the load steps, the under relaxation factor and the sub- iterations should be set. Under the field *Settings* the *RUN* options can be selected: On the one hand an

interactive analysis, on the other hand an automatic analysis. In Fig. 87 the GUI of the Settings is displayed.

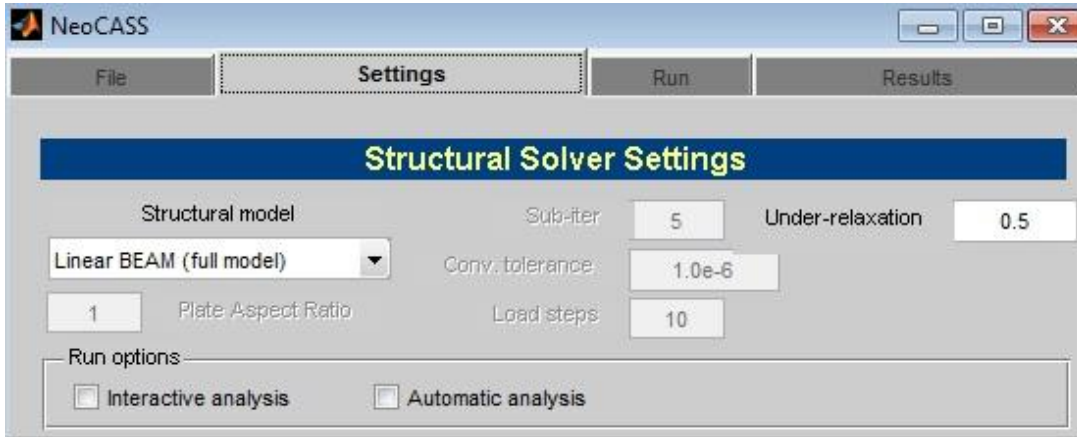


Fig. 87: GUI structural settings

Depending on the settings of the solver inputs the analytical possibilities are displayed. Under the field *Run* the wanted calculation can be started (Fig. 88). A static, modal and flutter calculation is run for the A320.



Fig. 88: GUI Run

3.7.4 Evaluation of the Results of SMARTCAD

The representation of the results is accomplished by the option *Results*. The according GUI is already depicted in Fig. 80. The several buttons give the possibility to plot the results that the user wants to see. Their labelling is precise. With the field *Scale* the results can be depicted more clearly. The deflection of the structural elements is multiplied by the scale factor and so the user can see the deformation more clearly. The field *Total frames* defines the number of pictures that are used for generating a mode animation. To specify which mode should be

shown to plot the deformed model, the field *Selected set* has to be used. The mode number has to be inserted.

The steady static analysis for the deformation of the aircraft is not available. The input data was checked conscientious. Currently, CFS Engineering deals with this problem to find a solution. As soon as the problem is solved the results can be checked. In this thesis it was planned to check the results with the help of the tool Aeroelastik by Torben Koberg. This tool is a result of a Master Thesis on the HAW Hamburg.

The first calculation, that is selectable, is the modal analysis. 20 frequencies are extracted as determined before under *settings*. These frequencies and the resulting deformation can be plotted. Fig. 89 depicts the model without a structural deformation. Next to this figure the deformation for mode shape 1 is presented (Fig. 90). The frequency is $1,947 \cdot 10^{-5}$ Hz. The scale factor is 100. The yellow nodes represent the deformed shape, the turquoise nodes the shape without deformation.

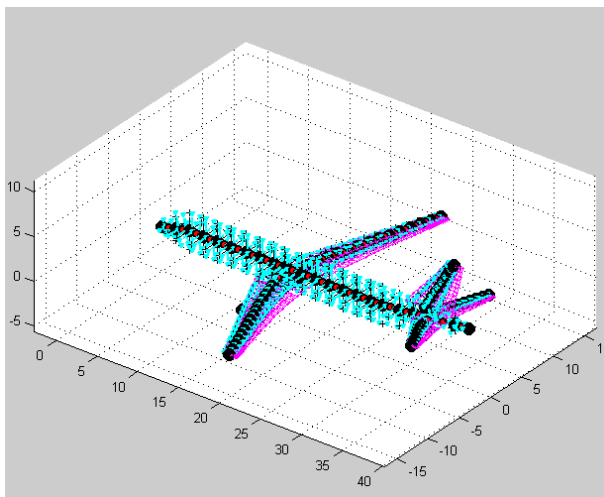


Fig. 89: Model

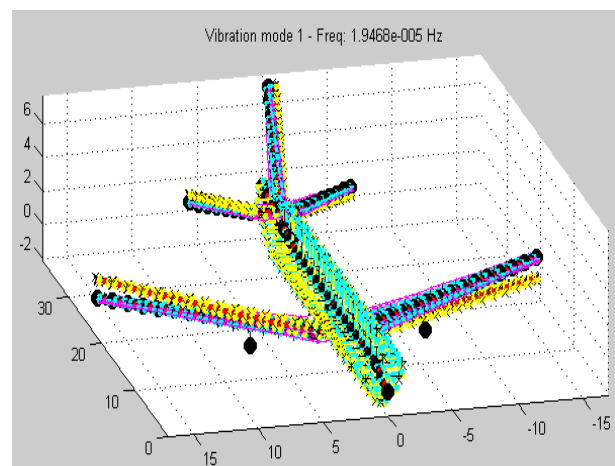


Fig. 90: Vibration mode 1

The deformation of the single modes will be important for a later analysis refers to the flutter computation.

The flutter calculation produces a V-g plot, where the damping g and the frequency f are plotted above the velocity. Thus the velocity is determined. The first six modes are rigid body modes. For the flutter calculation of a free aircraft the elastic body modes are required. The modes are defined at the *settings* for mode 7 to 20. Fig. 91 depicts the result of the flutter analysis. The striking modes are the modes 7 (0,97829 Hz), 8 (1,3812 Hz), 9 (2,5774 Hz), 12 (3,1785 Hz), 13 (3,3859 Hz) and 14 (3,5088 Hz). A closer look at these modes is done for a better understanding of the plot. Tab. 13 summarized this analysis.

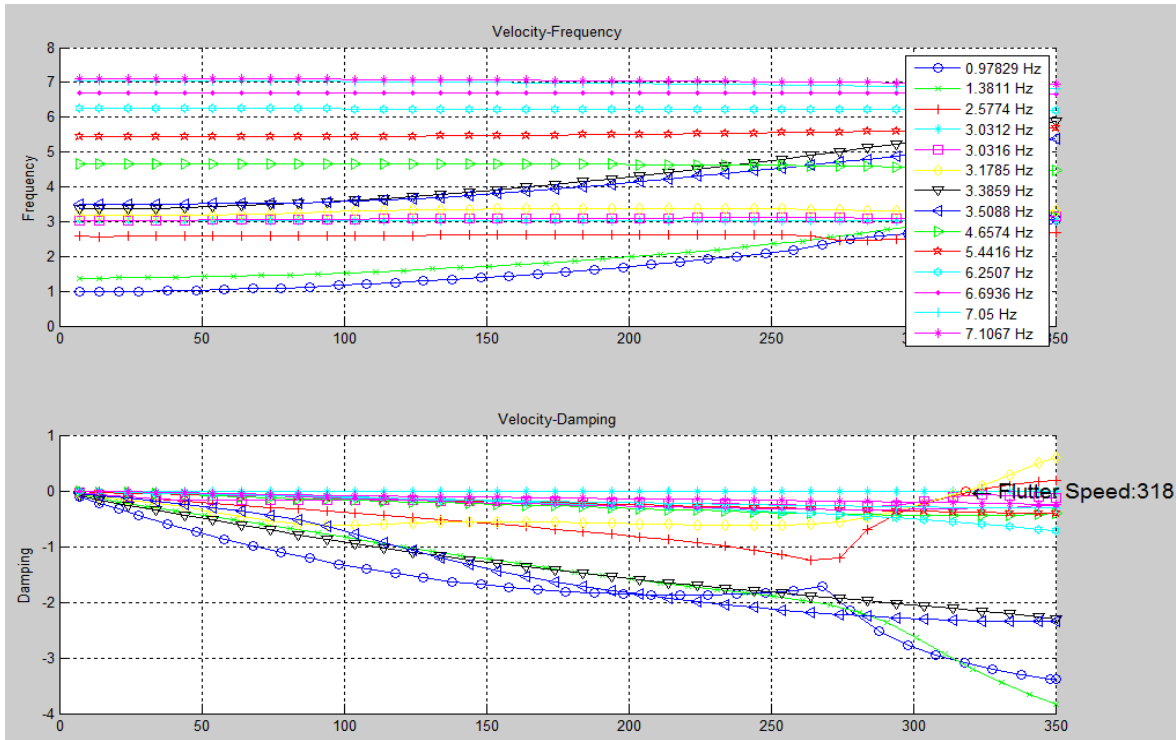


Fig. 91: V-g plot flutter analysis

A precise recalculation of the flutter phenomena is not possible. Therefore the course of the graph is estimated and analysed. The comparison is done by the help of generalised examples from the book Aeroelasticity (**Bisplinghoff 1983**). There are two statements that are important:

It is a general rule that the modes with the lowest frequencies are the ones which should be examined for evidence or flutter. (Bisplinghoff 1983)

Experiences have shown that either “first bending” or “first torsion” leads to the critical flutter mode. (Bisplinghoff 1983)

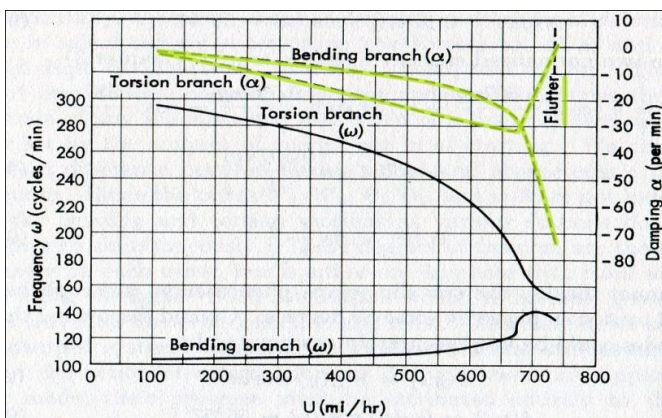


Fig. 92: Characteristic ratio of flutter and (**Bisplinghoff 1983**)

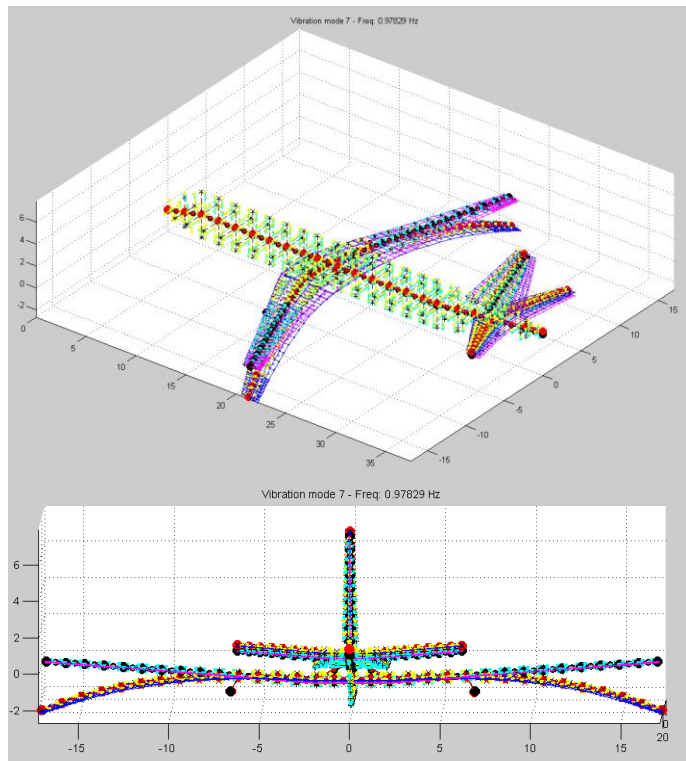
Moreover the graphs showed in Fig. 92 present the ratio of damping and frequency that is quite characteristic for all metal wings with stressed-skin construction.

Tab. 13: Mode description

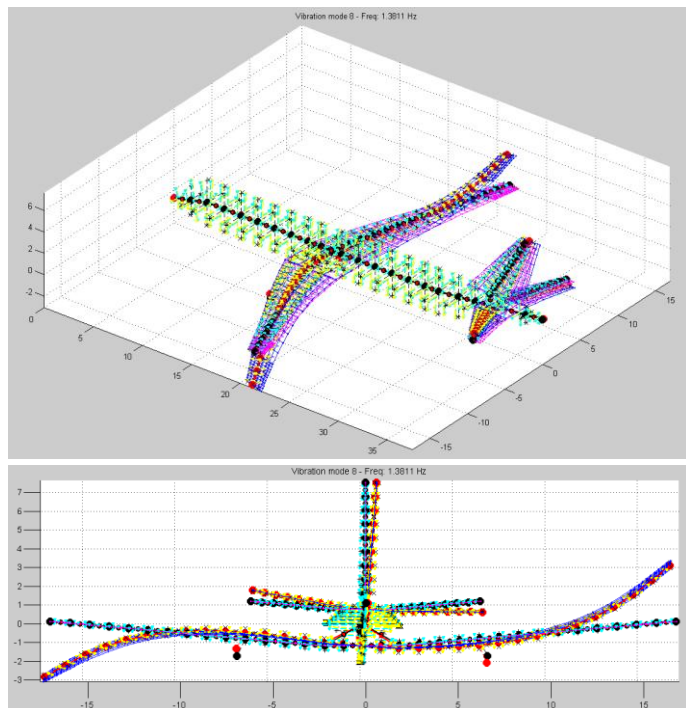
description

Vibration mode 7 represents a frequency of 0,97829 Hz (blue line with blue circles) . In Fig. 93 the first cantilever bending of the wing is seen. This mode does not go into an unstable state. As seen in Fig. 91 the damping does not approximate zero. Rather than the damping increases as from a certain speed (270 m/s). A closer look on Fig. 92 and the results of the flutter calculation of the A320 shows that the characteristic course of the damping for bending corresponds with the graph in the V-g plot of the A320.

visualisation of the mode shapes

**Fig. 93:** Mode shape 7 - deformed model

For 1,3812 Hz the first unrestrained anti-symmetrical bending appears. As seen in Fig. 94 the wing and the tail are deformed. Mode 8 does not go in an unstable state. The green line with the green star shows that. The curves for frequency and damping have the characteristic tendency.

**Fig. 94:** Mode shape 8 - deformed model

Mode shape 9 with a frequency of 2,5774 Hz results in a coupled deformation of Torsion and a second unrestrained symmetrical bending of the wing. The horizontal tail oscillates in a bending mode. The red line with the + (Fig. 91) shows that at first the mode is a stable one. At a speed of 270 m/s the mode shape changes more and more into an unstable one. The damping runs to zero and so at a speed of 318 m/s the aircraft goes into an unstable state. If one compares the graph for torsion of Fig. 92 with the course of the results of mode 9 (Fig. 91), the graphs match qualitatively.

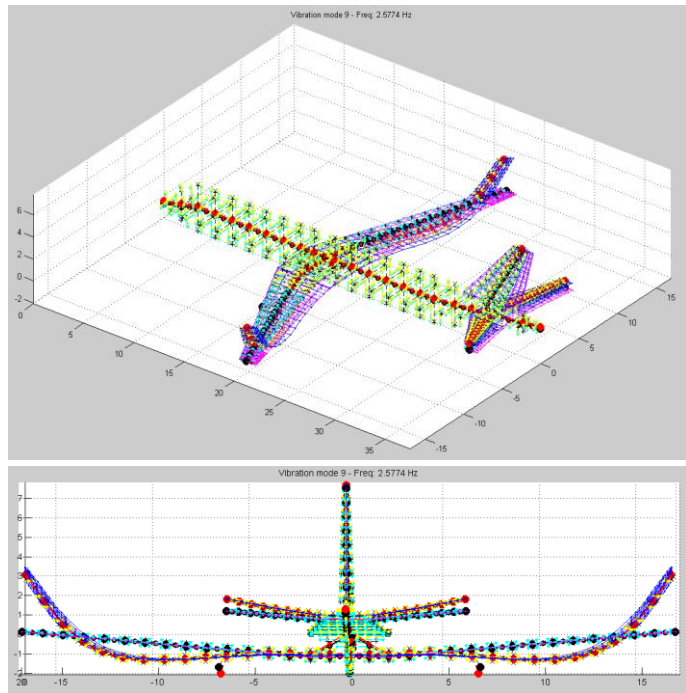


Fig. 95: Mode shape 9 - deformed model

Also mode 12 results in an unstable state. Here unsymmetrical bending and torsion are coupled. Both the wing and the horizontal tail are involved, while the horizontal tail has the main part. In Fig. 96 that is depicted quite well. The critical flutter speed is reached at 318 m/s.

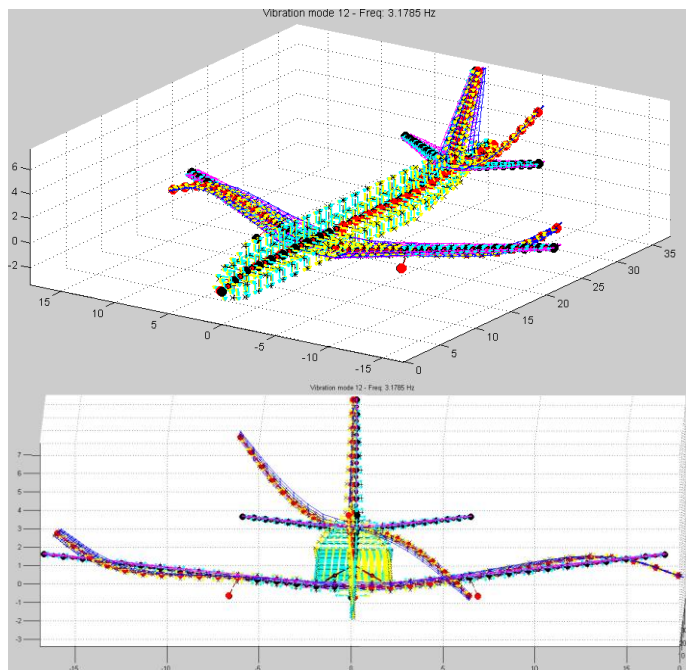


Fig. 96: Mode shape 12 - deformed model

Vibration mode 13 represents a frequency of 3,3859 Hz. Here the horizontal tail is deformed under bending. Mode 13 goes not in an unstable state. As seen in Fig. 97 the damping does not approximate to zero. The damping graph has a continuous development.

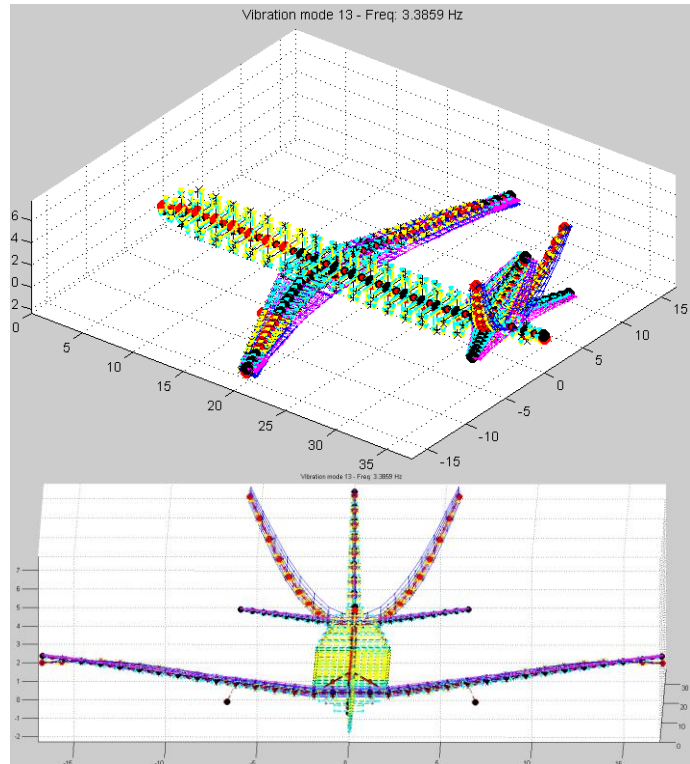


Fig. 97: Mode shape 13 - deformed model

An unsymmetrical deformation is seen in Fig. 98. Here torsion and bending are coupled, both for the horizontal tail and the wing. Mode shape 14 has a frequency of 3,5088 Hz. It does not go into an unstable state. The damping course is depicted by a blue line with blue tetrahedral in Fig. 91.

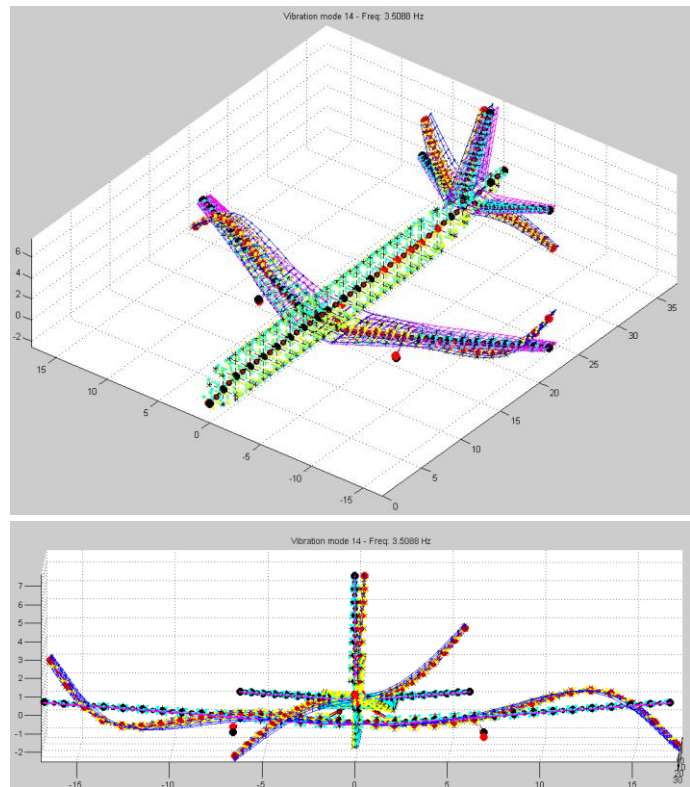


Fig. 98: Model shape 14 - deformed model

The vibration of the engine is not computed separately. The engine is modelled as mass and is included to the wing modes.

3.8 A320 in FCSDT

3.8.1 Implementation

The first thing that the user has to do is to define a new project. Afterwards one of the 5 integrated tools can be chosen. The FSCA tool is the one that is needed at the beginning when starting a new project. For the A320 the default flight control architecture (ub90.m) is loaded. Now single components can be chosen and edit or new one can be added. The graphical user interface is depicted in Fig. 99. It is obvious, that the structure of the flight architecture interface is well done and the user can easily understand the procedure.

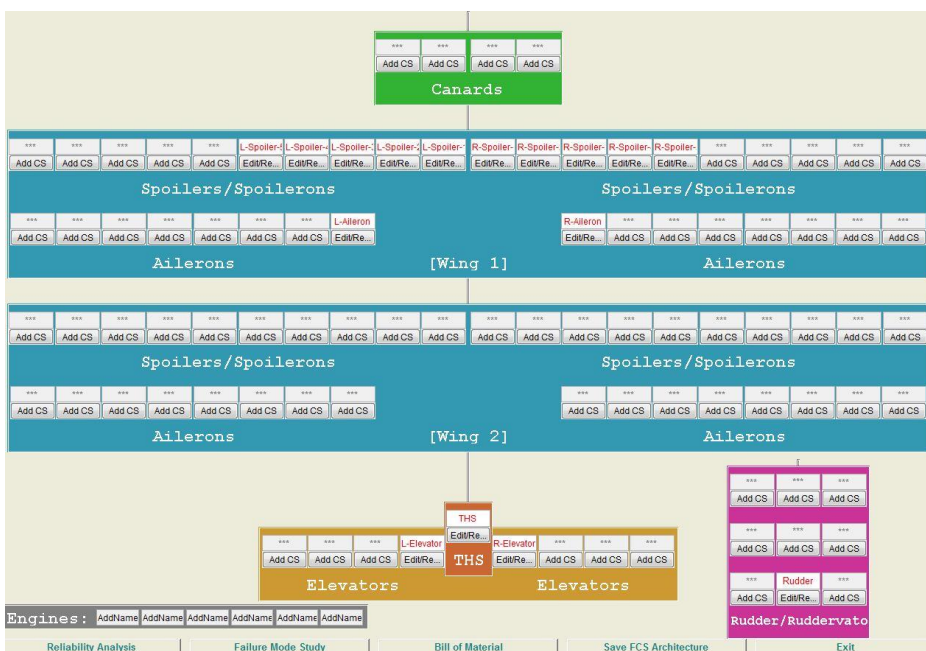


Fig. 99: GUI FSCA

Based to the architecture from the A320 represented in Fig. 100 the single components are inserted to the FCSDT tool.

The settings for the spoiler and the THS are left at the default values. The aileron, elevator and rudder settings are changed in order to reflect a fly by wire configuration. Therefore the failure rate has to be defined. This is necessary for later analysis.

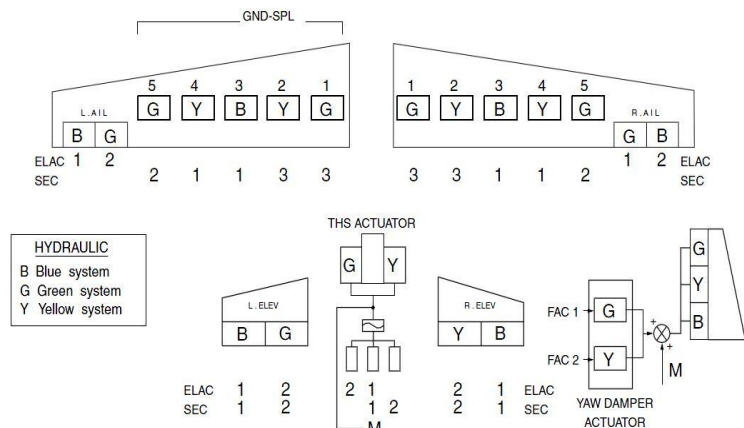


Fig. 100: FSCA A320 (Briere 2001)

The A320 was one of the first aircraft that replaced the manual flight control by a fly-by-wire (FBW) system. Before, the control movements were transmitted via hydraulic systems, push rods or steel cables. For the A320 flight controls given by the pilot, are converted into electronic signals. The signals are sent through wires to computers. With the help of the flight control computers the instructions for the actuators that are placed on the control surfaces are determined. From that the required aircraft responds results. The development of the fly-by-wire systems enables the integration of an automatic help system for the stability, where the computer can amend the flight attitude without an input of the pilot. Fig. 101 shows a sketched illustration of the system.

ELECTRICAL FLIGHT CONTROLS (FLY BY WIRE)

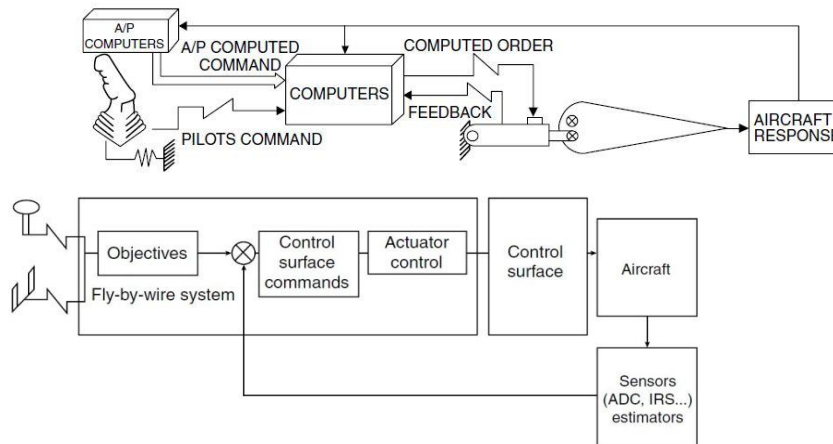


Fig. 101: Fly by wire (Briere 2001)

The definition of the control system architecture begins with the selection of the according component. Representatively the definition of the left aileron is documented. Clicking on the according button, a new window appears. Under *build in architecture* the system for the control can be set, for example fly-by-wire, fly-by-cable or fly-by-light. A set of the options can be found in the FCSDT manual (Maheri 2008). In this window the failure rate can be defined as well. The structure is shown in Fig. 102. Below this picture the visualisation via the tool is added (Fig. 103). With the help of this feature the understanding of the system is easier.

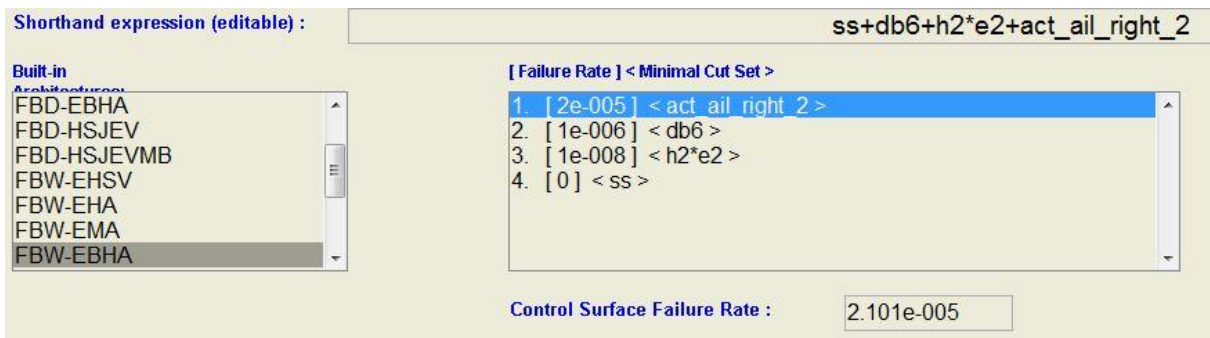


Fig. 102: Build up FCSA

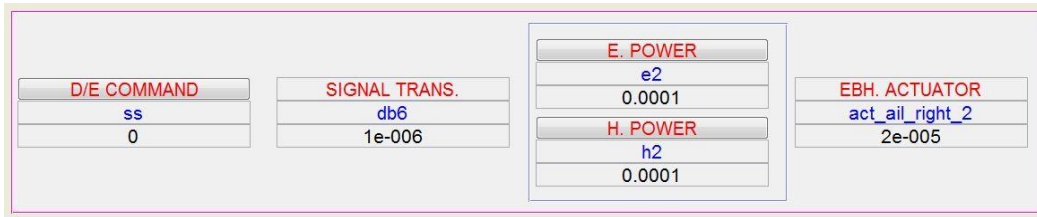


Fig. 103: Failure rate definition for the aileron

All components that are implemented into the process are listed and allocated with their own failure rate. The first row defines which component is meant, in the second row the name for the component can be set and the third row contains the failure rate. Here, the default failure rates for the system components are chosen. The window for the control surface definition can be closed after saving the changes. When opening this component again it is a little bit confusing that the *build in architecture* is removed to the initial settings. The input information which was defined before is still stored. It is just for the build up or modification. The old input will be overwritten by saving the new build structure. It is a bit circumstantial that if one just wants to change one parameter or add one more actuator to the system one has to build up the whole system from the beginning.

The FCSA is the basis for the *reliability analysis*. The handling of this tool is checked using the example of yaw control. It is a simply structured tool. The desired control action can be chosen. For it the failure probability is computed and with the help of a linked diagram the result is given. Fig. 104 shows the *reliability analysis* for the yaw control. The failure rate is about $2,1 \cdot 10^5$. Moreover the involved components and their failure rates are listed.

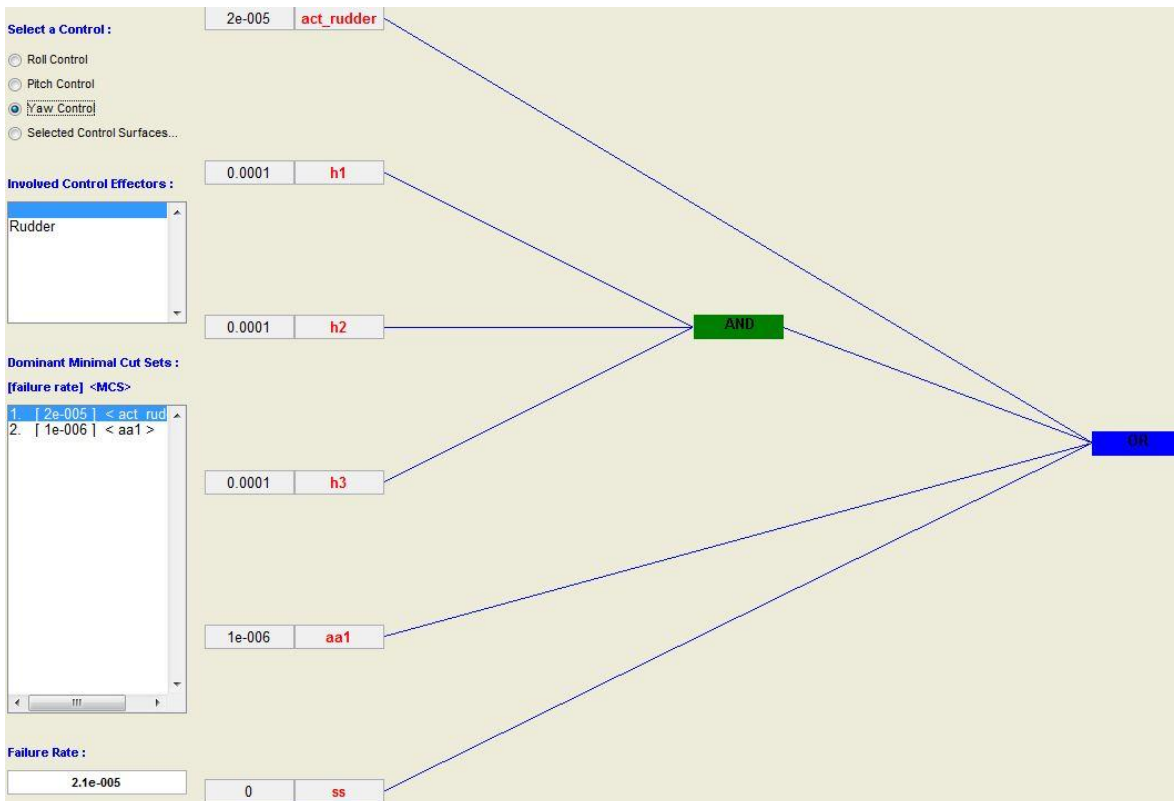


Fig. 104: Reliability analysis

The next button that can be selected is called *Failure Mode Study*. With this tool the user can select a series of control surfaces and engines as failed components. The vector of failed control surfaces or engines will be passed to SCAA or FSIM for failure mode study. The selected elements are engine 2 and L-aileron.

Under the FCSA interface the bill of material can be saved. The data is transmitted to an excel sheet. Because of that a running excel version is needed. The computer on which CEASIOM is installed has no licence for Microsoft Excel. It works with an Open Office version called calc. The FCSDT tool cannot communicate with this programme and so a problem appears. The bill of material cannot be saved or displayed.

The next sub tool of FCSDT is called SCAA. During the reading of the *.xml file from the project folder problems occur. Moreover the graphical user interface does not correspond with the GUI shown in the manual. Further work with this program results in following message:

Warning:

figure JFrame property will be **obsoleted in a future release**. For more information see the JFrame resource on the MathWorks Web site.

By trying to change the input data to the values determined in the previous CEASIOM tools further error messages appear. Therefore the sub tool cannot be used.

LTIS relates to SCAA and the bill of material. The computations are based on the results of these two files. Because they are not available, the tool LTIS cannot be started.

The tool CLS - control laws/protection can be used. The control laws and protections for the A320 are taken from the avionic handbook chapter 12 (**Briere 2001**). Fig. 105 shows the protection values of an A320. These conditions are included in the CLS tool. Depending on pitch roll and yaw in different flight phases the laws can be defined. As an example the laws and protection for the pitch are displayed in Fig. 106, Fig. 107 and Fig. 108.

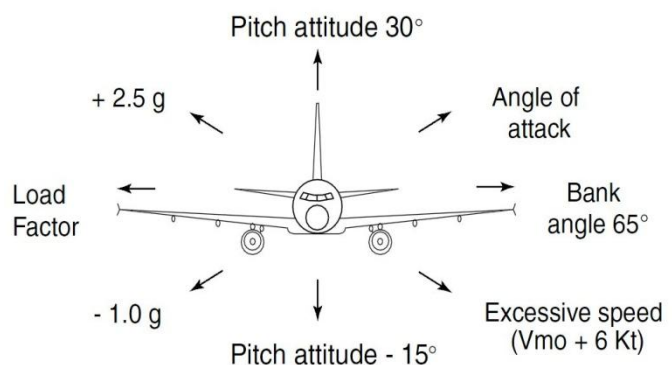


Fig. 105: A320 flight envelope protection (**Briere 2001**)

The first step is to select the attitude for which the law or the protection should be defined. Furthermore the flight phase has to be set. After that the user has to decide if the angle of attack, the Mach number, altitude or the vertical load factor is the determinant. The name can be given via the input field. Fig. 106 gives an overview of this procedure.

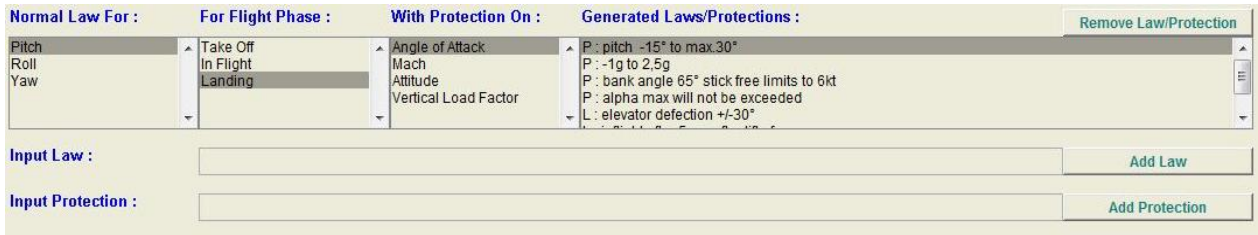


Fig. 106: Options for laws and protections

Fig. 107 presents the defined laws.



Fig. 107: Definition of the laws

Fig. 108 summarises the placed protections.

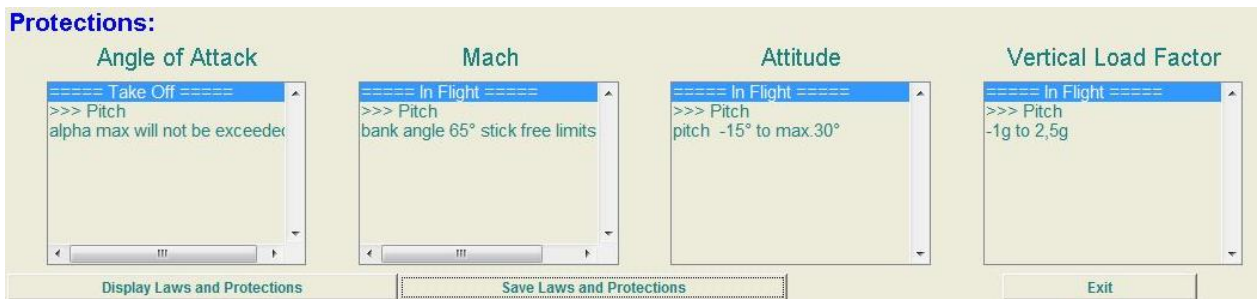


Fig. 108: Definition of the protections

The flight simulation tool of the FCSDT tool does not work, because the input data is not available.

3.8.2 Discussion on Practicability of FCSDT

The FCSDT tool is still in the process of development. The structure of the tool is understandable. Unfortunately, it is not possible to use all sub tools of the FCSDT to give a factual assessment.

4 Analysis of a Shoulder Wing Aircraft

4.1 Description of the Configuration

Based on a project of Aero called Airport 2030 a shoulder wing aircraft configuration is examined. The reason for that is a better ground handling and so a time saving of several minutes. This allows the reduction on ground-handling costs and an increase on aircraft utilization (**Krammer 2010**). The new shoulder wing aircraft model is named A320 SW. Therefore the A320-210 serves as reference airplane.

At the beginning of the analysis of the A320 SW, the A320 – 210 is precisely modelled in the A-C-Preliminary Sizing tool used in the lecture *Aircraft Design* of Prof. Scholz.

The preliminary sizing tool is structured as follows: It consists of four excel sheets. The first sheet includes the calculation for the flight phases approach, landing, take-off, 2nd segment and missed approach. Here, the requirements of the single flight phases have to be applied, for example landing field length, maximum lift coefficient in landing and weight ratio of landing and take-off. The second sheet deals with the maximum glide ratio in cruise and with an important characteristic of the flight. In the third sheet the calculation for cruise, masses and the matching chard takes place. Characteristics of the engines have to be set. Also the cruise Mach number should be defined. With the help of this data the matching chard is produced. Here the design point is depicted. Depending on this design point, which defines the wing loading and the thrust to weight ratio, the masses are determined. The reason for the rebuilding of the A320 – 210 with this tool is to get comparable data for the design of the shoulder wing in PreSTo. Also, the data that is available from Airbus is implemented on this way and some unknown values are worked out. To obtain traceable results, the A320 – 210 was rebuilt in different versions. That means the aircraft was computed with both the CFM56 engines and the V2500 engine, using the according characteristics. Moreover the aircraft was rebuilt with different payloads and the corresponding ranges. This data of the payload range diagram from Airbus refers to cruise conditions on ISA +10 and a Mach number of 0.76. Also the international reserve of en route 10% flight time reserve is given. The condition for ISA +10 leads to a factor for a thrust at cruise to a thrust to take-off ratio of 0.925. The reason for that is that for every 1 K above ISA conditions the thrust can be reduced by 0,75 % (**Raymer 1999**). Here, it is 10 K and so 7,5 %. In Tab. 14 the constant values are shown, on the one hand the given values with the reference and on the other hand the values that are worked out. Another special case is the glide ratio. Here the program computes a higher value than used. The Airbus data gives the same value without any effects of high speed for a Mach number of about 0.1, but for this calculation the cruise Mach of 0.76 serves as basis. The reason for the higher value of the A-C-Preliminary sizing tool is, that phenomena like wave drag are not considered in excel sheet 2 and just the C_{DO} is taken into account. For the redesign the value given by airbus for 0,76 Mach is used. Moreover the values of the mission fuel fraction are

adapted. The values given by Roskam (**Roskam 1989**) are from the year 1989 and very conservative. Besides the decisive parameters for the rebuilding of the A320 are given by Airbus and just the values of the mission fuel fraction do not fit. Now the effectiveness between climb and take-off is the same and amounts 0,995 as the effectiveness of decent and landing has the same value of 0,992. For a closer look the sheets of the A-C Preliminary sizing tool are attached on the CD belonging to the Master Thesis. All important values that are needed for the continued work are listed in Tab. 14.

Tab. 14: Values of A-C Preliminary sizing

| Characteristics | | Given by airbus data (Airbus 2003) | Worked out |
|-----------------|------------------------|--|------------|
| Excel Sheet 1 | Landing field length | 1700 m | |
| | $C_{L,max,L}$ | | 2,9 |
| | m_{ML}/m_{TO} | 0,878 | |
| | m_{MTO}/S_W | 601 kg/m ³ | |
| | Take-off field length | 2200 m | |
| | $C_{L,max,TO}$ | | 2,07 |
| | Thrust to weight ratio | 0,309 | |
| Excel Sheet 2 | Glide ratio | 17,7 | |
| Excel Sheet 3 | Estimated V/V_m | | 1,01 |
| | m_{OE}/m_{MTO} | 0,550 | |
| | Mach Cruise | 0,76 | |

The A320 SW has to fulfil the same requirements and the same missions like the A320 - 210. One difference is the type of the engine. The high wing airplane should be powered by a turboprop and not by a jet engine. To get fitting data for the aircraft, the Preliminary Sizing tool PreSTo is used. With the help of this tool the A320 SW is designed with props by meeting the same requirements for range and payload like the A320 - 210. Before starting the work with the PreSTo tool parameters for the turboprop and the cruise speed have to be defined. The parameters for the turboprop are ascertained by the comparison of turboprop aircraft that are developed in the last years and have nearly the same or a larger MTOW (see Tab. 15).

Tab. 15: Comparison of turboprop aircrafts

| | A400M | Antonow An 70 | Antonow An12BP | Tupolev TU 114 | Tupolev TU 95MS15PS | C13 Hercules |
|-----------------------------|------------------------|-----------------------|----------------------|----------------------|-----------------------------|---------------------|
| MTOW in tonnes | 141 | 135 | 61 | 171 | 156 | 70,3 |
| Aspect ratio | 8,5 | - | 11,86 | - | 8,7 | 10 |
| Turboprop | TP400-D6- Turboprop | Iwtschenko AI-24WT | Iwtschenko AI-20M | Kusnezow NK-12 MV | Kusnezow NK-4 2TW- 2F | Allison T56-A-15 |
| diameter - prop in meter | 5,5 | 4,49 | - | - | - | - |
| power in kW | 8 250 | 10 440 | 3 126 | 11 000 | 9 193 | 3 430 |
| number of engines | 4 | 4 | 4 | 4 | 4 | 4 |
| cruise speed | 0,695 | 0,694 | 0,62 | 0,72 | | 0,47 |
| max speed | 0,73 | 0,73 | | 0,82 | 0,84 | |
| SPC in mg/W/h | 228 | 307,8 | 265,5 | 217 | - | 325,9 |

The data are collected from the internet. The green marked fields in Tab. 15 show parameters that are used in PreSTo. The data for the power that can be reached serves as reference value. The cruise speed is calculated on another way, but the data from the table shows if the later determined value is realistic.

For the assessment of the cruise speed the time saving at the ground handling for a shoulder wing aircraft is important. The time that can be saved can lead to a smaller cruise mach number. The time saving is set to 10 minutes (**Krammer 2010**) during the ground handling. These 10 minutes have to be allocated to the flights during one day. The calculation of the cruise speed is based on the flight missions of an A320. In Tab. 16 the different flight missions are summarized.

Tab. 16: Flight mission

| | typical flight missions |
|---|------------------------------|
| A | 8 x 1,5 hours |
| B | 2 x 4,5 hours, 2 x 1,5 hours |
| C | 3 x 4,5 hours |
| D | 1 x 5 hours, 1 x 1,5 hours |
| E | 1 x 5 hours, 1 x 1 hours |

A detailed allocation and the needed cruise Mach number are shown in Tab. 17. The velocity v is the result of the determined endurance and the range of the A320 at 0,76 Mach.

Tab. 17: Determination of the cruise Mach number

| | | time saving | | endurance | altitude v | 11000 | 10000 | 9000 | 8000 | 7000 | 6000 |
|---|-----------|-------------|------------|------------|---------------|-------|-------|------|------|------|------|
| | | per day | per flight | | | Mach | | | | | |
| A | 8 flights | 70 min | 8,75 min | 98,75 min | 204 m/s | 0,69 | 0,68 | 0,67 | 0,66 | 0,65 | 0,65 |
| B | 2 flights | 10 min | 5 min | 95 min | 212 m/s | 0,72 | 0,71 | 0,70 | 0,69 | 0,68 | 0,67 |
| | 2 flights | 20 min | 10 min | 280 min | 216 m/s | 0,73 | 0,72 | 0,71 | 0,70 | 0,69 | 0,68 |
| C | 3 flights | 20 min | 6,67 min | 276,67 min | 219 m/s | 0,74 | 0,73 | 0,72 | 0,71 | 0,70 | 0,69 |
| D | 1 flight | 2 min | 2 min | 92 min | 219 m/s | 0,74 | 0,73 | 0,72 | 0,71 | 0,70 | 0,69 |
| | 1 flight | 8 min | 8 min | 314 min | 219 m/s | 0,74 | 0,73 | 0,72 | 0,71 | 0,70 | 0,69 |
| E | 1 flight | 2 min | 2 min | 62 min | 217 m/s | 0,74 | 0,72 | 0,71 | 0,70 | 0,69 | 0,69 |
| | 1 flight | 8 min | 8 min | 314 min | 219 m/s | 0,74 | 0,73 | 0,72 | 0,71 | 0,70 | 0,69 |

The parameter for the PreSTo computation is a cruise Mach number of 0,69. This speed can be realized by the turboprop engines that are used at aircrafts today and fulfil the requirements for flight mission A. The other flight missions are also feasible but then the altitude has to be adapted. Before starting with PreSTo the fuel fractions are also changed as in the tool A - C preliminary sizing. For turboprop aircrafts the values are modified as shown in Fig. 109.

| | | |
|-----------------------------|-----------------|-----------|
| Fuel-Fraction, engine start | $M_{ff,engine}$ | 0,999 [-] |
| Fuel-Fraction, taxi | $M_{ff,taxi}$ | 0,998 [-] |
| Fuel-Fraction, take-off | $M_{ff,TO}$ | 0,995 [-] |
| Fuel-Fraction, climb | $M_{ff,CLB}$ | 0,995 [-] |
| Fuel-Fraction, descent | $M_{ff,DES}$ | 0,992 [-] |
| Fuel-Fraction, landing | $M_{ff,L}$ | 0,995 [-] |

Fig. 109: Fuel fraction turboprop

The results of PreSTo and the comparison with the reference aircraft are shown in Tab. 18.

Tab. 18: Comparison with reference aircraft

| Components | A320 SW PreSTO | A320 – 210 |
|-----------------------|---|---|
| propulsion | turboprop | Jet CFM56 |
| number of engines | 2 | 2 |
| Wing location | shoulder wing aircraft | Low wing aircraft |
| Wing geometry | swept taper wing Sw= 98,4 m ² | Swept tapered wing Sw = 122,4 m ² |
| Mach cruise | 0,69 | 0,76 |
| Cruise altitude | 9 881 m | 11 800 m |
| Landing field length | 1 700 m | 1 700 m |
| Take off field length | 2 200 m | 2 200 m |
| Range at max. Payload | 1 500 NM | 1 500 NM |
| MTOW | 69 000 kg | 73 500 kg |
| Max.Payload | 20 000 kg | 20 000 kg |
| Number of Passanger | 150 | 150 |
| fuel weight | 11 975 kg | 12 500 kg |

All requirements are met, there for a fuel saving of 4,2 % per flight is possible. This result is for an aircraft with 2 turboprop engines that can fulfil all flight missions that are given. It is also possible to equip the aircraft with 4 engines. For that case the fuel saving increases to 12,7 % per flight and a higher altitude is possible. By correcting the altitude to lower heights it is also possible to save more fuel. Both preliminary sizing results from PreSTo are shown in Appendix D. The version with 2 engines is analysed more precisely with CEASIOM. But also the shoulder wing with 4 engines is implemented into the AcBuilder. It can be used in future works. For the moment the shoulder wing with 2 turboprops is more interesting because it is closer to the reference aircraft A320. The data of PreSTo serves as input for the AcBuilder. In the future it will be possible to produce an *.xml file for input in CEASIOM directly from PreSTo. The geometric data for the wings, the vertical tail and the horizontal tail with the according airfoil is given by PreSTo. Even the control surfaces are given. For the fuselage the data from the Airbus A320 -210 is taken.

4.2 Implementation in CEASIOM

4.2.1 AcBuilder

The data of PreSTo are inserted without any further problems. But there is an uncertainty refers to the definition of the engine. First of all the user can define the type of the engine. In the present case it is a turboprop engine. After that definition the GUI does not change and therefore the power has to be transmitted into thrust.

$$\frac{\text{Power of the turboprop}}{\text{velocity of the aircraft}} = Th_E \quad (4.1)$$

The maximum power of the engine was defined with 9700 kW per engine at the PreSTo tool. The velocity for cruise is about 207 m/s. The take-off velocity amounts 70 m/s. So, the maximum thrust is required for the take-off. When these values are inserted in the equation, the thrust is about 140 kN per engine. It implies the thrust to weight ratio that is also needed for the AcBuilder input. In PreSTo a MTOW of 68 800 kg is given. The equation for the thrust to weight ratio is:

$$\frac{Th}{W} = \frac{2 \cdot Th_E}{MTOW \cdot 9,81 \frac{m}{s}} = 0,4149 \quad (4.2)$$

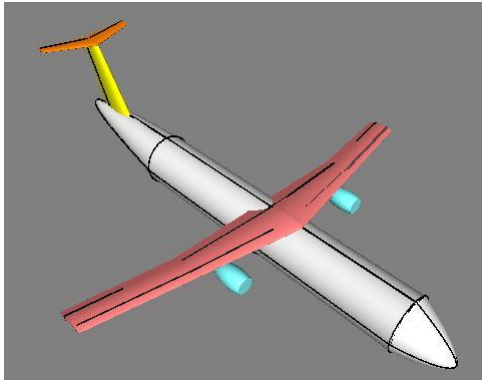


Fig. 110: SW – geometry

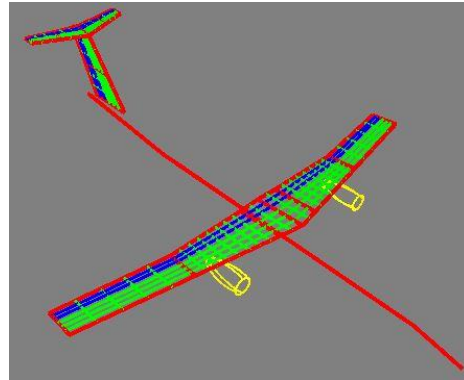


Fig. 111: SW - aero panel

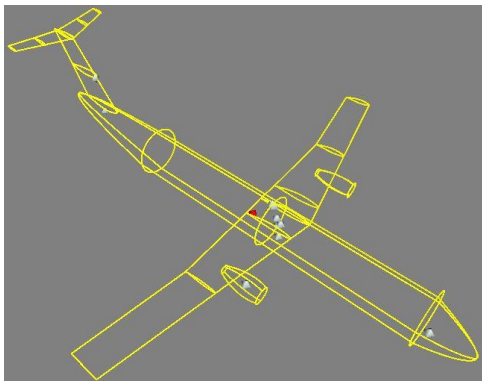


Fig. 112: SW - centre of gravity

| Parameter | Unit | Value |
|-------------------------|----------------|---------|
| taper_ratio | | 0,70316 |
| planform_AR | | 11,3893 |
| Weighted_area | m ² | 85,1413 |
| LE_sweep | deg. | 12,21 |
| MAC | m | 2,7618 |
| relative_apex | | 0,325 |
| Orig_root_chrd_at_ac_CL | | 4,1048 |
| Half_chord_sweep | deg. | 10,5247 |
| Quarter_chord_sweep | deg. | 11,3698 |
| non_dim_MAC_y_bar | | 0,47095 |
| Weighted_aspect_ratio | | 11,3893 |
| mean_thickness | | 0,1 |

Fig. 113: SW - reference data

Fig. 110 to Fig. 112 depict the visualisation of the AcBuilder sub-tools. The geometry is a result from the PreSTo input and hence the centre of gravity is computed. Moreover the aero panels are defined to get an even distribution. In Fig. 113 the reference data of the shoulder wing is summarized. This data is important for later calculations and for the input in NeoCASS.

The results of the weight estimation are compared with the estimation of PreSTo and with the reference aircraft A320-210 (Tab. 19).

Tab. 19: SW - weights

| | SW - AcBuilder | SW - PreSTo | A320-210 |
|---------------------|----------------|-------------|----------|
| MTOW in kg | 70 550 | 68 800 | 73 500 |
| OEW in kg | 46 700 | 36 800 | 40 500 |
| max. Payload in kg | 15 300 | 20 000 | 20 000 |
| max. Zero fuel mass | 62 000 | 56 800 | 60 500 |
| fuel in kg | 8 500 | 12 000 | 12 500 |

It is obvious that a weight saving can be realised in all sectors, compared with the A320 -210. The result of the AcBuilder deviates from the results of PreSTo. Here the same problem appears as described in chapter 3.2.2. The estimated weight for fuel and maximum payload is not right and therefore the OEW and MTOW deviate.

4.2.2 SUMO

The work with SUMO is without any difficulties. As for the A320 the fuselage given by the *.xml file of the AcBuilder is replaced by a more detailed one. Then the surface mesh and volume mesh is generated. Fig. 114 presents the outer surface of the shoulder wing aircraft. Fig. 115 presents the volume mesh that serves as basis for the Edge Euler calculation.

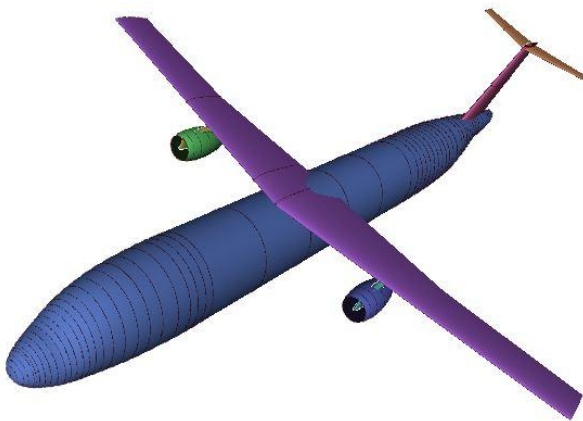


Fig. 114: SW - rendering in SUMO

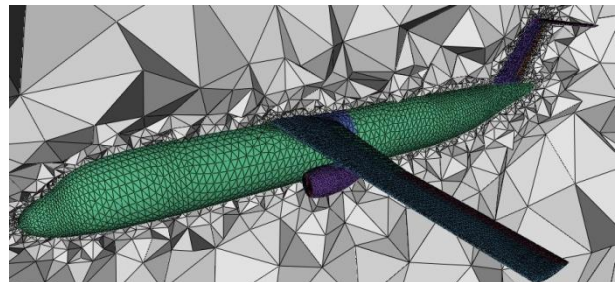


Fig. 115: SW - volume mesh

4.2.3 AMB

The aerodynamics are calculated with the help of AMB.

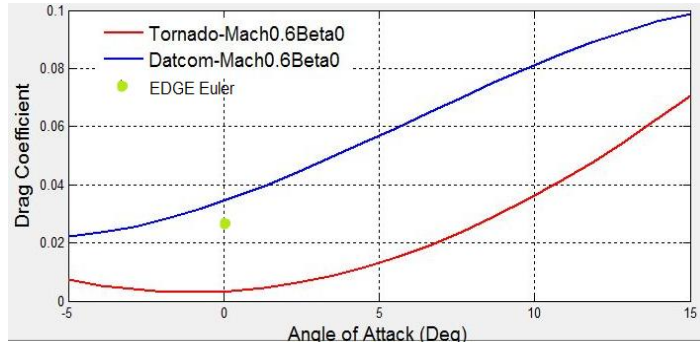


Fig. 116: SW - drag coefficient

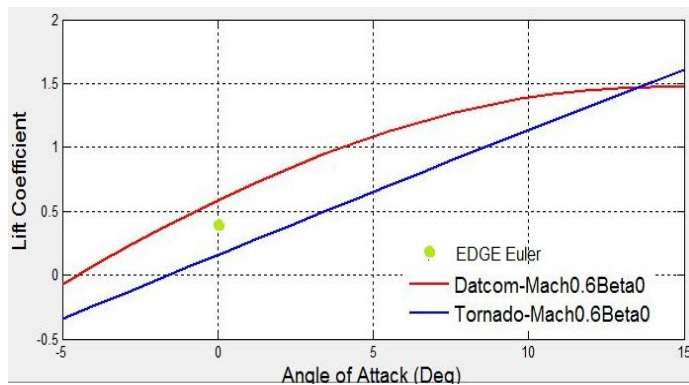


Fig. 117: SW - lift coefficient

Fig. 116 presents the drag coefficient over the angle of attack for the shoulder wing aircraft. The green dot represents the result of the EDGE Euler computation. Fig. 117 depicts the lift coefficient. The result of the EDGE Euler computation is marked with a green dot as well. The results for the drag coefficient and for the lift coefficient are acceptable. The output of Tornado and DATCOM differs. The same phenomenon appears in the calculation of the aerodynamics for the A320. But now the DATCOM results look better. A satisfying result for an angle of attack of 0° is given by the EDGE Euler computation. Here the cruise Mach number (0,69 Mach) is the basis and the altitude (9 900 m) can be set exactly.

The pitching moment coefficient and the rolling moment coefficient of the shoulder wing are compared to the coefficients of the A320 calculated by the AMB. The rolling moment coefficient of the shoulder wing for an angle of attack of 0° is determined by EDGE Euler with $0,3 \cdot 10^{-7}$. DATCOM sets the rolling moment coefficient to 0 and the rolling moment coefficient calculates by Tornado is $7,5 \cdot 10^{-7}$ (Fig. 118). The results for the A320 model calculated by DATCOM and Tornado are 0. If one considers the results of Tornado the rolling moment coefficient of the shoulder wing is higher. So, the longitudinal stability gets higher.

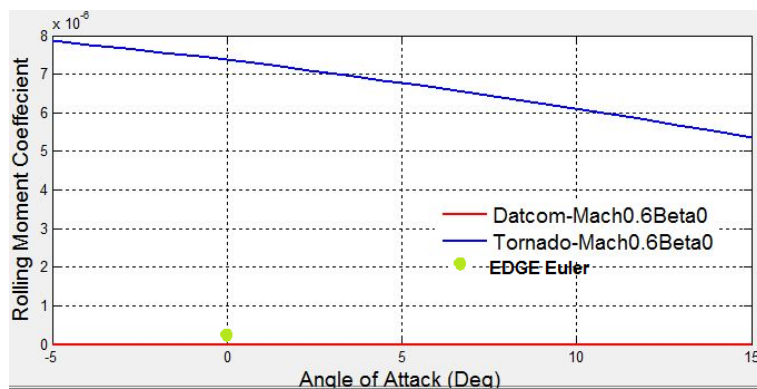


Fig. 118: SW - rolling moment coefficient

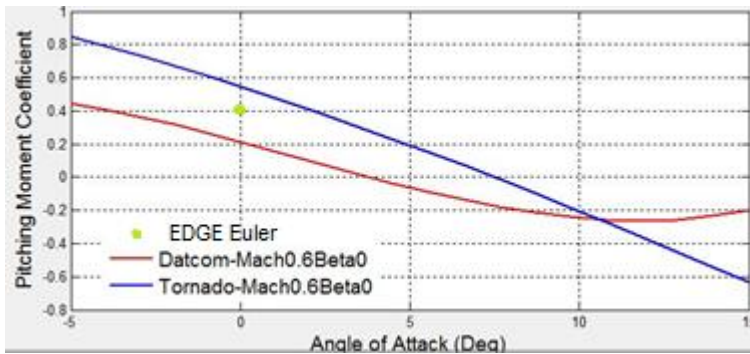


Fig. 119: SW - pitching moment coefficient

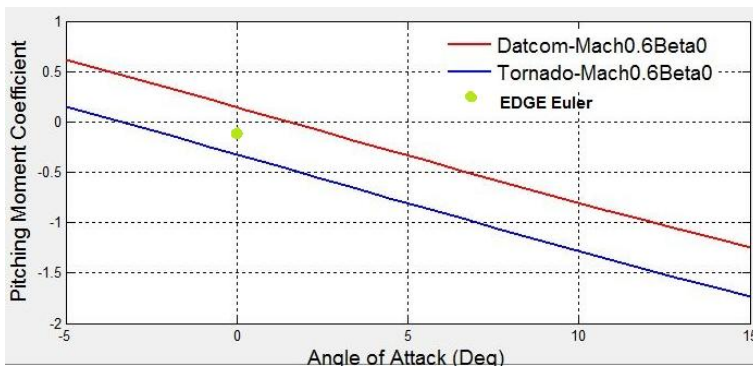


Fig. 120: A320 model - pitching moment coefficient

The pitching moment coefficient of the shoulder wing is depicted in Fig. 119. Here the results of EDGE Euler, DATCOM and Tornado are shown. Fig. 120 describes the results of the A320 model calculated by AMB. In both cases the results calculated with EDGE Euler are between the results of Tornado and DATCOM. Considering these values the pitching moment coefficient of the shoulder wing aircraft is higher than the one of the A320. The same applies for the Tornado calculation. DATCOM gives the same value for the shoulder wing aircraft and the A320.

The Mach distribution and the distribution of the pressure coefficient are depicted in Fig. 121 and in Fig. 122. The initial conditions are the cruise speed 0,69 Mach at a altitude of 9 900 m. Near the leading edge the velocity on the wing becomes 1 Mach. That will increase the wave drag. A higher sweep angle of the wing can minimize this problem.

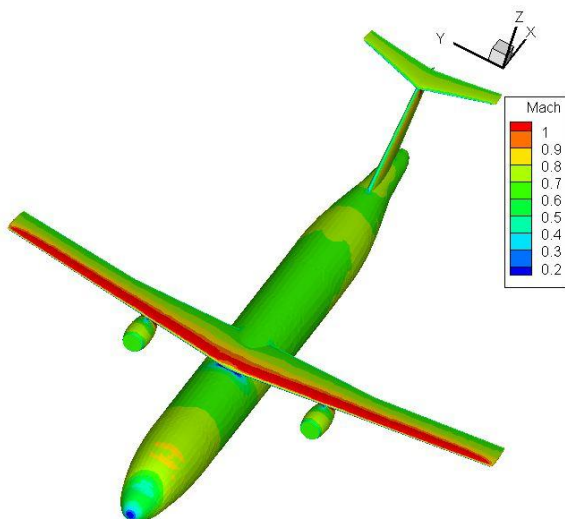


Fig. 121: SW - Mach distribution

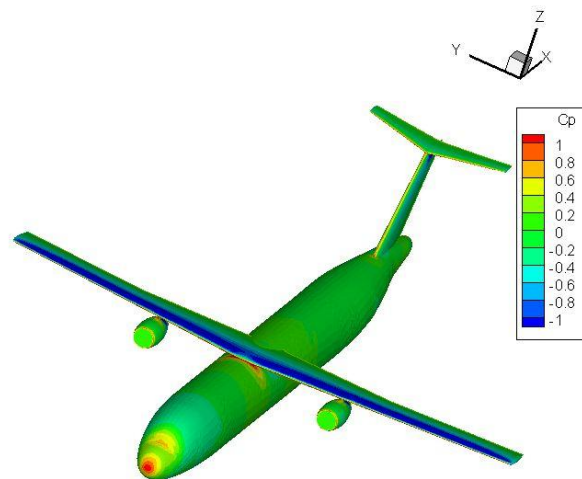


Fig. 122: SW - pressure coefficient distribution

In all aerodynamic calculations the aerodynamic effects of the turboprop are not considered. That can be proven by Fig. 121 and Fig. 122. The Mach distribution and the distribution of the pressure coefficient are constant along the upper surface of the wing. Close to the turboprops no change can be notice.

4.2.4 SDSA

With the help of the SDSA tool the short period characteristics and the phugoid characteristics are considered for the cruise conditions (0,69 Mach , h = 9 900 meter). The results are shown Fig. 123 and Fig. 124. The ICAO criteria are used for evaluation as for the A320.

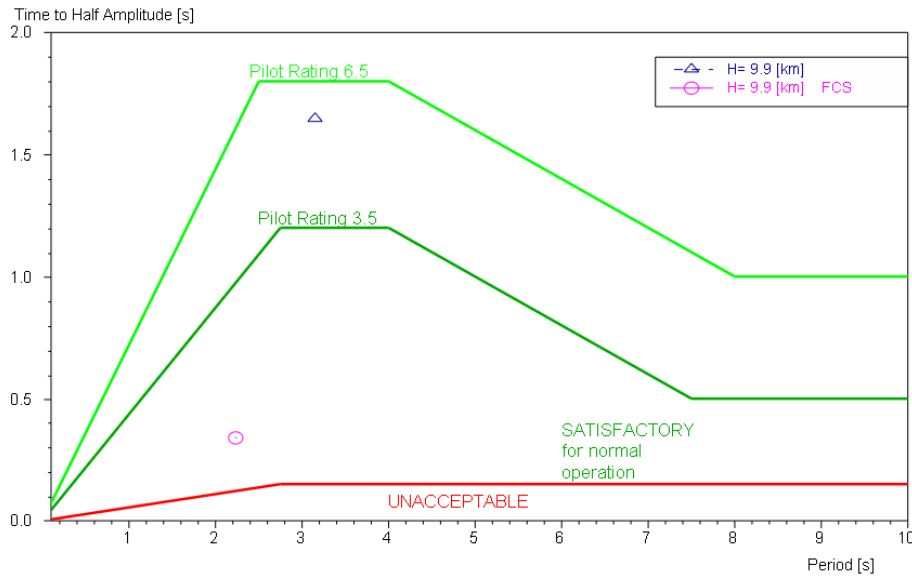


Fig. 123: SW - short period

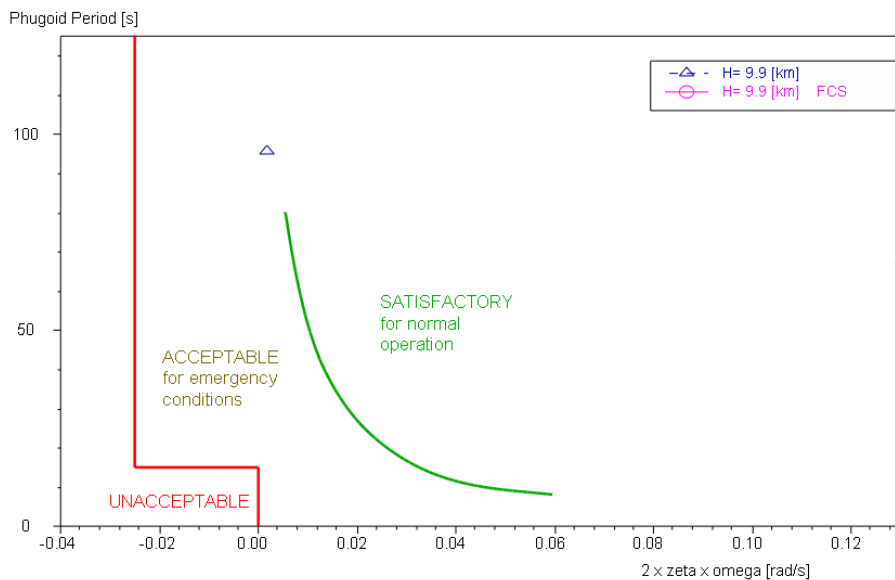


Fig. 124: SW – Phugoid

Looking at the short period characteristics, the shoulder wing aircraft is in a stable state during the flight. The support of a flight control system is not necessary. Otherwise the flight control system is important to control the aircraft in a satisfactory state with regard to the phugoid criteria.

SDSA calculates the range that the shoulder wing aircraft can realise. Fig. 125 depict the results. The initial conditions are a constant CL, an altitude between 8 000 and 9 000 meters and an airspeed range from 100 m/s to 220 m/s. The engine type is a turboprop with a SFC of 0,217 kg/kw/h.

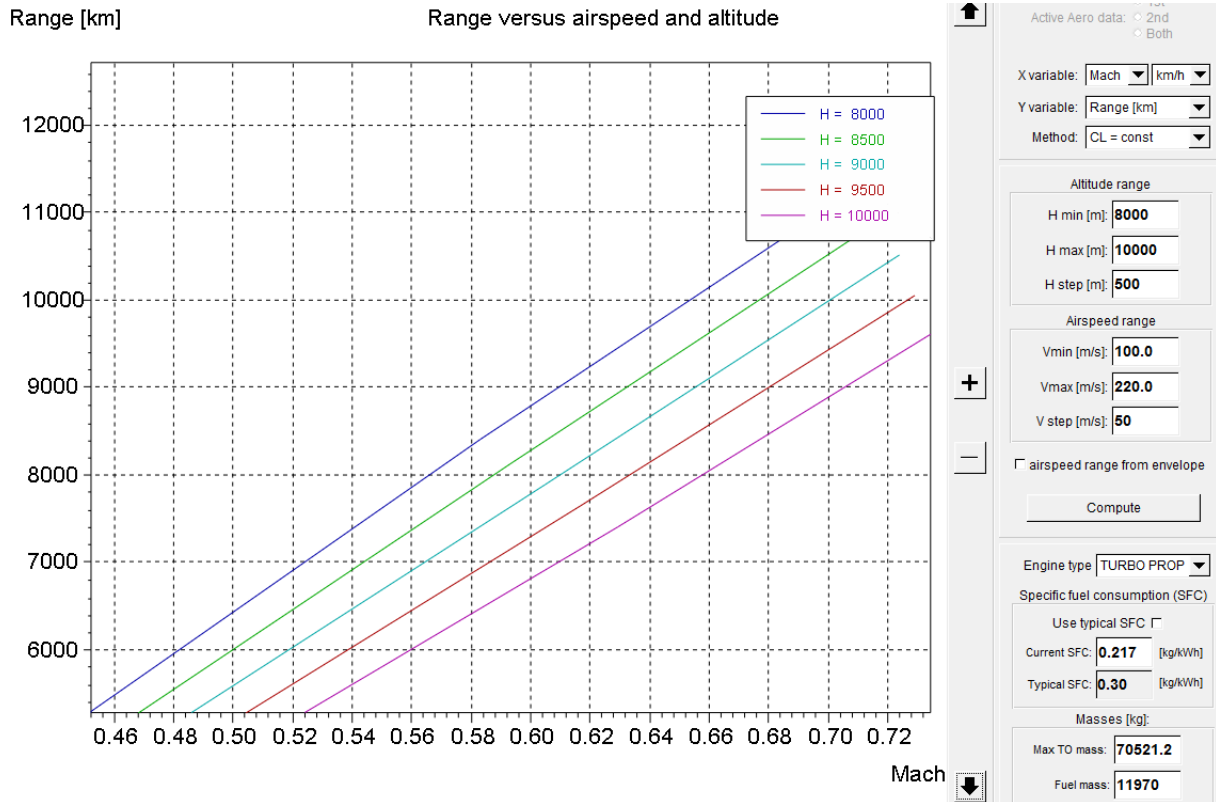


Fig. 125: SW - range

For a cruise Mach of 0,69 Mach and an altitude of 9 900 meter the range is about 8 700 km. According to the SDSA calculation the flight missions summarized in Tab. 16 can be fulfilled.

4.2.5 NeoCASS

GUESS gives a first view of the forces that works on the wing. The weight estimation of the shoulder wing aircraft is not analysed in more detail. That can be done when the input of the AcBuilder has no more discrepancies. The results of the bending moment and the shear forces also depend on the weight, but it is possible to compare the force curves of the A320 and the shoulder wing aircraft computed by GUESS, to get a generalized overview. Fig. 126 presents the shear force of the shoulder wing aircraft along the spanwise. Fig. 127 depicts the bending moment along the spanwise. Fig. 128 and Fig. 129 give the result for the calculation of the A320 – 200 model.

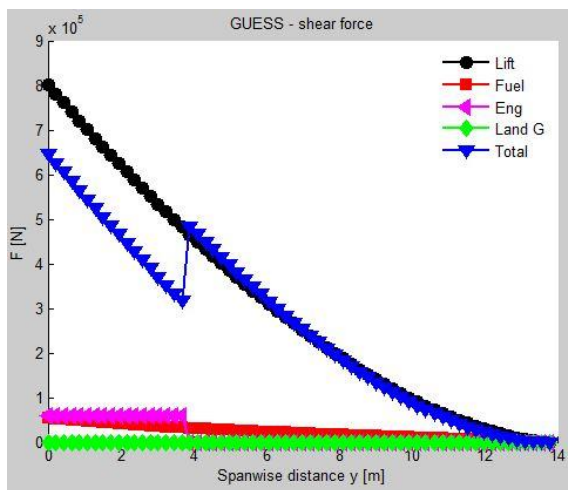


Fig. 126: SW - shear force

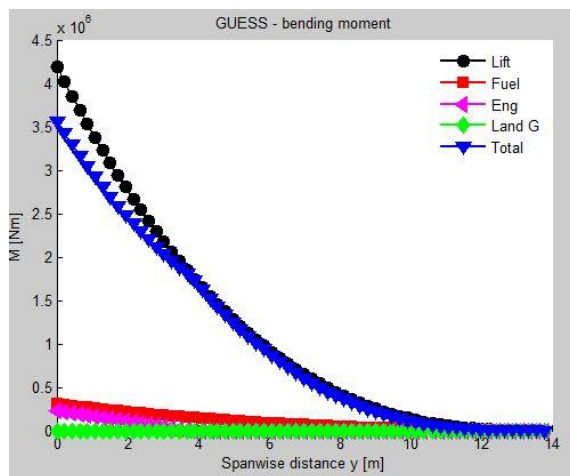


Fig. 127: SW - bending moment

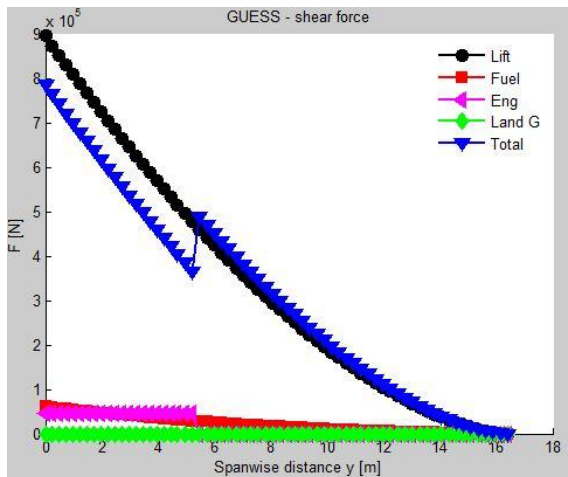


Fig. 128: Model A320 - shear force

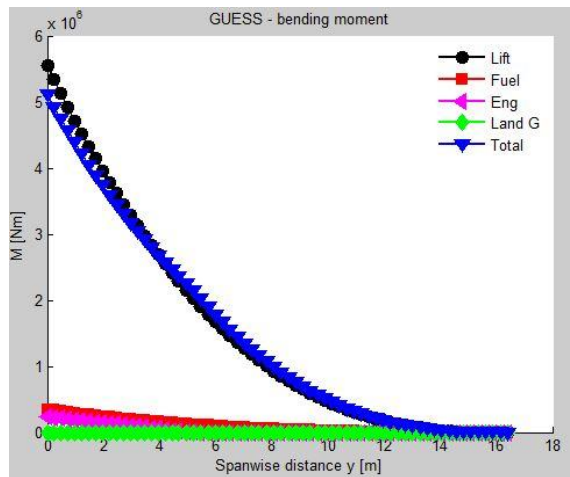


Fig. 129: Model A320 - bending moment

It is identifiable that the forces on the shoulder wing are lower than the one on the Airbus wing. For one thing the whole aircraft (SW) has a lighter weight and therefore the lifting forces can be smaller. That results in lower loads. Further studies can optimise the material selection and the structural construction. For the moment both aircraft are calculated with the same material and the same structural philosophy.

The computations that are run on SMARTCAD are the one that are available at the moment. A modal analysis and a flutter analysis can be run. The result of the modal analysis is used for the visualisation of the mode that goes into an unstable state. The flutter calculation is done for four Mach number to get the critical flutter speed. Tab. 20 summarizes the flutter speeds for the Mach numbers at an altitude of 0 and 9 900 meters. The according V-g plots are depicted in Appendix E.

Tab. 20: Flutter speed for SW

| Mach number | flutter speed 0 meter altitude | flutter speed 9 900 meter altitude |
|-------------|--------------------------------|------------------------------------|
| 0.2 | 92,10 m/s | - |
| 0.4 | 90,70 m/s | - |
| 0.6 | 88,50 m/s | 162,85 m/s |
| 0.8 | 86,70 m/s | 156,75 m/s |

The cruise speed is about 207 m/s. The flutter speed is for all velocities and at both altitudes smaller than the required velocity. To have the exact flutter speed for the cruise Mach of 0,69 at the altitude of a single computation is done. The resulting V-g plot of the computation is seen in Fig. 130. Mode shape 11 (pink line with squares) is the one that goes into an unstable state. The flutter speed is about 160 m/s.

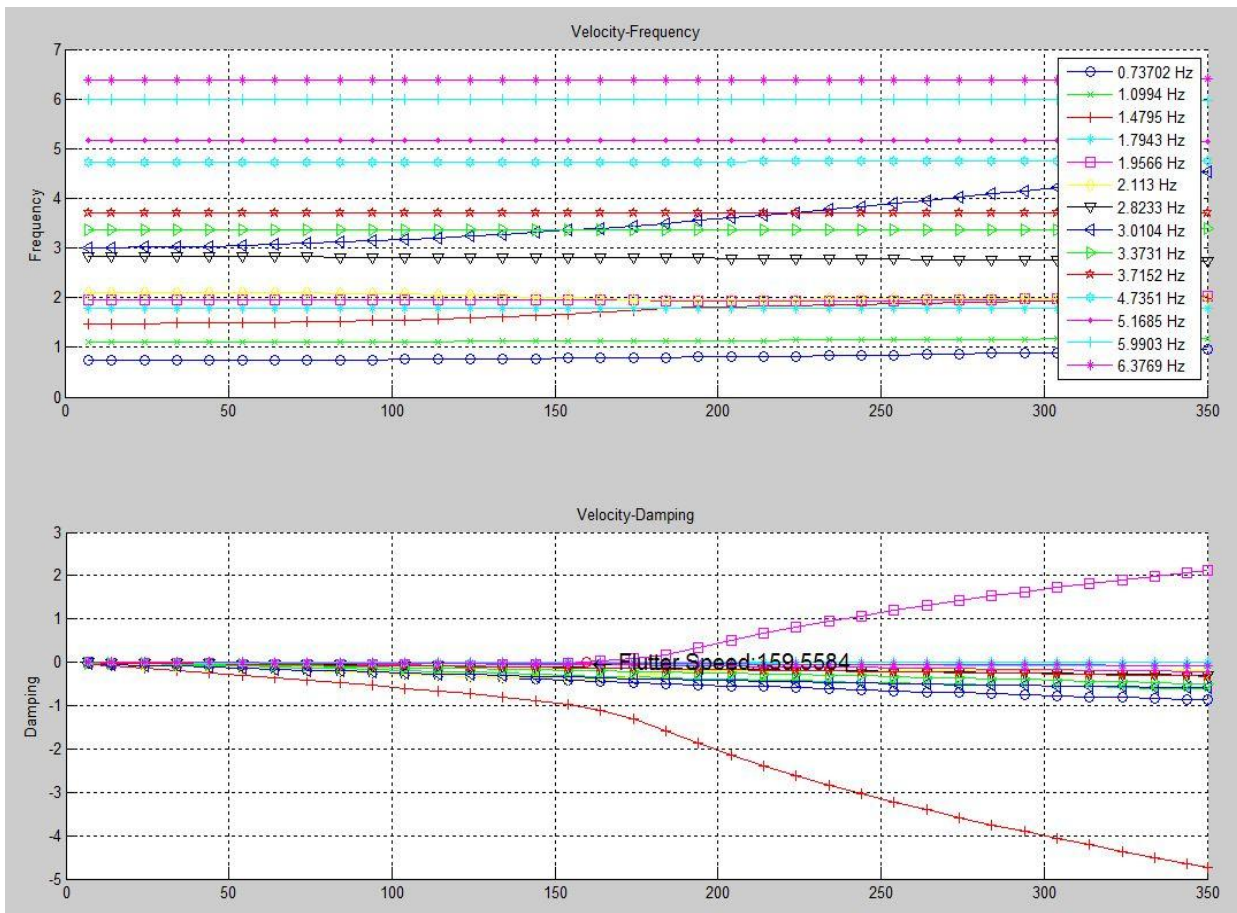


Fig. 130: V-g plot Mach 0,69 altitude 9 900 meters

The according deformation is shown in Fig. 131. The scale factor to illustrate the deformation is 50. The vibration mode 11 is at a frequency of 1,9566 Hz.

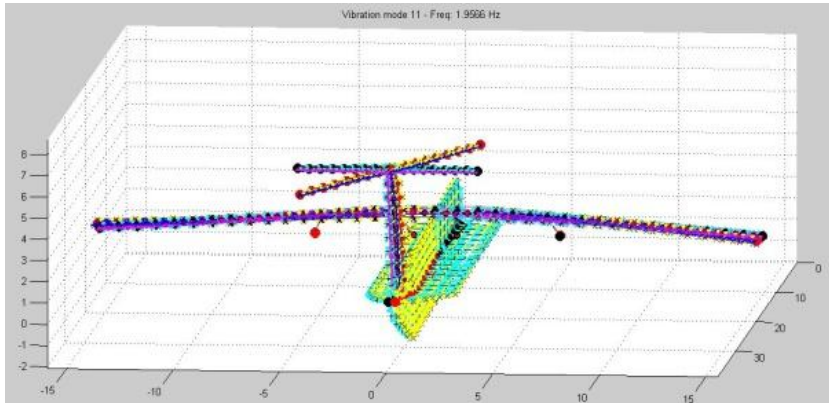


Fig. 131: Mode shape 11 - deformed model SW

The critical component is the horizontal tail. The oscillation in a bending mode leads to the unstable state. Here the structure has to be improved and the geometry has to be adapted.

Thus, SMARTCAD gives clues where the design of the shoulder wing has to be changed and edited. On a fast way the structure and the critical loads can be estimated.

5 Conclusion and Outlook

CEASIOM is tested in a detailed way referring to the Airbus A320. All tools are considered in this process. At the moment it is not possible to redesign the A320 in a proper way. The main reason for the deviations during the work with CEASIOM can be lead back to AcBuilder. The AcBuilder output`s is the basis for all following modules. Discrepancies appear in the estimation of weight. The key to these problems is still in process and will be corrected in the next version of CEASIOM. After that it will be useful to run the generated *.xml files on the new version to have them checked again. The results of AMB, SUMO and SDSA are comprehensible. Inaccuracies will be minimised by more precise input from AcBuilder. Definitely, the user has to consider the results of these tools precisely, to notice possible failures. The handling of NeoCASS is still complicated. Not all features working, but the features that can be tested give realistic results. Currently the problems are being solved by CFSEngineering. Apparently, there are problems by transmitting the input data to the solver of SMARTCAD. As soon as this is solved the results can be quickly checked. The FCSDT tool is still in the process of development. Unfortunately, it is not possible to use all sub tools of the FCSDT to give a factual assessment.

A shoulder wing configuration is analysed by CEASIOM as well. Therefore the tools are used that give satisfactory results for the A320. The shoulder wing aircraft refers to the Airbus A320 and fulfils the same requirements. The shoulder wing configuration makes it possible to save time during the ground handling procedure. The cruise speed of the shoulder wing aircraft can be smaller, because the time that is saved at the ground can allocate to the flights per day. Instead of a jet engine, turboprop powers the shoulder wing aircraft. A fuel saving of 4,2% per flight compared to the A320 can be realised with this configuration. There is still a potential to save more fuel, for example, by using four turboprops instead of two. In further steps the structure has to be optimised. It has to be considered if the T tail is the best option for this configuration or if a conventional tail may give better results. Furthermore the material can be adapted to the loads and the position of the wing can be optimised.

In conclusion it can be said that CEASIOM will become a readily accessible and also timesaving tool for the conceptual design phase as soon the failures are solved. It provides first clues which assumption should be reconsidered and where improvement and development of the initial design is potentially necessary.

6 References

- Aerospace 2010** URL:http://www.aerospaceweb.org/aircraft/jetliner/a320/a320_schem_01.jpg (08.Dec. 2010)
- Airbus 2003** AIRBUS: *Airplane Characteristics For Airport Planning AC*. Blagnac Cedex, France : Airbus S.A.S., 2003
- Bisplinghoff 1983** BISPLINGHOFF, Raymond L.; ASHLEY, Holt; HALFMAN, Robert L.: *Aeroelasticity*. New York : Dover publication, 1983
- Briere 2001** BRIERE, Dominique; FAVRE, Christian; TRAVERSE, Pascal.: *The avionics Handbook. Electrical Flight Controls, From Airbus A320/A330/340 to Futur Military Transport Aircraft: A Family of Fault-Tolerant Systems Aeroelasticity*. CRC Press LLC, 2001
- Cavagna 2009** CAVAGNA, L.; DA RONCH, A.; RICCI, S: *NeoCASS Next generation Conceptual Aero Structural Sizing*. Milano: Dipartimento di Ingegneria Aerospaziale - Politecnico di Milano, 2009
- Cavagna 2009a** CAVAGNA, L.; RICCI, S.; RICCOBENE, L: *Bringing Aeroelastic Analysis in the conceptual design of future aircraft*. In: IFASD - International Forum on aeroelasticity and Structural Dynamics (Seattel, Washington 21th – 25th Sep. 2009). Stockholm/Milano: FOI/ Dipartimento di Ingegneria Aerospaziale - Politecnico di Milano, 2009
- CASIOM 2010** URL: <http://www.cfse.ch/cfse/site/about-introduction.php> (09.Dec. 2010)
- CFS 2005** URL: <http://www.ceasiom.com/ceasiom-modules.html> (11.Nov. 2010)
- DaRonch 2007** DA RONCH, A., CAVAGNA, L.: *A Doublet-Lattice Method for Calculating Lift Distributions on Planar and Non-Planar Configurations in Subsonic Flows*. Stockholm/Milano: Department of Aeronautical and Vehicle Engineering KTH/ Department of Aerospace Engineering, Politecnico di Milano, 2007

- DaRonch 2009** DA RONCH, A.: *AMB Interface for external CFD Solver*. Liverpool: University of Liverpool, 2009
- DWS aviation 2010** URL: <http://www.dancewithshadows.com/aviation/wp-content/uploads/2008/12/winglets.jpg> (16.Nov 2010)
- ELLER 2009** URL: <http://www.larosterna.com/sumo.html> (16. Nov.2010)
- FOI 2008** FOI: *Edge User Guide*. Defence and Security, Systems and Technology FOI dNr 03-2870, 2008
- Harris 2010** URL: http://www.airlinercafe.com/Walkarounds/a320/A320_Wingtip_port_and_winglet.JPG (16. Nov.2010)
- ISO 1151-1** ISO 1151-1. *Flight dynamics - Concepts, quantities and symbols - Part 1: Aircraft motion relative to the air*
- Krammer 2010** KRAMER, PHILIP., JUNKER, O, SCHOLZ, DIETER: *Aircraft Design for low cost ground-handling - The final results of the ALOHA project*. In: ICAS 2010 - 27th Congress of the International Council of the Aeronautical Sciences (Nizza, Italy 2010) Hamburg: AERO, 2010
- Krauss 2010** <http://www.worldofkrauss.com/foils/164> (24. Nov. 2010)
- Maheri 2008** MAHERI, A.; BEAVERSTOCK, C.,; SIDORYUK, M: *Flight Control System Designer Toolkit - Technical Report and User Manual*. Bristol: SimSAC, 2008
- Moura 2000** FERNANDES DA MOURA, Eurico J.: *Vergleich Verschiedener Verfahren zur Masseprognose von Flugzeugbaugruppen im frühen Flugzeugentwurf - Flügel, Leitwerk, Einsatzausrüstung* -. Hamburg: Poject HAW, 2000
- Moura 2001** FERNANDES DA MOURA, Eurico J.: *Vergleich verschiedener Verfahren zur Masseprognose von Flugzeugbaugruppen im frühen Flugzeugentwurf*. Hamburg: Thesis HAW, 2001
- Molitor 2009** MOLITOR, P.: *CEASIOM tier 1 and 1+ module for simulation of aircraft stability and control characteristics*. Stockholm: KTH, 2009

- Nguewo 2009** NGUEWO, D.: *Vorlesung Flugzeugmechanik 2*. Hamburg, HAW Hochschule für angewandte Wissenschaften, Department F+F, lecture notes, 2009
- Prado 2010** PRADO.: *Berechnung A320-200*. Ausgabe Dateien, Hamburg, 2010
- Puelles 2010** PUELLES, A.: *CEASIOM XML file Definition*. Stockholm: Royal Institute of Technology, 2010
- Raymers 1992** RAYMERS, Daniel P.: *Aircraft Design. A Conceptual Approach*. Washington: AIAA education series, 1992
- Roskam 1989** ROSKAM, J.: *Airplane Design.Bd.2: Preliminary Configuration Design and Integration of the Propulsion System*. Ottawa, 1989
- Scholz 1999** SCHOLZ, Dieter: *Flugzeugentwurf*. Hamburg, HAW Hochschule für angewandte Wissenschaften, Department F+F, lecture notes, 1999
- Schulz 2007** SCHULZ, Detlef: *Aerodynamik mit Labor* Hamburg, HAW Hochschule für angewandte Wissenschaften, Department F+F, lecture notes, 2007
- Seibel 2008** SEIBEL, M.: *Eine Vorlesung zur Gestaltung und Auslegung von Flugzeugzellen*. Hamburg, HAW Hochschule für angewandte Wissenschaften, Department F+F. lecture notes, WS 2008/09
- SimSAC 2009** SIMSAC: *SDSA - Theoretical Basics*. Stockholm, 2009
- Wiki 2010** http://en.wikipedia.org/wiki/Flight_dynamics (01. Dec. 2010)
- Young 2001** YOUNG, T.: *Flight Mechanics Course ME 4726* . Department of Mechanical and Aeronautical Engineering, University of Limerick. lecture notes, 2001

7 Appendix

Appendix A

A1: Input Data - AcBuilder

| Parameter | Unit | Value |
|--------------------------------|-------|-----------|
| omega_nose | deg. | 35,0 |
| phi_nose | deg. | 12,0 |
| epsilon_nose | (0-) | 0,815 |
| Forefuse_X_sect_vertical_d... | m | 4,141 |
| Forefuse_X_sect_horizontal... | m | 3,95 |
| Forefuse_Xs_distortion_coe... | m | 0,5 |
| Nose_length | m | 3,374915 |
| omega_tail | deg. | 13,0 |
| phi_tail | deg. | 6,0 |
| epsilon_tail | (0-) | 2,557 |
| Aftfuse_X_sect_vertical_dia... | m | 4,141 |
| Aftfuse_X_sect_horizontal_... | m | 3,95 |
| Aftfuse_Xs_distortion_coeff... | m | 0,5 |
| Tail_length | m | 10,588537 |
| fraction_fore | (0-1) | 0,5 |
| shift_fore | --- | 0,0 |
| Total_fuselage_length | m | 37,57 |
| a0_fore | m | 2,02275 |
| a1_fore | m | 0,0 |
| b1_fore | m | -0,04775 |
| a0_aft | m | 2,02275 |
| a1_aft | m | 0,0 |
| b1_aft | m | -0,04775 |
| x | m | 0,0 |
| y | m | 0,0 |
| z | m | 0,0 |

Fig.A1 1: Input fuselage

| Parameter | Unit | Value |
|---------------------------------|----------------|-------------------------------------|
| area | m ² | 31,0 |
| Span | m | 12,45 |
| AR | | 5,0001 |
| spanwise_kink | [0-1] | 0,5 |
| taper_kink | [0-1] | 0,65 |
| taper_tip | [0-1] | 0,33 |
| root_incidence | deg. | 0,0 |
| kink_incidence | deg. | 0,0 |
| tip_incidence | deg. | 0,0 |
| LE_sweep_inboard | deg. | 32,317 |
| LE_sweep_outboard | deg. | 32,317 |
| dihedral_inboard | deg. | 5,0 |
| dihedral_outboard | deg. | 5,0 |
| airfoilRoot | name | 0012 |
| airfoilKink | name | 0012 |
| airfoilTip | name | 0012 |
| thickness_root | | 0,12 |
| thickness_kink | | 0,12 |
| thickness_tip | | 0,12 |
| empennage_layout | | <input type="checkbox"/> |
| Elevator.present | | <input checked="" type="checkbox"/> |
| Elevator.chord | [0-1] | 0,32 |
| Elevator.Span | [0-1] | 0,95 |
| Elevator.limit_deflection_up | deg. | 30,0 |
| Elevator.limit_deflection_do... | deg. | 15,0 |
| limit_tailplane_deflection_up | deg. | 30,0 |
| limit_tailplane_deflection_d... | deg. | 15,0 |
| vertical_locale | fusva | 0,191 |
| apex_locale | fusln | 0,82 |
| x | m | 30,8074 |
| y | m | 0,0 |
| z | m | 0,790931 |

Fig.A1 2: Input horizontal tail

| Parameter | Unit | Value |
|-------------------------------|---------|-------------------------------------|
| area | m^2 | 122,4 |
| Span | m | 33,913 |
| AR | | 9,3962 |
| spanwise_kink1 | [0-1] | 0,11016 |
| spanwise_kink2 | [0-1] | 0,3735 |
| taper_kink1 | [0-1] | 0,88 |
| taper_kink2 | [0-1] | 0,6186 |
| taper_tip | [0-1] | 0,2462 |
| root_incidence | deg. | -1,25 |
| kink1_incidence | deg. | -1,25 |
| kink2_incidence | deg. | 0,5127 |
| tip_incidence | deg. | -1,38 |
| LE_sweep_inboard | deg. | 27,418 |
| LE_sweep_midboard | deg. | 27,418 |
| LE_sweep_outboard | deg. | 27,418 |
| dihedral_inboard | deg. | 5,0 |
| dihedral_midboard | deg. | 5,0 |
| dihedral_outboard | deg. | 5,0 |
| airfoilRoot | name | SC20612 |
| airfoilKink1 | name | SC20612 |
| airfoilKink2 | name | SC20612 |
| airfoilTip | name | SC20612 |
| thickness_root | | 0,12 |
| thickness_kink1 | | 0,1 |
| thickness_kink2 | | 0,12 |
| thickness_tip | | 0,12 |
| reference_convention | | <input checked="" type="checkbox"/> |
| configuration | 0,1,... | 0 |
| winglet.present | | <input checked="" type="checkbox"/> |
| winglet.Span | m | 1,1 |
| winglet.taper_ratio | [0-1] | 0,2 |
| winglet.LE_sweep | deg. | 66,0 |
| winglet.Cant_angle | deg. | 60,0 |
| winglet.root_incidence | deg. | 0,0 |
| winglet.tip_incidence | deg. | 0,0 |
| flap.present | | <input checked="" type="checkbox"/> |
| flap.root_chord | [0-1] | 0,275 |
| flap.kink1_chord | [0-1] | 0,275 |
| flap.kink2_chord | [0-1] | 0,275 |
| aileron.present | | <input checked="" type="checkbox"/> |
| aileron.chord | [0-1] | 0,275 |
| aileron.Span | m | 0,213 |
| aileron.position | 0,1,2 | 1,0 |
| aileron.limit_deflection_up | deg. | 25,0 |
| aileron.limit_deflection_d... | deg. | 25,0 |
| slat.present | | <input checked="" type="checkbox"/> |
| slat.chord | [0-1] | 0,22 |
| slat.root_position | [0-1] | 1,0 |
| slat.tip_position | [0-1] | 0,808 |
| fairing.present | | <input checked="" type="checkbox"/> |
| fairing.Forward_chord_fra... | % | 20,0 |
| fairing.Aft_chord_fraction | % | 30,0 |
| fairing.flushness | % | 20,0 |
| placement | fusva | 0,223 |
| apex_locale | fusln | 0,3134 |
| x | m | 11,774438 |
| y | m | 0,0 |
| z | m | -1,147057 |

Fig.A1 3: Input wing

| Parameter | Unit | Value |
|-------------------------|-------|-------------------------------------|
| area | m^2 | 21,5 |
| Span | m | 5,865 |
| AR | | 1,5999 |
| spanwise_kink | [0-1] | 0,5 |
| taper_kink | [0-1] | 0,68 |
| taper_tip | [0-1] | 0,349 |
| root_incidence | deg. | 0,0 |
| kink_incidence | deg. | 0,0 |
| tip_incidence | deg. | 0,0 |
| LE_sweep_inboard | deg. | 40,3982 |
| LE_sweep_outboard | deg. | 40,3982 |
| dihedral_inboard | deg. | 0,0 |
| dihedral_outboard | deg. | 0,0 |
| airfoilRoot | name | 0012 |
| airfoilKink | name | 0012 |
| airfoilTip | name | 0012 |
| thickness_root | | 0,12 |
| thickness_kink | | 0,12 |
| thickness_tip | | 0,12 |
| Rudder.present | | <input checked="" type="checkbox"/> |
| Rudder.chord | [0-1] | 0,23 |
| Rudder.Span | [0-1] | 0,95 |
| Rudder.limit_deflection | deg. | 30,0 |
| Twin_tail | | <input type="checkbox"/> |
| Twin_tail_span | wspn | 0,0001 |
| vertical_locale | fusva | 0,4 |
| apex_locale | fusln | 0,797 |
| x | m | 29,94329 |
| y | m | 0,0 |
| z | m | 1,6564 |

Fig.A1 4: Input vertical tail

| Parameter | Unit | Value |
|------------------------------|---------|-------------------------------------|
| Layout_and_config | 0..5 | 0 |
| Propulsion_type | 0..3 | 0 |
| Nacelle_body_type | shor... | <input checked="" type="checkbox"/> |
| symmetry | | <input checked="" type="checkbox"/> |
| Y_locale | wspn | 0,399 |
| X_locale | fusln | 0,35 |
| Z_locale | fusva | 0,0 |
| fineness_ratio | >0 | 1,661 |
| d_max | m | 1,9 |
| toe_in | deg. | 0,0 |
| pitch | deg. | 2,0 |
| Thrust_to_weight_ratio | | 0,4 |
| Propeller_diameter | m | 1,276 |
| Max_thrust | kN | 104,173 |
| Bypass_ratio_to_emulate | | 6,0 |
| Thrust_reverser_effectivness | | 0,3 |
| Fan_cowl_length_ratio | % | 0,0 |
| x | m | 13,69005... |
| y | m | 0,0 |
| z | m | -1,772884... |

Fig.A1 5: Input engine

| Parameter | Unit | Value |
|---------------------------|----------------|-------------------------------------|
| Design_classification | 0,1,2 | 0 |
| installation_type | | <input checked="" type="checkbox"/> |
| gross_volume | m ³ | 90,0 |
| baggage_combined_length | m | 22,0 |
| baggage_apex_per_fuselgt | [0-1] | 0,1 |
| Cabin_length_to_aft_cab | m | 22,0 |
| Cabin_max_internal_height | m | 2,22 |
| Cabin_max_internal_width | m | 3,696 |
| Cabin_floor_width | m | 3,5 |
| Cabin_volume | m ³ | 151.29177... |
| Cabin_attendant_number | | 4 |
| Flight_crew_number | | 2 |
| Passenger_accomodation | | 150 |
| Seats_abreast_in_fuselage | | 6 |
| Seat_pitch | m | 0,8 |
| Maximum_cabin_altitude | m | 11000,0 |
| Max_pressure_differential | Pa | 0,0 |
| Target_operating_ceiling | m | 0,0 |

Fig.A1 6: Input Weight & Balance

| Parameter | Unit | Value |
|------------------|------|-------|
| nwing_inboard | | 2 |
| nwing_midboard | | 4 |
| nwing_outboard | | 8 |
| nwing_carryth | | 2 |
| nfuse | | 22 |
| nvtail_inboard | | 4 |
| nvtail_outboard | | 4 |
| nhtail_inboard | | 4 |
| nhtail_outboard | | 4 |
| nhtail_carryth | | 1 |
| ncanard_inboard | | 1 |
| ncanard_outboard | | 1 |
| ncanard_carryth | | 1 |
| nwing2_inboard | | 0 |
| nwing2_midboard | | 0 |
| nwing2_outboard | | 0 |
| nwing2_carryth | | 0 |

Fig.A1 7: Input beam model (technology)

| Parameter | Unit | Value |
|----------------------------|------|-------|
| nx.wing_inboard | | 4 |
| nx.wing_midboard | | 4 |
| nx.wing_outboard | | 4 |
| nx.vert_inboard | | 4 |
| nx.vert_outboard | | 4 |
| nx.hori_inboard | | 4 |
| nx.hori_outboard | | 4 |
| nx.canard_inboard | | 1 |
| nx.canard_outboard | | 1 |
| nx.wing2_inboard | | 0 |
| nx.wing2_midboard | | 0 |
| nx.wing2_outboard | | 0 |
| nx.sup_control.wing_in... | | 2 |
| nx.sup_control.wing_mi... | | 2 |
| nx.sup_control.wing_ou... | | 2 |
| nx.sup_control.vert_inb... | | 2 |
| nx.sup_control.vert_out... | | 2 |
| nx.sup_control.hori_inb... | | 2 |
| nx.sup_control.hori_out... | | 2 |
| nx.sup_control.canard_... | | 1 |
| nx.sup_control.canard_... | | 1 |
| nx.sup_control.wing2_i... | | 0 |
| nx.sup_control.wing2_... | | 0 |
| nx.sup_control.wing2_o... | | 0 |
| ny.wing_inboard | | 2 |
| ny.wing_midboard | | 3 |
| ny.wing_outboard | | 8 |
| ny.vert_inboard | | 3 |
| ny.vert_outboard | | 3 |
| ny.hori_inboard | | 3 |
| ny.hori_outboard | | 3 |
| ny.canard_inboard | | 1 |
| ny.canard_outboard | | 1 |
| ny.wing2_inboard | | 0 |
| ny.wing2_midboard | | 0 |
| ny.wing2_outboard | | 0 |

Fig.A1 8: Input aero panel (technology)

| Parameter | Unit | Value |
|-----------------------------|-------|-------|
| Wing1.Fore_W2_spar_I... | [0-1] | 0,066 |
| Wing1.Aft_W2_spar_lo... | [0-1] | 0,744 |
| Wing1.Fore_W2_spar_I... | [0-1] | 0,066 |
| Wing1.Aft_W2_spar_lo... | [0-1] | 0,744 |
| Wing1.Fore_W2_spar_I... | [0-1] | 0,066 |
| Wing1.Aft_W2_spar_lo... | [0-1] | 0,744 |
| Wing1.Fore_W2_spar_I... | [0-1] | 0,066 |
| Wing1.Aft_W2_spar_lo... | [0-1] | 0,744 |
| Wing2.Fore_W2_spar_I... | [0-1] | 0,0 |
| Wing2.Aft_W2_spar_lo... | [0-1] | 0,0 |
| Wing2.Fore_W2_spar_I... | [0-1] | 0,0 |
| Wing2.Aft_W2_spar_lo... | [0-1] | 0,0 |
| Wing2.Fore_W2_spar_I... | [0-1] | 0,2 |
| Wing2.Aft_W2_spar_lo... | [0-1] | 0,8 |
| Wing2.Fore_W2_spar_I... | [0-1] | 0,0 |
| Wing2.Aft_W2_spar_lo... | [0-1] | 0,0 |
| Horizontal_tail.Fore_HT... | [0-1] | 0,15 |
| Horizontal_tail.Aft_HT_s... | [0-1] | 0,65 |
| Horizontal_tail.Fore_HT... | [0-1] | 0,15 |
| Horizontal_tail.Aft_HT_s... | [0-1] | 0,65 |
| Horizontal_tail.Fore_HT... | [0-1] | 0,15 |
| Horizontal_tail.Aft_HT_s... | [0-1] | 0,65 |
| Canard.Fore_CA_spar_I... | [0-1] | 0,15 |
| Canard.Aft_CA_spar_lo... | [0-1] | 0,65 |
| Canard.Fore_CA_spar_I... | [0-1] | 0,15 |
| Canard.Aft_CA_spar_lo... | [0-1] | 0,65 |
| Canard.Fore_CA_spar_I... | [0-1] | 0,15 |
| Canard.Aft_CA_spar_lo... | [0-1] | 0,65 |
| Vertical_tail.Fore_VT_s... | [0-1] | 0,15 |
| Vertical_tail.Aft_VT_spa... | [0-1] | 0,7 |
| Vertical_tail.Fore_VT_s... | [0-1] | 0,15 |
| Vertical_tail.Aft_VT_spa... | [0-1] | 0,7 |
| Vertical_tail.Fore_VT_s... | [0-1] | 0,15 |
| Vertical_tail.Aft_VT_spa... | [0-1] | 0,7 |

Fig.A1 9: Input spar location (technology)

| Parameter | Unit | Value |
|-------------|-------------------|----------------|
| wing.esw | N/m ² | 73800000000... |
| wing.fcs | N/m ² | 27600000000... |
| wing.dsw | kg/m ³ | 2854,0 |
| wing.kcon | - | 2,0 |
| fus.kcon | - | 4,0 |
| fus.fts | N/m ² | 403222950,0 |
| fus.fcs | N/m ² | 73800000000... |
| fus.es | N/m ² | 73800000000... |
| fus.ef | N/m ² | 73751890000... |
| fus.ds | kg/m ³ | 2795,7174 |
| fus.df | kg/m ³ | 2854,0 |
| vtail.kcon | - | 2,0 |
| vtail.esw | N/m ² | 73800000000... |
| vtail.dsw | kg/m ³ | 2854,0 |
| vtail.fcs | N/m ² | 27600000000... |
| htail.kcon | - | 4,0 |
| htail.esw | N/m ² | 73800000000... |
| htail.dsw | kg/m ³ | 2854,0 |
| htail.fcs | N/m ² | 27600000000... |
| canard.kcon | - | 4,0 |
| canard.esw | N/m ² | 73751890000... |
| canard.dsw | kg/m ³ | 2795,7174 |
| canard.fcs | N/m ² | 385991200,0 |
| wing2.kcon | - | 4,0 |
| wing2.esw | N/m ² | 73751890000... |
| wing2.dsw | kg/m ³ | 2795,7174 |
| wing2.fcs | N/m ² | 385991200,0 |

Fig.A1 10: Input Material (technology)

A2: Comparison of all Computed Variants AcBuilder

| | |
|----|---|
| V1 | max. fuel (att all not in onls in wing) |
| V2 | without unusable fuel option - max fuel in wing 12500 kg |
| V3 | Target operating ceiling = 0 -> automatical calculation; max fuell in wing = 12500 kg |
| V4 | Payload increased deu single parameters of the AcBuilder ; max fuell in wing = 12500 kg |
| V5 | max. fuel in wings 14000 kg |

| | Janes 1 | Prado | V1 | V2 | V3 | V4 | V5 |
|----------------------|----------|-------|-------|-------|-------|-------|-------|
| MTOW | 73500,00 | 73500 | 60452 | 77541 | 73397 | 78190 | 75860 |
| OEW | 42100,00 | 41000 | 47679 | 52268 | 48123 | 49628 | 48797 |
| max zero fuel weight | 61000,00 | 60188 | 62989 | 67578 | 63434 | 68227 | 64397 |
| max. payload | 18633,00 | 19099 | 15310 | 15310 | 15310 | 18600 | 15600 |
| GMEW | | 36230 | 40543 | 45132 | 40987 | 42492 | 41662 |
| Landinggear | | 2547 | 2541 | 3301 | 3116 | 3330 | 3226 |
| Wing weight | | 8297 | 7719 | 9088 | 8766 | 9138 | 8958 |
| HT weight | | 590 | 757 | 870 | 844 | 875 | 860 |
| VT weight | | 434 | 440 | 505 | 490 | 507 | 499 |
| Fuselage weight | | 9119 | 10214 | 10258 | 7207 | 7448 | 9558 |
| Engine group | | 7822 | 7542 | 9779 | 9235 | 9865 | 7231 |
| fuel | 12500,00 | 13312 | -2537 | 9963 | 9963 | 9963 | 11463 |

Deviations in %

| | Prado-Janes | V1-Prado | V2-Prado | V3 - Prado | V4 Prado | V5 Prado | V3 - Janes |
|----------------------|-------------|----------|----------|------------|----------|----------|------------|
| MTOW | 0,00 | -17,75 | 5,50 | -0,14 | 6,38 | 3,21 | -0,14 |
| OEW | 2,68 | 16,29 | 27,48 | 17,37 | 21,04 | 19,02 | 14,31 |
| max zero fuel weight | 1,35 | 4,65 | 12,28 | 5,39 | 13,36 | 6,99 | 3,99 |
| max. payload | -2,44 | -19,84 | -19,84 | -19,84 | -2,61 | -18,32 | -17,83 |
| GMEW | | 11,90 | 24,57 | 13,13 | 17,28 | 14,99 | |
| Landinggear | | -0,24 | 29,60 | 22,34 | 30,74 | 26,66 | |
| Wing weight | | -6,97 | 9,53 | 5,65 | 10,14 | 7,97 | |
| HT weight | | 28,31 | 47,46 | 43,05 | 48,31 | 45,76 | |
| VT weight | | 1,38 | 16,36 | 12,90 | 16,82 | 14,98 | |
| Fuselage weight | | 12,01 | 12,49 | -20,97 | -18,32 | 4,81 | |
| Engine group | | -3,58 | 25,02 | 18,06 | 26,12 | -7,56 | |
| fuel | -6,10 | -119,06 | -25,16 | -25,16 | -25,16 | -13,89 | -20,30 |

Appendix B

Select aerodynamic data:

- Lift coefficient versus AoA
- Drag coefficient versus AoA
- Pitching moment coefficient versus AoA
- Max. angle of attack
- Side force derivative with respect to sideslip angle
- Rolling moment derivative with respect to sideslip angle
- Yawing moment derivative with respect to sideslip angle
- Lift derivative with respect to pitch rate versus Mach number
- Pitching moment derivative with respect to pitch rate
- Pitching moment derivative with respect to Alpha dot
- Rolling moment derivative with respect to roll rate
- Rolling moment derivative with respect to yaw rate
- Yawing moment derivative with respect to roll rate
- Yawing moment derivative with respect to yaw rate
- Lift derivative with respect to elevator deflection
- Pitching moment derivative with respect to elevator deflection
- Rolling moment derivative with respect to ailerons deflection
- Side force derivative with respect to rudder deflection
- Rolling moment derivative with respect to rudder deflection
- Yawing moment derivative with respect to rudder deflection

Fig.B 1: List for aerodynamic output (SDSA)

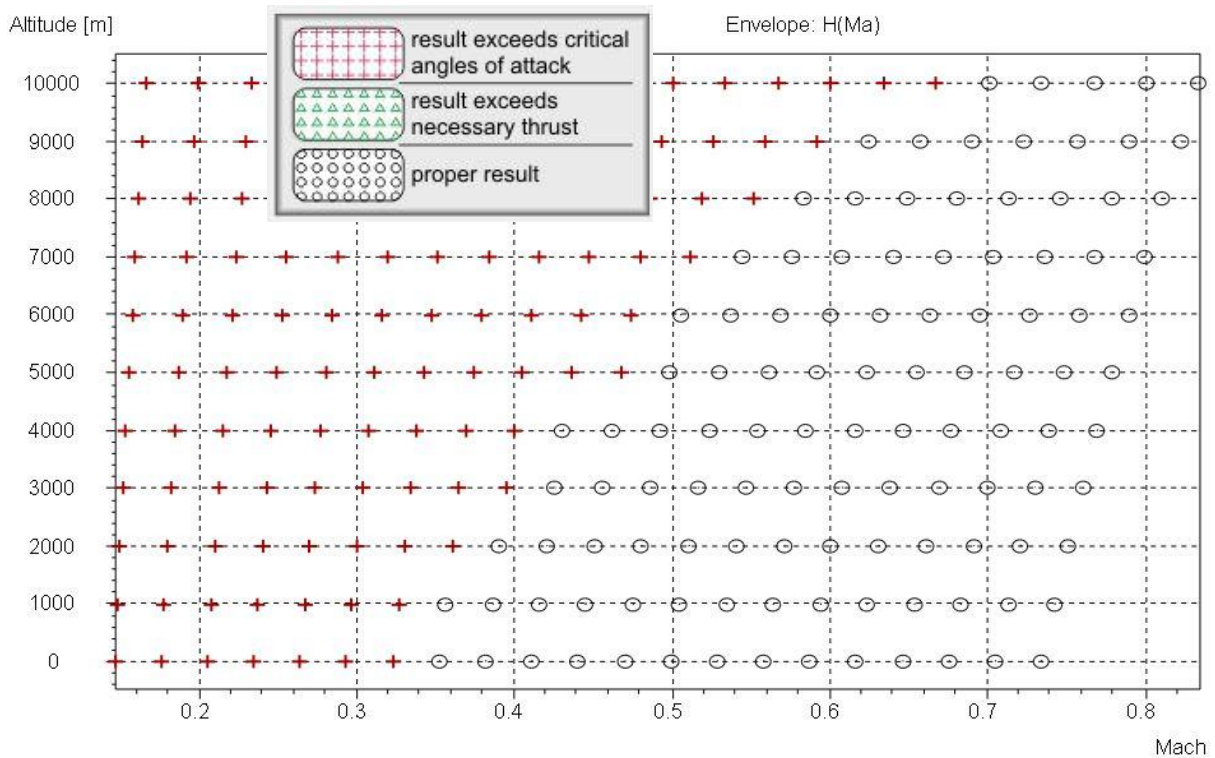


Fig.B 2: LQR matrix

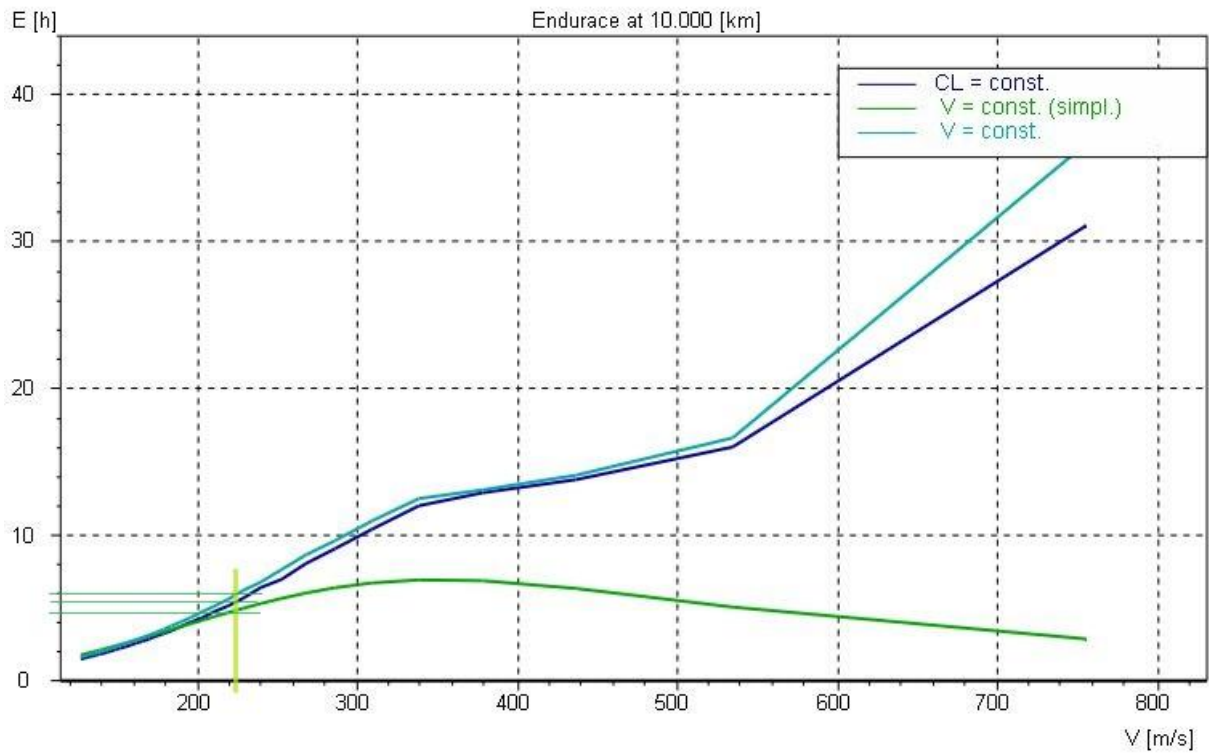


Fig.B 3: External SDSA tool endurance

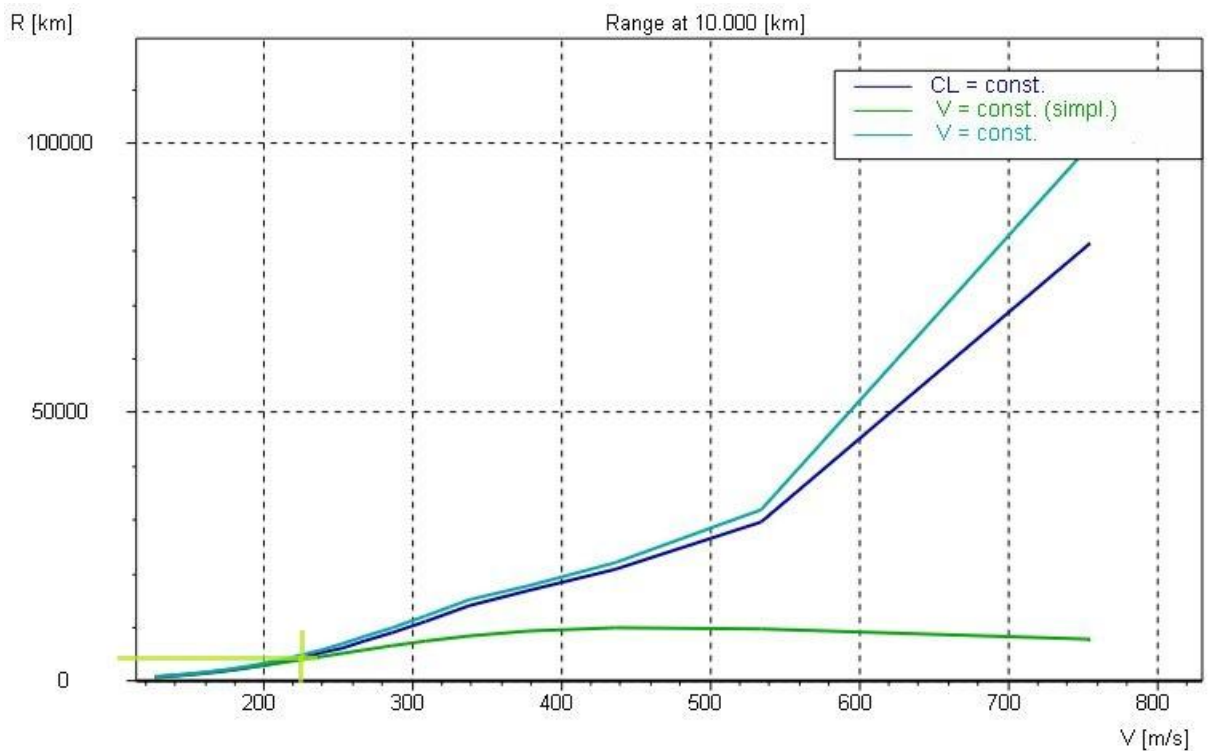


Fig.B 4: External tool range

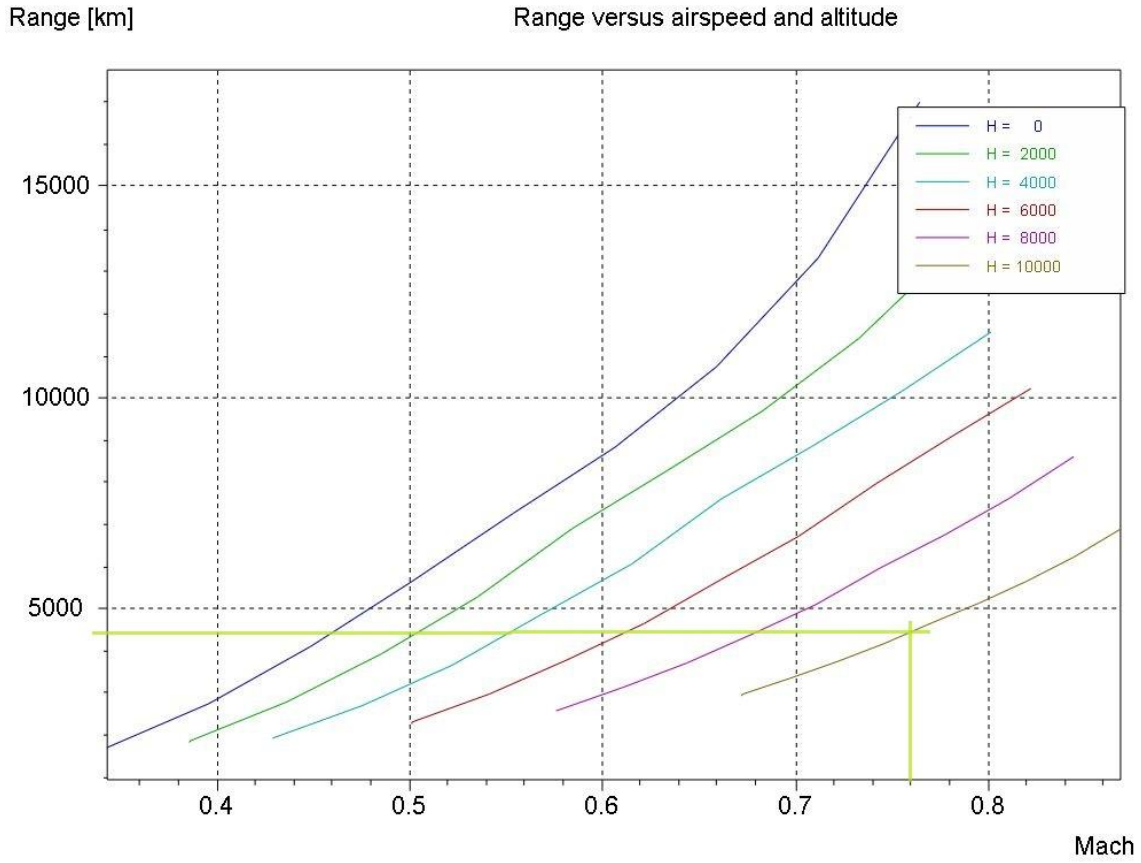


Fig.B 5: SDSA range - C_L constant

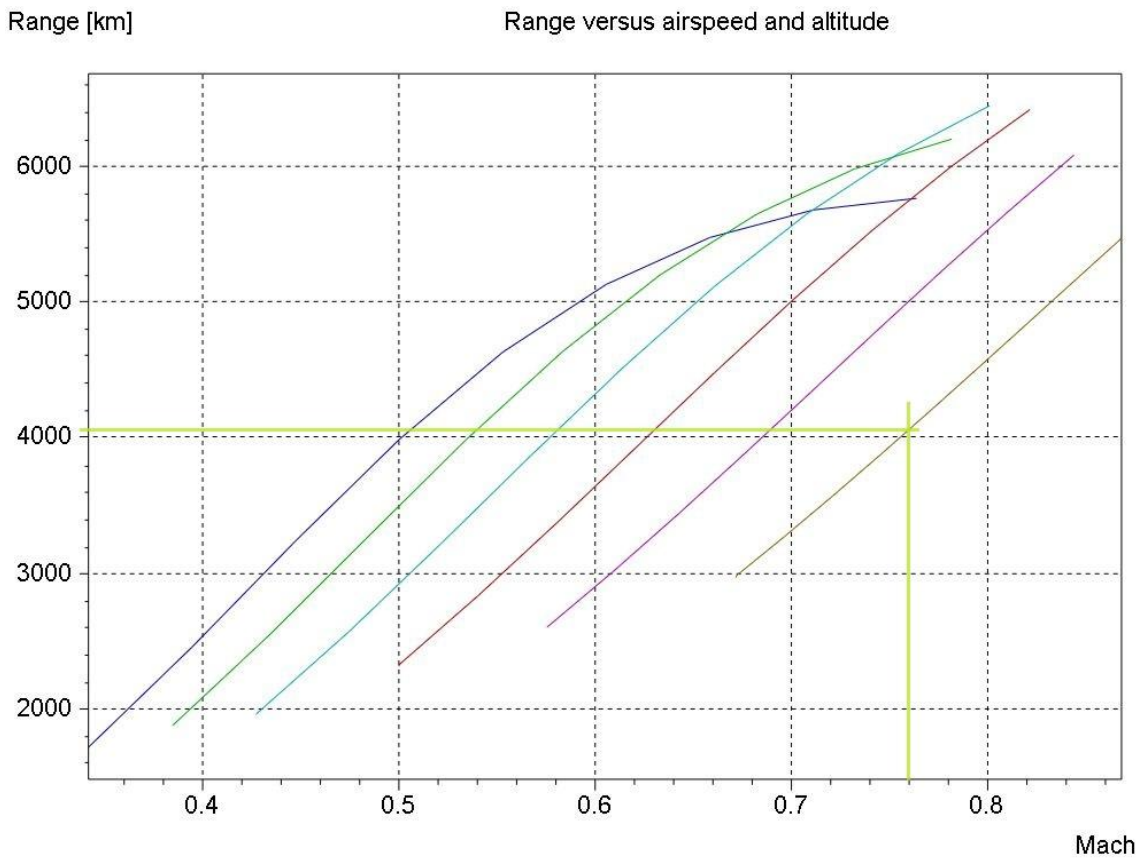


Fig.B 6: SDSA range - V constant (simple)

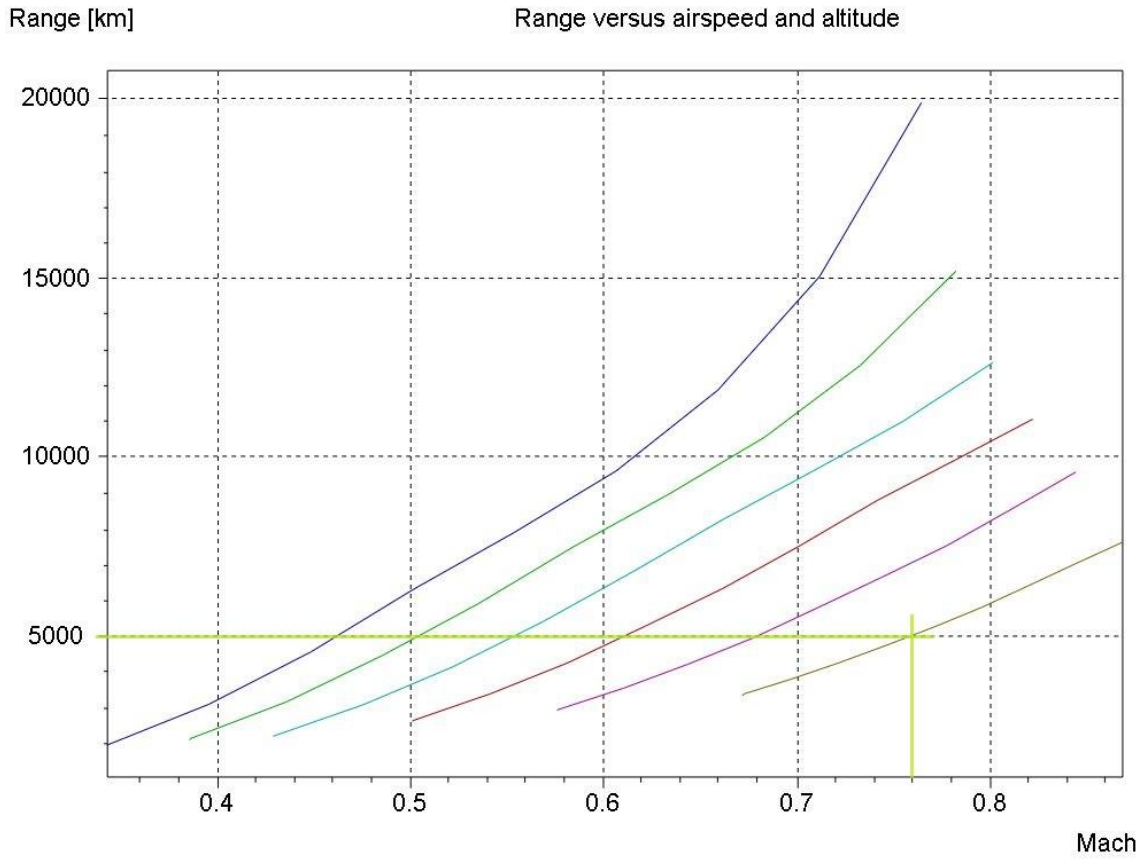


Fig.B 7: SDSA range - V constant

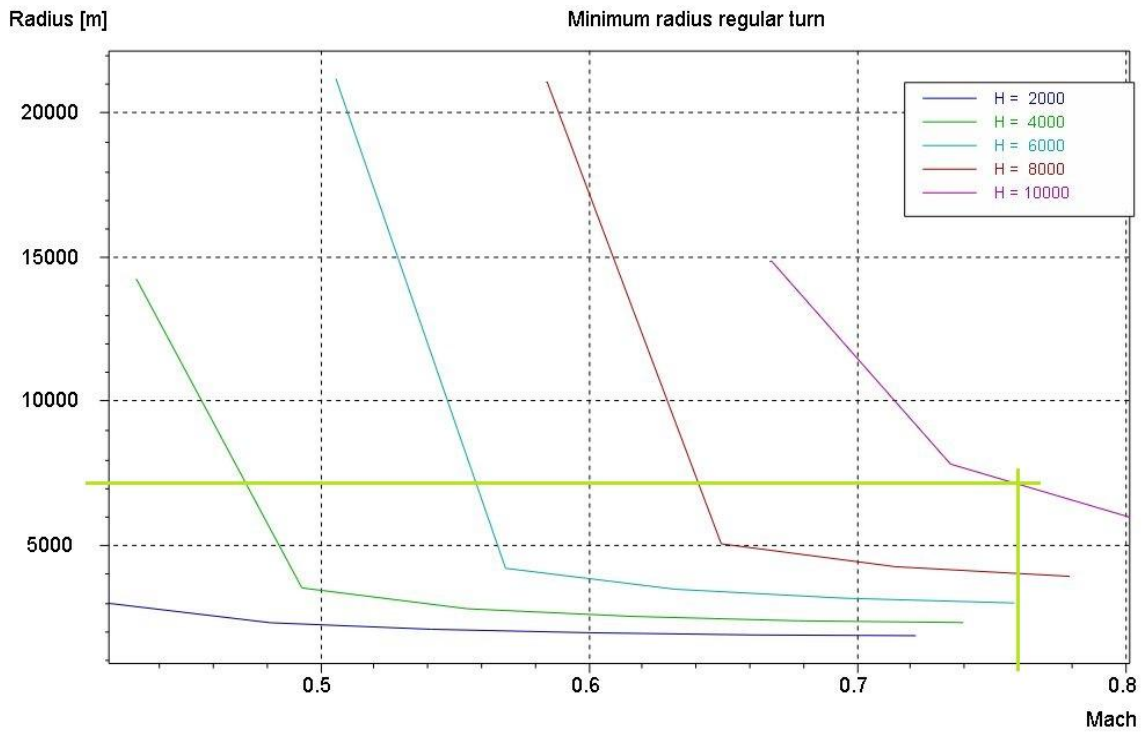


Fig.B 8: SDSA radius regular turn

Appendix C

Input EXCEL sheet – bending moment and shear force

| | | | |
|------------------|------------|------------------------|---------------------------------------|
| data | | | |
| wing area | S = | 65,27 m ² | g = 9,81 m/s ² |
| half span | b = | 16,60 m | nz = 2,5 |
| chord tip | ct = | 1,5541 m | mFL = 3086 kg |
| chord root | cr = | 6,3124 m | mT = 4621 |
| taper ratio | λ | 0,246 | mK = 6250 kg |
| swep angle | Φ | 24,71° | delta η = 0,6638 m |
| VS-position | | 6,6 % | e = 0,153 |
| HS-position | | 74 % | q=0,5* ρ h*v ² = 8722 |
| rel.thickness | δ = | 12 % | hTr = 6,767 m |
| wing load * nz = | G/S = | 13675 N/m ² | Tr = 104000 N |
| airfoil | SC(2)-0612 | | v = 224 m/s |
| | | | altitude = 10000 m |

(according Excel sheet is attached on the CD)

Appendix D

| Cruise flight | | | |
|--------------------|----------|------------------------------------|--------|
| Cruise Mach number | M_{CR} | <input type="text" value="0.69"/> | [-] |
| Cruise altitude | h_{CR} | <input type="text" value="9881"/> | [m] |
| Cruise speed | V_{CR} | <input type="text" value="207"/> | [m/s] |
| Cruise altitude | h_{CR} | <input type="text" value="32416"/> | [ft] |
| Cruise speed | V_{CR} | <input type="text" value="402"/> | [kt] |
| Cruise speed | V_{CR} | <input type="text" value="745"/> | [km/h] |

| Aircraft data | | Comparative data | |
|--|------------------|------------------------------------|-------------------|
| Max. take-off mass | m_{MTO} | <input type="text" value="68763"/> | [kg] |
| Max. landing mass | m_{ML} | <input type="text" value="61887"/> | [kg] |
| Operating empty mass | m_{OE} | <input type="text" value="36788"/> | [kg] |
| Payload | m_{PL} | <input type="text" value="20000"/> | [kg] |
| Max. zero-fuel mass | m_{MZF} | <input type="text" value="56788"/> | [kg] |
| Mission fuel fraction, standard flight | m_F | <input type="text" value="11975"/> | [kg] |
| Fuel mass, required | $m_{F,req}$ | <input type="text" value="12145"/> | [kg] |
| Fuel mass, all reserves | $m_{F,res}$ | <input type="text" value="2971"/> | [kg] |
| Fuel volume, required | $V_{F,req}$ | <input type="text" value="15.47"/> | [m ³] |
| Wing area | S_W | <input type="text" value="98.4"/> | [m ²] |
| Take-off power | $P_{s,TO}$ | <input type="text" value="19333"/> | [kW] |
| Take-off power of ONE engine | $P_{s,TO}/n_E$ | <input type="text" value="9666"/> | [kW] |
| Number of engines | n_E | <input type="text" value="2"/> | [-] |
| Max. Take-off mass | m_{MTO} | <input type="text" value="73500"/> | [kg] |
| Max. landing mass | m_{ML} | <input type="text" value="64500"/> | [kg] |
| Operating empty mass | m_{OE} | <input type="text" value="40430"/> | [kg] |
| Mission fuel fraction, standard flight | m_F | <input type="text" value="12500"/> | [kg] |
| Wing area | S_W | <input type="text" value="122.4"/> | [m ²] |
| T-O power of ONE engine | $P_{s,TO} / n_E$ | <input type="text" value="9700"/> | [kW] |

Fig.D 1: PreSTo result - SW 2 turboprop engines

| Cruise flight | | | |
|--------------------|----------|------------------------------------|--------|
| Cruise Mach number | M_{CR} | <input type="text" value="0.69"/> | [-] |
| Cruise altitude | h_{CR} | <input type="text" value="10361"/> | [m] |
| Cruise speed | V_{CR} | <input type="text" value="206"/> | [m/s] |
| Cruise altitude | h_{CR} | <input type="text" value="33993"/> | [ft] |
| Cruise speed | V_{CR} | <input type="text" value="400"/> | [kt] |
| Cruise speed | V_{CR} | <input type="text" value="740"/> | [km/h] |

| Aircraft data | | Comparative data | |
|--|------------------|------------------------------------|-------------------|
| Max. take-off mass | m_{MTO} | <input type="text" value="66481"/> | [kg] |
| Max. landing mass | m_{ML} | <input type="text" value="59833"/> | [kg] |
| Operating empty mass | m_{OE} | <input type="text" value="35567"/> | [kg] |
| Payload | m_{PL} | <input type="text" value="20000"/> | [kg] |
| Max. zero-fuel mass | m_{MZF} | <input type="text" value="55567"/> | [kg] |
| Mission fuel fraction, standard flight | m_F | <input type="text" value="10914"/> | [kg] |
| Fuel mass, required | $m_{F,req}$ | <input type="text" value="11080"/> | [kg] |
| Fuel mass, all reserves | $m_{F,res}$ | <input type="text" value="2711"/> | [kg] |
| Fuel volume, required | $V_{F,req}$ | <input type="text" value="14.11"/> | [m ³] |
| Wing area | S_W | <input type="text" value="91.8"/> | [m ²] |
| Take-off power | $P_{s,TO}$ | <input type="text" value="18132"/> | [kW] |
| Take-off power of ONE engine | $P_{s,TO}/n_E$ | <input type="text" value="4533"/> | [kW] |
| Number of engines | n_E | <input type="text" value="4"/> | [-] |
| Max. Take-off mass | m_{MTO} | <input type="text" value="73500"/> | [kg] |
| Max. landing mass | m_{ML} | <input type="text" value="64500"/> | [kg] |
| Operating empty mass | m_{OE} | <input type="text" value="40430"/> | [kg] |
| Mission fuel fraction, standard flight | m_F | <input type="text" value="12500"/> | [kg] |
| Wing area | S_W | <input type="text" value="122.4"/> | [m ²] |
| T-O power of ONE engine | $P_{s,TO} / n_E$ | <input type="text" value="4600"/> | [kW] |

Fig.D 2: PreSTo result - SW 2 turboprop engines

(for a closer look : the excel sheets are attached at the CD)

Appendix E

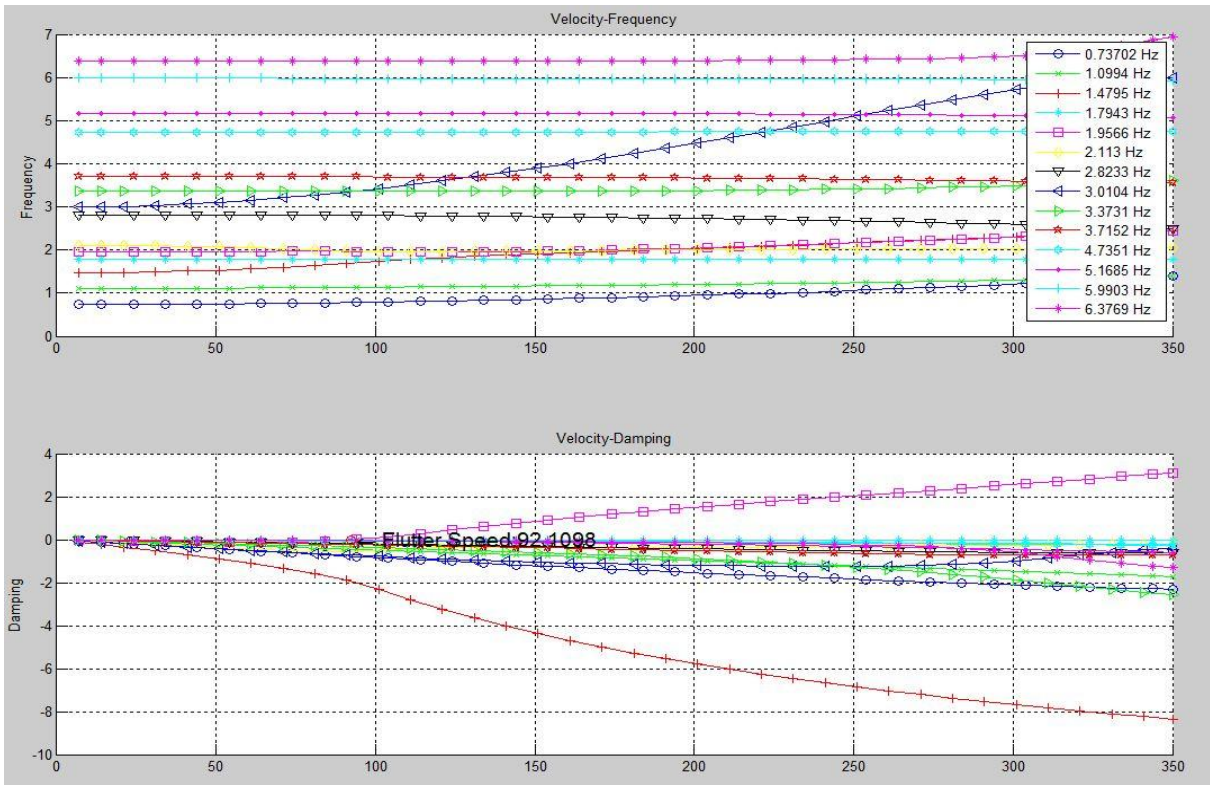


Fig.E 1: V-g plot 0.2 Mach h=0 m

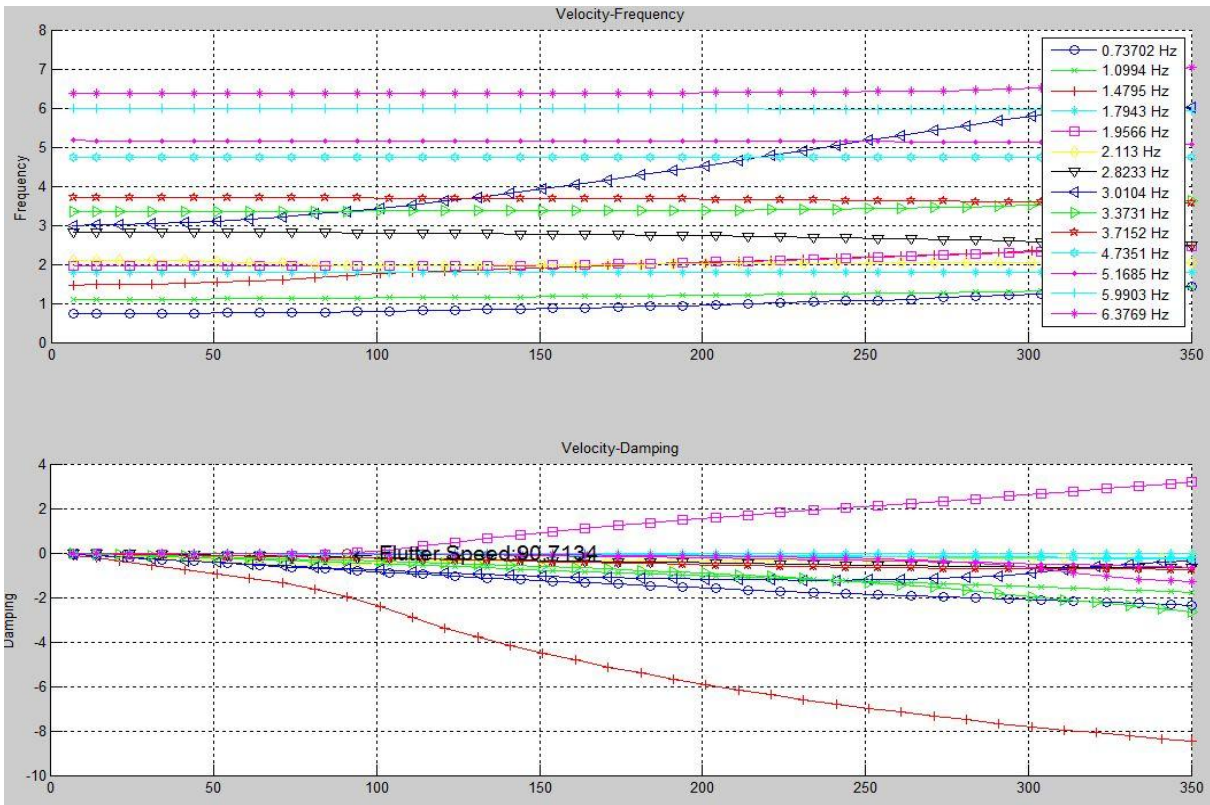


Fig.E 2: V-g plot 0.4 Mach h=0 m

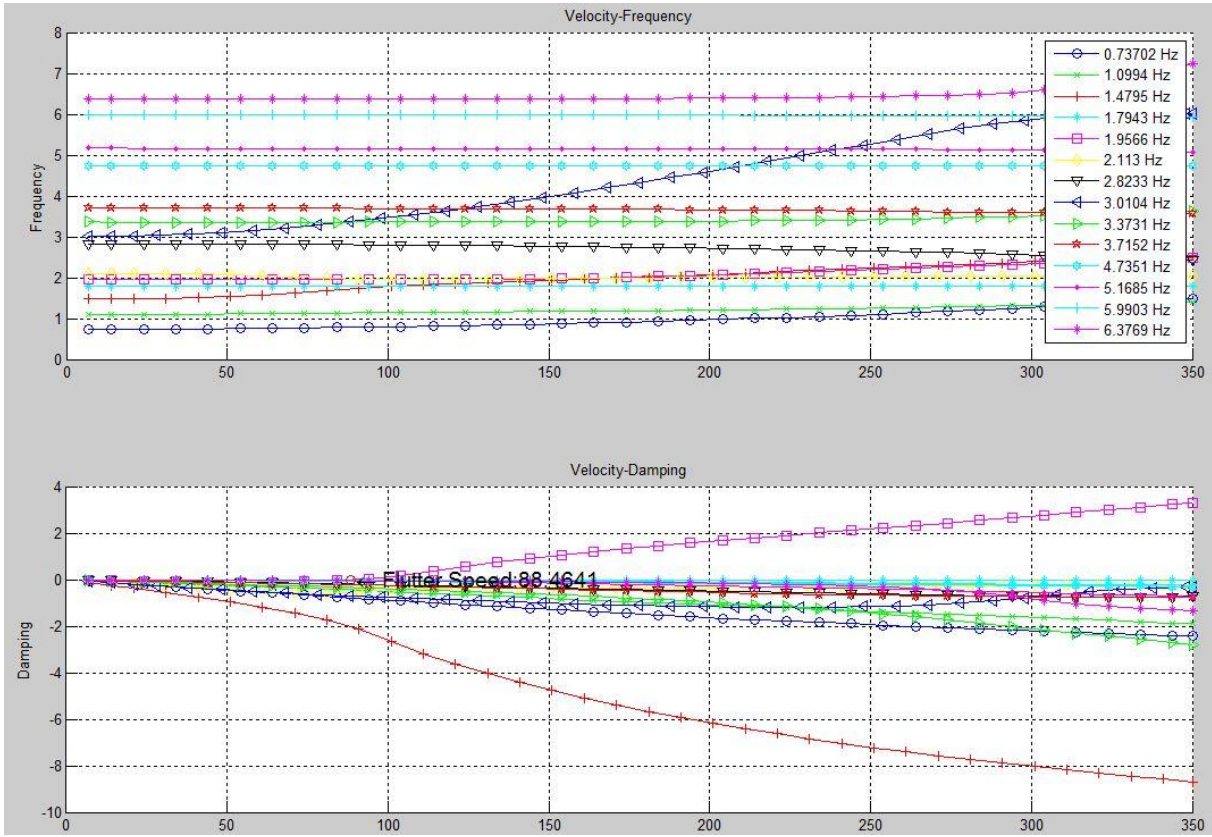


Fig.E 3: V-g plot 0.6 Mach h=0 m

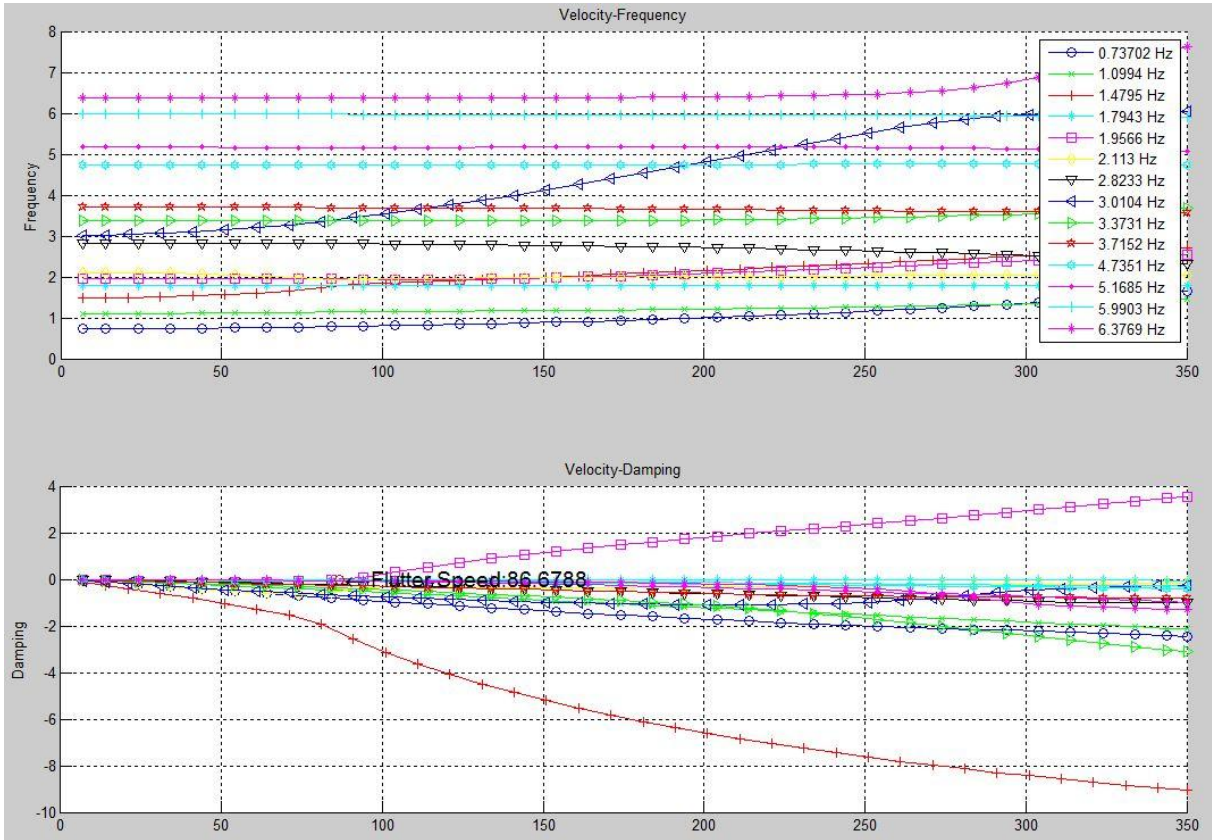


Fig.E 4: V-g plot 0.8 Mach h=0 m

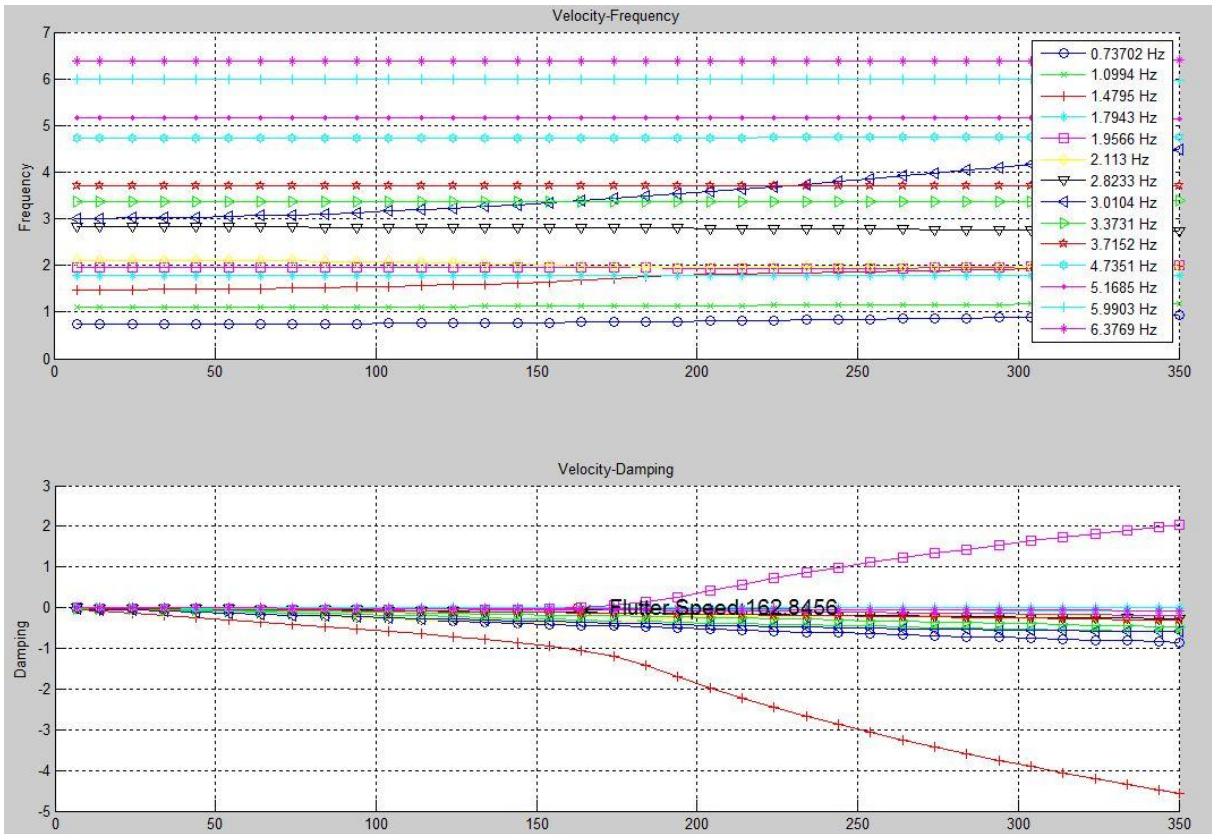


Fig.E 5: V-g plot 0.6 Mach h=9 900 m

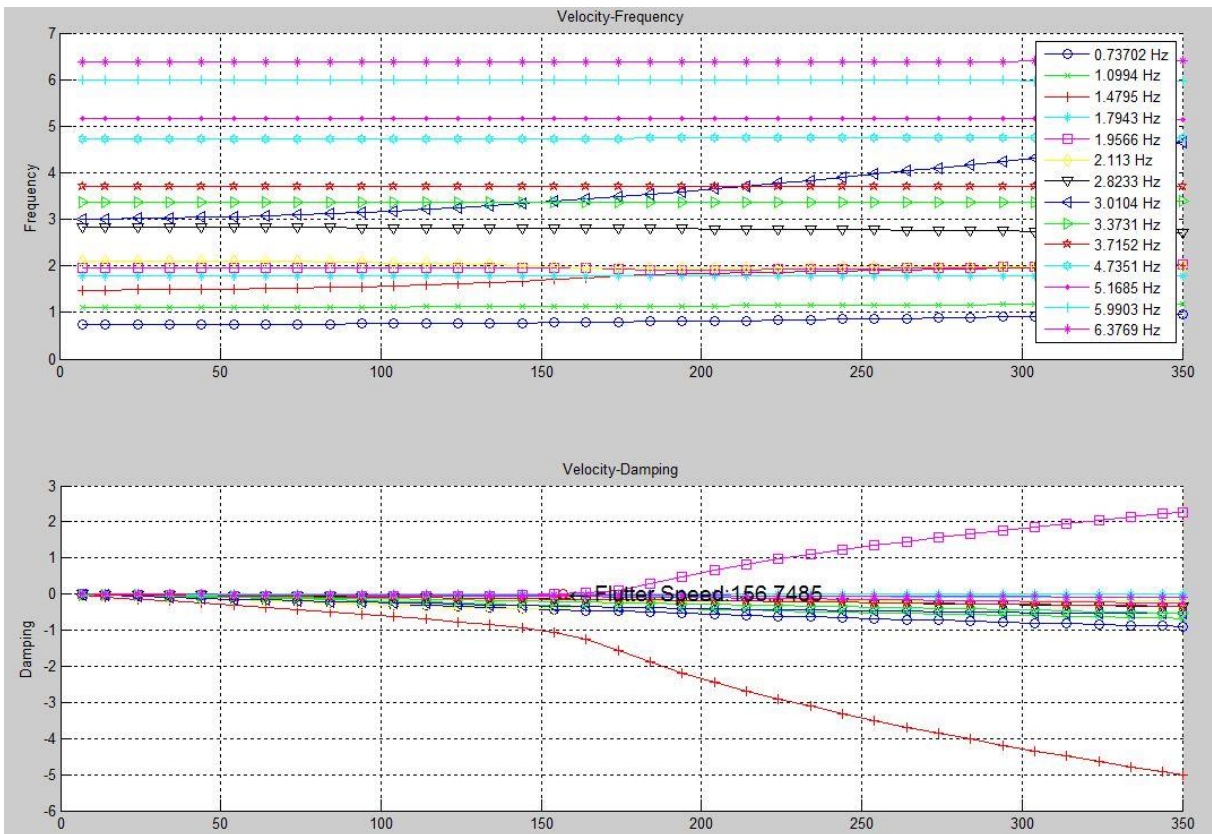


Fig.E 6: V-g plot 0.8 Mach h=9 900 m

Appendix F

Contents of the CD:

Folder: Master thesis

- Written content
 - Abstarct.pdf
 - Abstract.docx
 - Thesis.doc
 - Thesis.pdf
 - Announcement_presentation.pdf
 - Poster.pdf

- Calculations
 - Excel sheets
 - PreSTo_3.3_0,69.xls
 - PreSTo_3.3_0,69_4T.xls
 - A-C_Preliminary_SizingA320_cfm56.xls
 - Aml.xls
 - Structure.xls

- CEASIOM
 - SW (including all *.xml files for each tool of CEASIOM)
 - A320 (including all *.xml files for each tool of CEASIOM)